GENE EXPRESSION IN HUMAN KERITINOCYTES CONTAINING INTEGRATED COPIES OF THE SV40 EARLY REGION

By

SUQING LIU

A dissertation submitted to the Graduate Faculty in Biochemistry in partial fulfillment of the requirements for the degree of Doctor of Philosophy, The City University of New York

2013

This manuscript has been read and accepted for the Graduate Faculty in Biochemistry in satisfaction of the dissertation requirement for the degree of Doctor of Philosophy.

Mark L. Steinberg

Date

Chair of Examining Committee

Edward J. Kennelly

Date

Executive Officer

Karen Hubbard

Jeanne Poindexter

Ann Shinnar

Wilma Saffran

Paul Gottlieb

Supervisory Committee

THE CITY UNIVERSITY OF NEW YORK

ABSTRACT

GENE EXPRESSION IN HUMAN KERATINOCYTES CONTAINING INTEGRATED COPIES OF SV40 EARLY REGION

By

Suqing Liu

Advisor: Professor Mark L. Steinberg

Simian Virus 40 (SV40) large T antigen is one of the simplest and most reliable agents for induction of immortalization of cultured cells. It is known to act by blocking the activities of the cellular tumor suppressors of p53 and pRb proteins. However, other factors that may act downstream from T antigen and the mode of its regulation in SV40 transformed human keratinocytes remain unknown. In the present study we demonstrate that loss of functional T antigen results in a comprehensive gene regulation pattern that is exploited by p53 during the conversion of immortalized cells into primary cells.

We employed line 130, a permanent line of SV40-immortalized human keratinocytes with a unique integrated copy of the virus to study altered gene expression after silencing of the viral early genes using RNA interference methodology. We characterized the viral integration site in 130 cells by sequence analyses of a cloned XbaI fragment isolated from a lambda bacteriophage library as well as by primer walking using various PCR techniques. The viral integrant was found to consist of two tandemly integrated viral DNA copies but with only a single intact copy

of the viral early genes. The viral DNA was found to be joined, at one end, to human chromosome 21q within an intronic region of the homeobox gene, PKNOX1 and, at the other end to a site within a noncoding region of chromosome 10. The late region of the second copy adjacent to chromosome 10 was found to contain numerous rearrangements which may have occurred during the integration process that also brought about the chromosomal breakage and joining of chromosomes 21 and 10. Sequence analyses of the viral mRNAs (via cDNAs cloned in a T vector) showed that there was only a single viral transcript encoding a full length, intact early gene mRNA.

SV40 large T antigen (LT) binds to the cell cycle regulators p53 and pRb, and we found that down regulation of LT antigen expression brought about an accumulation of cells at the G1/S interface, associated with cell cycle arrest. We also found increased expression of BTG2, a novel anti-proliferation protein, as well as induction of the cell cycle inhibitor $p21^{WAF1/CIP1}$, murine double minute-2 promoter activity, expression of murine double minute-2 gene product and expression of GADD45A. Expression of p53 was down-regulated, but we observed an increase in p53 activity that was correlated with reduced binding to LT, suggesting that LT silencing led to p53-independent and BTG2-dependent cycle control in cell 130 line. No evidence of apoptosis was found. We attempted to establish a stable LT knock-down subline of 130 using an miRNA expression vector, but we found that while the presence of the plasmid vector was stably maintained over long-term culture, long-term LT silencing was not maintained, supporting the idea that even after long-term culture immortalization remains dependent upon SV40 T antigen expression.

Acknowledgments

I am deeply grateful to Dr. Mark L. Steinberg and Dr. Simon Simms for providing me an opportunity to study in the field of Biochemistry, which will benefit me for the rest of my life.

I am sincerely and heartily grateful to my mentor, Dr. Mark L. Steinberg, for his encouragement and academic advice. His profound guidance helped me pass the most difficult time during the dissertation. Without his support, the completion of this work would be impossible.

I am very grateful to the remaining members of my dissertation committee, Ann Shinnar, Jeanne Poindexter, Wilma Saffran and Paul Gottlieb. Their academic support and input and personal cheering are greatly appreciated.

Besides this I would like to thank to my whole families, especially, my father, Yuan-Zhu Liu and my daughter, Feiran Lou, their inspiration of pursuit of higher education encourages me to finish my Ph.D. program.

Table Contents **Pages**

List of Tables **pages**

List of Figures **pages**

INTRODUCTION

SV40 large T antigen gene, an oncogene, encodes a powerful oncoprotein T antigen which is capable of transforming a variety of cell types and inducing cell immortalization through its effect on p53 protein and retinoblastoma protein (pRb). However, the Large T antigen's effect may not be limited to these two pathways. In this research, we investigated Large T antigen's effect on gene expression using siRNA silencing technique and a SV 40 transformed immortalized human epithelial cell line, 130 cell line. It is hypothesized that inactive of large T antigen may be associated with growth arrest, senescence, apoptosis, and differentiation. The phenotype changes and molecular level changes by which inactive of the large T antigen were studied. The gene expression was easily screened by the real-time PCR array; the translation of the gene was determined by Western blotting. We found that silencing of T antigen affects the regulation of several genes which are related to cell cycle arrest, senescence, apoptosis and differentiation. The most interesting gene to be regulated is B-cell Translocation Gene-2 Tumor Suppressor Gene (BTG2). In many cancer cells, the BTG2 gene was found at a very low level. A recent study revealed that HPV, which causes human cervical cancer, depresses the BTG2 expression (1).

I. Simian Virus 40 and Its Roles in Cell Transformation

Simian virus 40(SV40) is the member of pol yomaviruses family. It was first identified in cultures of rhesus monkey kidney cells that were being used to produce vaccines and was a contaminant in polio vaccines and adenovaccines (2). It was found that virus did not produce cytopathic effects in rhesus monkey origin cells but produced cytopathic effects in kidney cell

cultures derived from the African green monkey (3). Later, it was shown that tumors were induced in newborn hamsters by injection of rhesus monkey kidney cell extracts (4). Since millions of people were injected inadvertently between 1955 and 1963, SV40 as a human carcinogen (5) was intensively studied since then.

1.1 Structural Features of SV40 Virus and Viral Genome

SV40 virus is an icosahedral shaped virus with a diameter of about 45 nm. Its genome consists of a covalently closed circular double-stranded DNA of 5243 base pairs in length. The SV40 genomic DNA comprises three regions: Regulatory region, early region and late region. The early and late regions are defined in term of order of being expressed either before or after viral genome replication. The non-translated viral regulatory region (RR; nt 5163 to 320) controls replication and late promoter initiator that contains the origin (*ori*) of replication, early promoter, and enhancers. The early region (ER) encodes three nonstructural proteins which are designated large T- antigen (LT), small t- antigen (ST) and 17K T antigen (17KT)). These are all generated by alternative splicing from a single mRNA precursor, so that LT, ST and 17kT have identical N-termini but differ in their C-termini. Many studies have shown that the early region of the SV40 viral genome is necessary for cell transformation (6, 7).

The late region (LR) transcription begins near the origin and extends around the opposite strand from that transcribed to produce the early mRNA (8). It encodes three structural proteins, VP1, VP2 and VP3, which comprise the viral capsid. SV40 encodes a fourth small late protein, agnoprotein containing 66 amino acids. It accumulates in the perinuclear region during the late

phase of the infection cycle and enhances the efficiency of viral cell to cell spread. Gene expression is accomplished using the host cellular transcription apparatus.

Figure 1

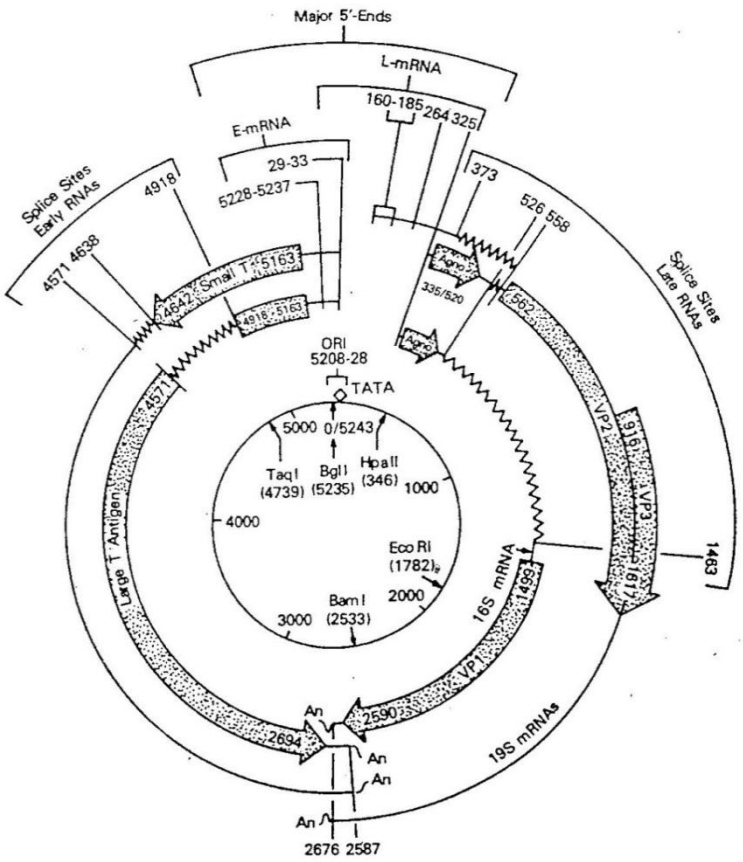

Figure 1. Genetic Structure and Function Map of SV40 Genome. Source: John N. Brandy and Norman P. Salzman (9)

Given on the map are structural features of DNA transcription, RNA processing, and RNA translation. Cleavage site of five single-site restriction endonucleases are indicated for reference. The origin of replication (*ORI)*, 5'and 3'ends of early (small t- and large T-antigens) and late (16S and 19S) mRNA, and the early gene TATA box are shown on the map. Open arrows designate the protein coding regions of mRNAs. Within the arrows, the first number locates the AUG codon, and the second number identifies the nucleotide that immediately precedes the termination codon. mRNA splicing sites are indicated by wavy lines. Early and late transcription proceed on the viral minus and plus strands in counterclockwise and clockwise directions, respectively.

1.2 Structural Features and Biochemical Properties of SV40 Large T antigen

T- antigen is a nuclear phosphoprotein containing 708 amino acids, with a molecular weight of 90 kDa. The T antigen, serving as a multiple regulatory protein, determines the progress in the infection of permissive cells and abortive infection of non-permissive cells by controlling its own transcription and DNA synthesis and the transcription of other viral mRNAs.

1.2.1 DNA binding of T antigen induces the viral replication

SV40 T antigen possesses intrinsic DNA, RNA helicase and ATPase activity, and binds to specific SV40 regulatory region with high affinity (Figure. 2). There are three T antigen binding sites in SV40 regulation region: site I, site II and site III. Site I contains two important GAGGC elements separated by a seven base pairs of AT-rich spacer (10). SV40 T antigen binds to this 17-bp sequence forming a complex covering 5-7 base pairs on either side of this core element. The binding of SV40 T antigen to site I appear to regulate transcription from the early gene promoter (11). Site II contains four GAGGC elements which are organized as two pairs in

opposite orientations, the binding of T antigen in site II results in proper location an orientation of T antigen on the origin. And the binding of ATP to T antigen increases the binding affinity of T antigen to the origin region. It seems that ATP induces the conformational change within T antigen that stabilizes its binding to the binding site. Studies of the protein-DNA complex at the origin showed that T antigen assembles into a two-lobed structure, each lobe contains a T antigen hexamer, and double strands DNA at the origin region are partially separated (12). The hydrolysis of bound ATP by the intrinsic ATPase activity of T antigen causes further separation of the double strands DNA at the origin region, driven by the DNA helicase activity of T antigen. T antigen moves from the 3' to 5' direction on the DNA strands and unwinds the double strand DNA to create a replication bubble (13, 14). The exact function of site III has not been determined. *In vivo*, the binding of T antigen to site III may involve in the interaction of host proteins either with T antigen or Site III (15, 16).

Thus, the binding of T antigen to specific sites at viral *ori* initiates and drives viral DNA replication also applies to cellular origins of replication, much as it does on the viral *ori*, and all the properties of T antigen vitalize transformed cells into S phase(15, 17).

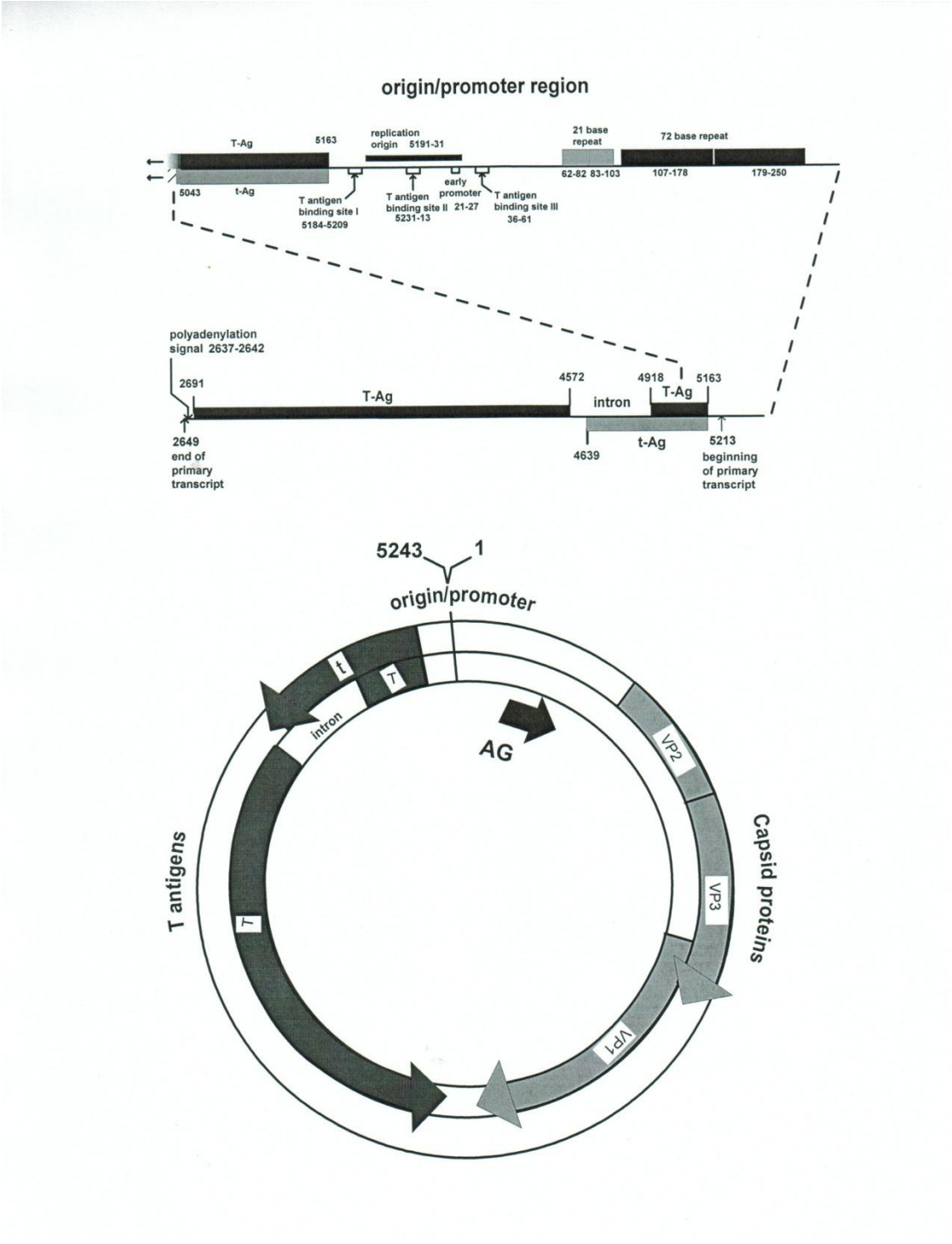

Figure 2. Diagrammatic illustration of the transcription map and T- antigen binding sites at and near the SV40 replication origin.

1.2.2 Functional domains of T antigen

There are several domains with T antigen associating with its multi-regulation functions. There are DNA binding sites which bind to double stranded DNA to initiate viral DNA synthesis *ori* binding; The ATPase act (18), which enables T antigen to translocate from cytoplasm to the nucleus; the Zinc-finger motif responsible for protein –protein interaction (19); The J domain interacts with chaperone protein (Dnak-like protein such as hsc 70); two binding sites for the tumor suppressor protein p53 (20); and a binding site for the retinoblastoma suppressor protein Rb-protein-binding motif (LXCXE) (21), and hostrange domain (HR).

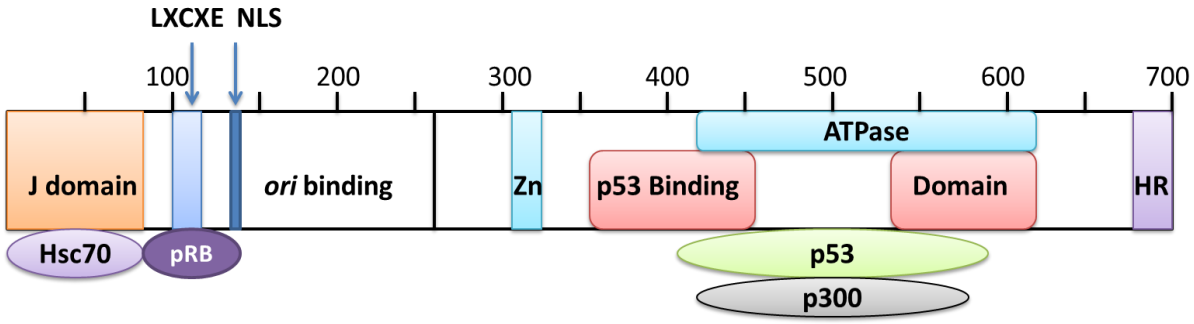

Figure 3. Structure of SV40 Large T antigen and binding proteins

1.2.2.1 Transformation and Immortalization of Cells

Numerous studies have reported that expression of large T antigen alone is necessary and sufficient for cell transformation and immortalization (22). During cellular transformation (23), two tumor suppressors, p53 (24) and pRb (25) proteins, are bound to T antigen, and stabilized, so that their activities are inhibited. As a result, increased p53 levels are correlated with an enhanced transformation frequency (26, 27).

1.2.2.2 T antigen interacting with p53

The p53 tumor suppressor protein, 393 amino acids, has a number of roles in normal cells, the most important of which is in blocking the cell cycle after DNA damage and inducing apoptosis. Since certain promoters of genes contain specific p53 binding site (TGCCT), the transcriptional activation of gene can be modulated by p53 binding, as transcription of p21. In cells containing undamaged DNA, p53 is highly unstable and is present at very low concentrations. Since in the unstable state p53 interacts with an ubiquitin ligase, murine double minute oncoprotein (Mdm2). Consequently the p53 protein is ubiquitinlated and immediately recognized and degraded in proteosomes. DNA damage activates p53 by activating protein kinases that in turn, phosphorylate p53. Phosphorylated p53 reduces binding to Mdm2 and stimulates and turns on the transcription of one of downstream gene p21 (waf1). Thereby, p21 inhibits the phosphorylation of important cell-cycle regulatory factors such as a number of cyclin- cyclin-dependent kinase (Cdk) complexes: cyclin D1–Cdk4, cyclin E–Cdk2, cyclin A–Cdk2, and cyclin A–Cdc2, and inhibits kinase activity and blocks cell cycle progression. p21 alone can regulate the G1 checkpoint and arrest the cell at the G1 to S phase transition, that allows the impaired DNA to be repaired before the cell enters S phase.

When DNA is damaged, the apoptosis of cells can be stimulated by the production of high concentrations of p53, because p53 promotes transcription of proapoptotic genes such as Bax, DR5, Fas/ APO1 and antiapoptotic genes that include Bcl-2, Bcl-XLand IAPs. Activity of apoptotic genes ultimately leads to efficient cell death. At least part of this mechanism is that

p53 can activate the transcription of genes that encode proteins as the Bcl-2 family, that promote the release of cytochrome C from mitochondria,

p53 was initially identified as a co-precipitating protein of SV40 T antigen protein in immunoprecipitation assays. Two bipartite sites of large T antigen can bind the p53 protein (amino acid residues 351~450, and 533~626) and form the SV40 large T-p53 complex (28), the function of p53 blocking cell division was abolishes and cells with genetic damage can survive and enter S phase; which is potentially oncogenic by virtue of its functional involvement in the control of cell proliferation. Therefore, this leads to an accumulation of T-antigen-expressing cells with wild type inactivated p53 that may promote cell immortalizing and transforming activities as well as tumorigenic growth (29-31).

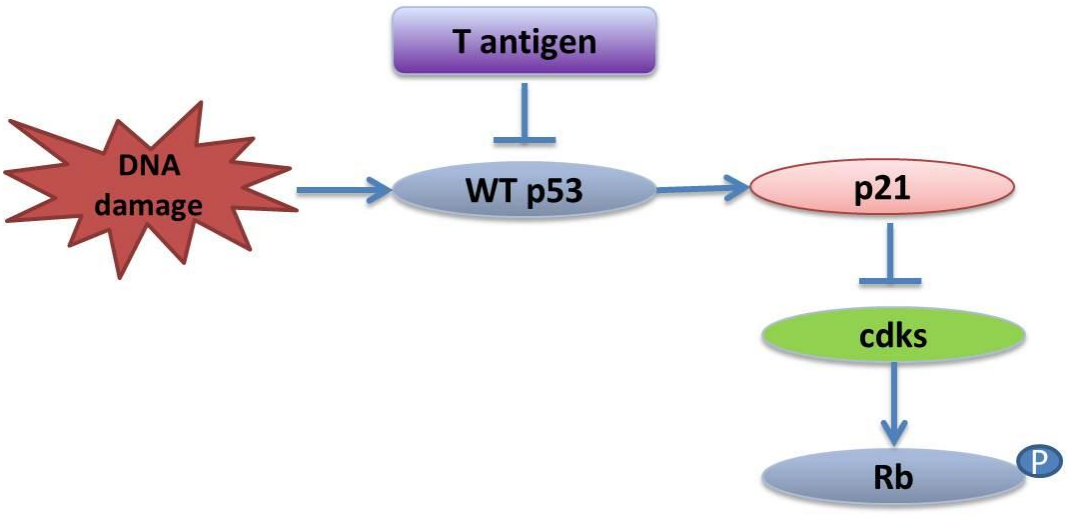

Figure 4. SV40 large T antigen inhibits p53 transactivation.

1.2.2.3 T antigen interacting with Retinoblastoma Protein

The retinoblastoma protein (pRb) is a nuclear protein with a negative regulatory effect on cell growth as a tumor suppressor. pRb has a number of functions but the most important one is regulating the cell cycle. In dividing cells,pRb undergoes a cycle of phosphorylation and dephosphorylation at various times. Cells that are arrested in G1 or G0 phase contain underphosphorylated pRb that interacts with F2F transcription factors. Thereby, their activities are inhibited. For cells to progress into S phase, Rb must be phosphorylated by cyclin-dependent kinases (Cyclin D-cdk4). This releases E2F, which functions in the activation of genes involved in DNA synthesis. T antigen binds to underphosphorylated pRb which is the active form of protein (32, 33). Allowing E2F to escape and activate transcription, thereby promoting progression through the cell cycle. This is a major mechanism whereby T antigen induced the inappropriate cell proliferation characteristic of oncogenically transformed cells.

1.2.2.4 T antigen interacting with p300/CBP indirectly

P300 (early region 1A binding protein p300) and CBP (cAMP-responsive – element-binding factor binding protein) are both large nuclear phosphoprotein and transcriptional coactivators (adapters). They both share the two transcriptional adapter motifs. p300 (34) and CBP play multiple roles in cellular biological processes, including cell growth and transformation. The simian virus 40 large T antigen (SV40 LT) induces cell transformation through the binding and inactivation of p53 and the retinoblastoma family members. Usually p53 function requires an association with the CREB binding protein (CBP)/p300 coactivators, which forms a ternary complex containing SV40 LT, p53, and CBP/ p300. p300/CBP associates with large T antigen

indirectly, through its interaction with p53. Thus, SV40 LT can inhibit the p53, CBP and p300 functions during the cell DNA damaged, and extends the life span of human cells.

1.2.2.5 J Domain and Other Activities Associate with N-terminal End

The two major early proteins encoded by SV40 Large T antigen and small t antigen have identical sequences through their first 82 amino acids called J domain. Since the J domain has the similar amino acid sequence with DnaJ co-chaperone protein (35), it can functionally substitute for the J domains of *E.coli* Dna J in a phage λ growth assay. The J domain can bind Hsc70, a heat shock chaperone protein. The T antigen-hsc 70 interaction supports a stable binding between pRb and T antigen and stimulated the ATPase activity of the heat shock protein by several fold, because hsc70 disrupts the interaction between pRb and E2F in an ATPase-dependent reaction. The J domain of T antigen has a regulatory role in stabilizing T antigen-p53 complexes. The J domain of LT and small t antigen is a functional molecular chaperon J protein.

1.2.2.6 Role of Small T Antigen and 17K antigen

The small t antigen contains a J domain adjacent to a Zinc binding domain that directs the association of small t antigen with protein phosphatase 2A (PP2A)(36), a serine/threonine phosphatase, which is a significant regulatory protein including cell growth and specific signaling pathways. It consists of three subunits—a catalytic subunit C, a regulatory subunit A and a second regulatory subunit B (37). Protein phosphatase 2A is the only cellular protein known to bind to SV40 small t antigen (38).

When hsc70 binds to J domain (39), the B regulatory subunit of PP2A is released and is replaced by small t antigen on the trimer. Small t antigen forms a stable complex with A and C subunits of PP2A, and inhibits PP2A dephosphorylation enzyme activity. Inhibition of PP2A phosphatase activity may influence cell transformation and anchorage-independent growth.

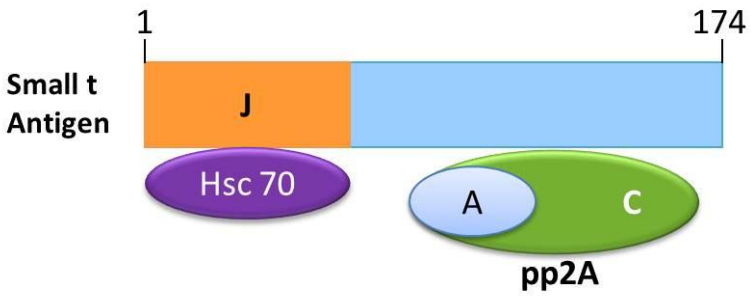

Figure.5.The structure of small T antigen and binding proteins

PP2A can regulate a variety of signaling pathways and cell processes including several classes of protein kinases, transcription factors, and cell cycle regulators. Small t antigen targets PP2A to overcome its negative role in some signaling pathways leading to increased cell proliferation. For example, PP2A dephosphorylates the activating phosphorylation of sites on mitogen-activated protein kinase kinase kinase (MEKK) and the mitogen-activated protein kinase *in vitro*. Thus, there is a decrease in their respective kinase activities. SV40 small t antigen interacts with PP2A to inhibit PP2A activity and up-regulate mitogen-activated protein kinase (ERK1) and the mitogen-activated protein kinase kinase (MEK1). Many signaling pathways have been reported to be affected by PP2A (40). In conclusion, Small t antigen can promote the cell cycle

progression by inhibiting PP2A enzyme activity. ST cannot transform cells alone, although it may enhance the efficiency with which transformation occurs (41).

The third early protein 17k T, which is expressed from an alternatively spliced third SV40 early mRNA, consists of 135 amino acids. Of these, 131 correspond to the amino-terminus of large T, the four carboxy-terminal amino acids are unique and encoded by a different reading frame. In other words, the expression of the transforming amino-terminal domain of large T antigen is as an independent 17kT protein (42). 17K T protein binding Hsc 70 and pRb provides a means for individually regulating the various functions as N-terminal of LT antigen doing. During infection the 17K T antigen is present only in small amounts, compared with other T antigens. Thus, the 17K T antigen will not be further discussed here.

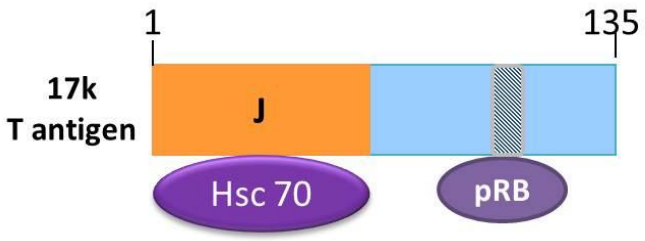

Figure.6.The structure of 17K T antigen and binding proteins

2. Cellular Senescence

Cellular senescence is a state of irreversible cell cycle arrest. The observation that, in vitro, cells derived from normal tissues undergo a defined number of cell divisions before entering a quiescent state has been termed " In replicative senescence" (43). In replicative senescence cells are non-mitotic, but remain metabolically active. Phenotypically, cells in the senescent state show an altered morphology and display a striking increase in the number of lysosomal vacuoles and increased cytoplasmic beta galactosidase activity. Cellular senescence is divided into two different categories; replicative and premature senescence. Replicative senescence is widely believed to reflect an internal program that underlies the aging process. Premature cellular senescence is thought to have evolved, at least in part, as a tumor suppressive mechanism. This process is triggered either by telomere erosion or by acute stress signals, including oncogenic stress induced by overactive oncogenes or underactive tumor suppressor genes (44). Oncogenic stress induces at least three intrinsic pathways, p16/pRb-, p53/p21-, and the DNA damage response (DDR-) pathways. In keeping with this idea are the observations that the senescent process is abrogated in cells derived from tumors and also after activation of a certain oncogenes. Significantly the p53 and pRb genes which are tumor suppressors are also essential for establishing and/or maintaining the state of growth arrest characteristic of senescence (45). Loss of cellular senescence resulting in immortalization is a hallmark of oncogenic transformation of cells *in vitro*.

2.1 The p16/pRb pathway of senescence induction

The G1 to S phase transition in cell cycle is controlled by the p16/ pRb pathway. pRb can be inactivated by cyclin-dependent kinase (Cdk)-mediated phosphorylation. During the normal cell cycle, pRb is phosphorylated by cyclin D/Cdk4 or 6 and cyclin E/Cdk2 near the G1/S phase

transition. Oncogene activation or loss of tumor suppressor genes results in oncogenic stress that induces the Cdk-inhibitor p16. p16 binds to CDK4/6 inhibiting its kinase activity, thereby preventing pRb phosphorylation. The Cdk inhibitor p27 is induced by external growth inhibitory signals such as TGF-β and inhibits cyclin E/Cdk2. Therefore pRb remains associated with the transcription factor E2Fs localizing it to the cytoplasm. Thus, E2F transcription factors are not capable of activating the transcription of S-phase genes and the G1/S phase transition is arrested. p16 expression is also regulated by pRb via a feedback loop between p16 and pRb. Phosphorylation of pRb results in increased levels of p16 expression which inhibits Cdk4/6 resulting in increased levels of hypophosphorylation of pRb which, in turn, leads to decreased p16 expression. pRb mediates senescence by repressing E2F transcription factors (46). However, viral oncogenic proteins such as SV40 large T antigen can bind pRb and suppress the activity of pRb which causes cell immortalization.

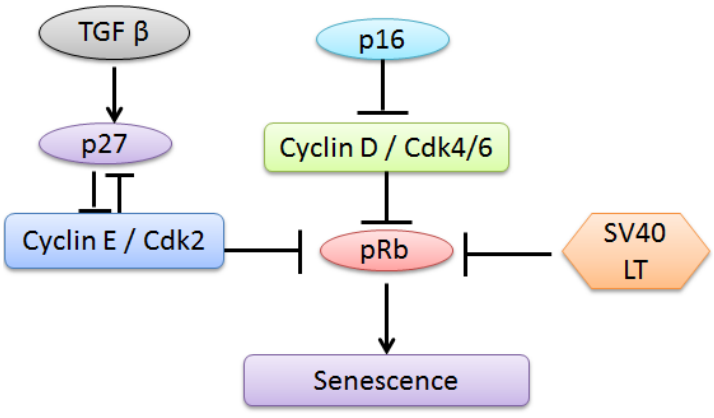

Figure 7. The p16/pRb pathway of senescence

2.2 Induction of the p53/p21 senescence pathway

The tumor suppressor protein p53 is normally degraded via the E3 ligase Mdm2 (murine double minute-2). Oncogenic stress inhibits Mdm2, thereby activating p53. p53 activates transcription of the Cdk inhibitor p27 that contributes to senescence induction by inhibiting Cdk2 (Figure. 7).transcription of p21 is also induced by p53 and is repressed by Myc (v-myc myelocytomatosis viral oncogene homolog). mTOR (mechanistic target of rapamycin), a serine/threonine kinase, stimulates p53 translation and thereby contributes to induction of senescence, but is inhibited by PTEN (phosphatase and tensin homolog) (47, 48). SV40 large T antigen binds to p53 inhibiting its activity and counteracts cellular senescence.

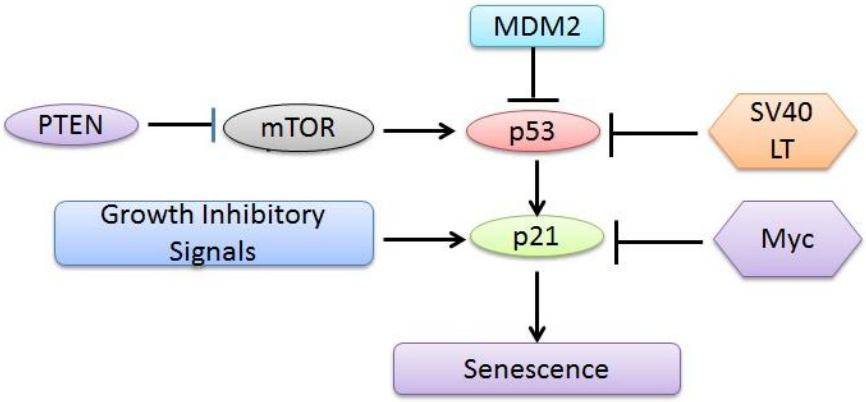

Figure 8. The p53/p21 pathway of senescence

2.3 The DNA damage response (DDR) pathway

Telomere erosion or oncogenic stress induces DNA damage that activates the DDR response, including the kinases ATM (ataxia telangiectasia mutated), ATR (ataxia telangiectasia and Rad3 related), Chk2 (checkpoint kinase 2) and Chk1 (checkpoint kinase 1). ATM and Chk2 phosphorylates and activates p53, which induces senescence via p21. DDR signaling also

induces different DNA repair systems. If DNA repair is successful, DDR signaling will be shut off and p53 inactivated, thereby aborting senescence signaling(49). Some repair proteins are reported to inhibit p53 or p21 directly. Myc enhances DDR signaling, but might also stimulate DNA repair, and counteracts telomere erosion through induction of hTert.

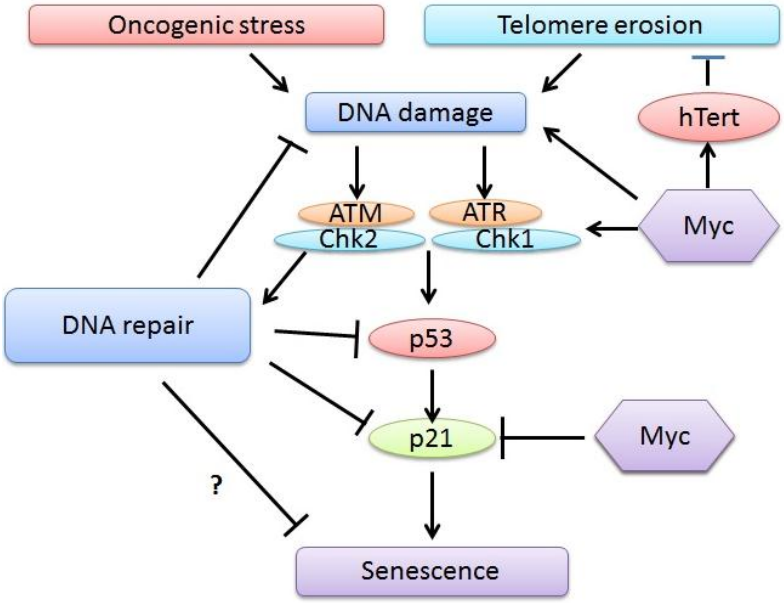

Figure 9. The DDR pathway of senescence

2.4 Chromosomes associated with Senescence genes

Cellular immortalization is one of the critical steps in human carcinogenesis. During this process cells must escape senescence and acquire an infinite lifespan. It has long been known that loss of a key tumor suppressor gene, such as p53 and pRb, is necessary, but not sufficient. There must be additional mutation or epigenetic alterations necessary for immortalizations to occur. In Simith and Berube's somatic cell genetic complementation studies (50), they found that in somatic cell hybrids of mortal and immortal cells, the senescence phenotype is dominant over the immortal phenotype (51, 52). They also found two unrelated immortal cell lines with defects in different genes were fused together. The hybrid cells were found to undergo senescence. They suggested that there are at least four senescence genes must be abrogated in order to achieve cellular immortalization. Microcell-mediated transfer of chromosomes into immortalized cells was used to identify putative senescence genes. Several chromosomes were identified as potentially encoding senescent genes including chromosomes 1, 2, 3, 4, 6, 7, 10, 11, 16, 17, 18, and X. To date, only the MORF4 (mortality factor 4) gene has been identified on chromosome 4(53). Other senescence-specific genes have not yet been identified.

3. Immortalization of Human Epidermal Keratinocytes by SV40

Since most human cancers are derived from epithelial cells, immortalized epithelial cells are good models of normal and abnormal epithelial cell growth and differentiation (54). The early genes of Simian virus 40 (SV40) are known to be effective in inducing immortalization of cells without cytotoxic effects (7). In 1979, Dr. Steinberg's group first reported the transformation and immortalization of human epidermal keratinocytes by SV40 *in vitro* (55). SV40-immortalized human epithelial cells have been shown to express many of the phenotypic

properties of the untransformed host at early passages following infection (56, 57). For this reason low passaged SV40-infected human epithelial cells have been used as a model system to study epithelial function and the essential factors required for cellular processes.

The early region (31~2599) of SV40 can induce the transformed properties exhibited by tumor cells grown in culture. Introduction of the early region of SV40 DNA into the cell is necessary and sufficient for complete transformation of cultured cells. Human epithelial cells are nonpermissive for infection, so that intact SV40 virus can be used to introduce the immortalizing gene without cytopathic effects. Transformation of human keratinocytes by SV40 is a progressive process. The progressive takes many cell generations during which different transformed phenotype emerges and becomes fixed in the cultured cells. The entire process can be divided into three distinct stages: early phase, crisis stage and late phase as shown in Figure 7.

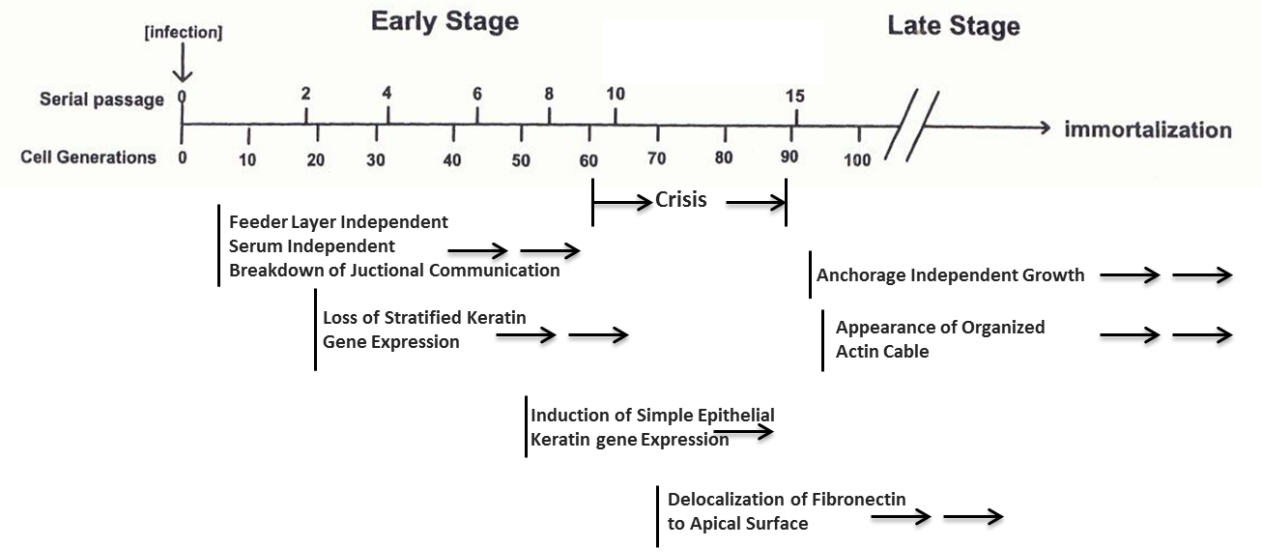

Figure 10. Schematic representation of changes in properties of growth and differentiation over time following infection of human epidermal keratinocytes by SV40.

SV40 gene expresses T antigen, which is critical for cell immortalization. In the early stage-phase, the T antigen–positive subpopulation, initially comprising only about 2% of the cells exposed to virus, gradually increases with each generation. Uninfected cells undergo senescence in approximately 60 generations. In the early phase the transformed cells lose dependence on fibroblast feeder layer, growth serum independence and lose the stratification characteristic of epidermal differentiation. Between 10 and 15 serial passages (63-91 generations), they enter a "crisis" period in which cell number remains constant as successful cell division is balanced by cell death, or even declines. T-antigen extends lifespan of cells in culture, so that crisis occurs when there is more population growth than senescence in uninfected cells. The cells then enter the late phase. Anchorage independent growth can be used as a marker of the late phase. During this phage changes in actin filaments occur and undifferentiated carcinoma-like tumours develop in nude mice.

4. RNA Interference and mRNA silencing

RNA interference (RNAi) is the process by which double-stranded RNA molecules silence a target gene through the specific destruction of the target gene's mRNA. It was discovered in 1998 (58) . Recently RNAi has been very successfully applied in cancer research and gene regulation study, because of its specificity, selectivity, efficiency of RNA interference in targeting mRNAs, and lack of cytotoxic effects(59, 60).

RNA interference is triggered by small interfering RNAs (siRNAs), which are 21-23 nucleotides that hybridize to each double-stranded RNA(61). After hybridization, each strand of the siRNA with the two nucleotide 3' single-stranded tails is prevented from encoding protein. siRNAs can be generated by chemical synthesis or from three different precursor RNAs: long double-stranded RNA (dsRNAs), plasmid-(retrovirus/Adenovirus) vector synthesized short hairpin RNAs (shRNAs) (62), and endogenous hairpin RNA with a few base-pair mismatches in the stem micro RNAs (miRNAs). For the entire process, the ribonuclease-III activity of the Dicer enzyme is required to generate 21–23-nt siRNAs. These siRNAs are then incorporated into an RNA-induced silencing complex (RISC) (63), which in turn uses its ATP-dependent RNA-helicase activity to unwind the duplex siRNA into single-stranded siRNA. The antisense strand of the duplex siRNA guides the RISC to the target mRNA. Under proper conditions and concentrations, the antisense and sense strands anneal to form double-stranded RNA if the RNA sequence is a perfect match to a target mRNA, resulting in target mRNA degradation. An RNA sequence with a partial match to the target mRNA functions as a miRNA and causes translational repression.

siRNA, shRNA and miRNA increase stability of RNA then elicit RNA interference through common biochemical pathways summarized in Figure 11. RNA interference increase stability due to the double-strand. The technique is specific in silencing mRNA, and is very efficient in delivering siRNA. In addition, the 21-23 nucleotide siRNA has antiviral properties. All of the above make RNA interference a powerful experimental tool for studying gene function.

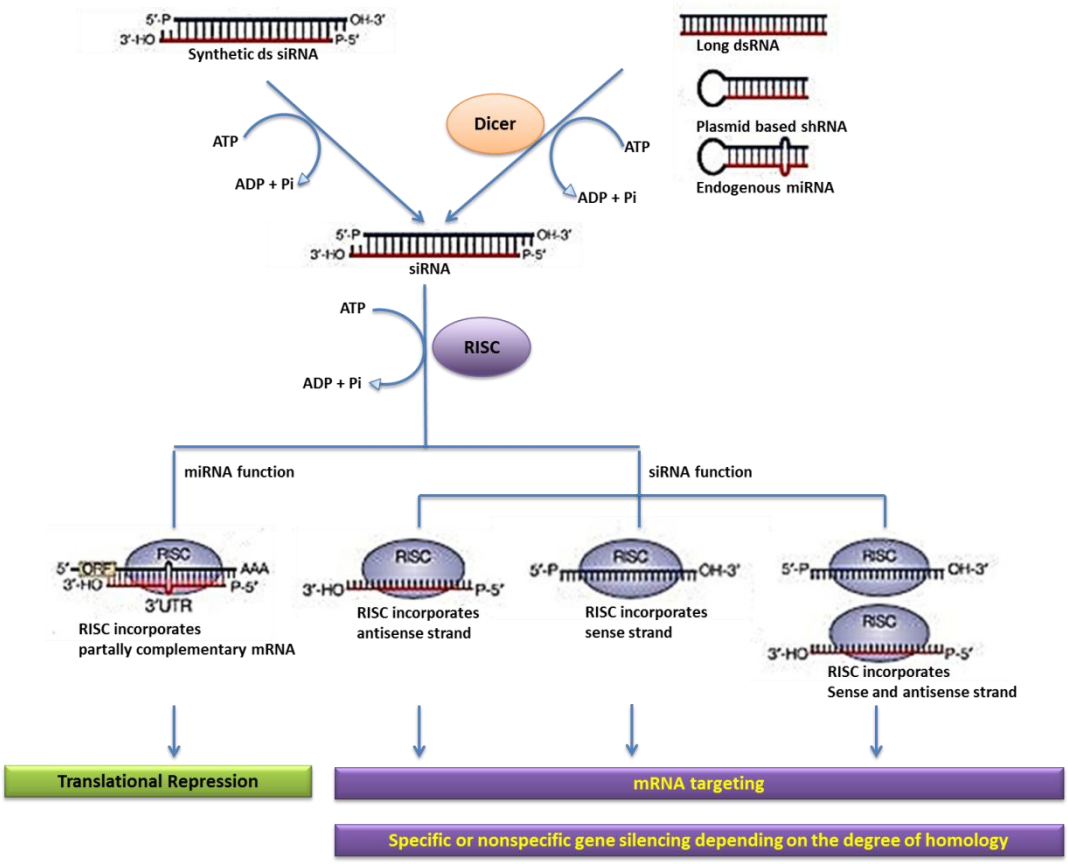

Figure 11. siRNA pathways in targeted mRNA silencing.

5. The B-cell Translocation Gene-2 Tumor Suppressor Gene (BTG2)

After LT antigen silencing, we studied a pathway in cell cycle. Particularly, we examined changes in B-cell translocation gene 2(BTG2). BTG2 is a member of a novel BTG/Tob family of anti-proliferative genes (APRO), in which there are six protein members, Tob1, Tob2, BTG1, BTG2, BTG3 and BTG4, in human cells (64). The protein products of human BTG/Tob family share common structural motifs, including two highly conserved domains (BTG boxes A and B) separated by 20–25 non-conserved amino acids. The BTG/Tob gene family often contains some

copies of an ATTTA motif that is known as the most common determinant of the RNA stability in mammalian cells.

5.1 Structural BTG2 Gene and Its Protein

The homo sapiens BTG2 (BTG2) gene is composed of 4790 bps, localized to chromosomal locus 1q32.1. It contains exon 1 and 2 and one intron of 1359 bp. There is 2954 bp of the 5'-flanking region upstream from the ATG start codon (65). There is a CCATT box in -70-80 upstream from the initial transcription site ATG, to bind for the RNA transcription factor, but a TATA box in promoter DNA region. There are three binding sites for specificity protein 1 (Sp1), a human transcription factor. A CpG (Cytosine-phosphate-guanine) island is located in promoter region; cytosine can be methylated to form 5-methylcytosine by DNA methyltransferases, which turns off the gene transcription. Six p53 binding sites (p53BS1-6) are located in 5'-flanking region and the intron (Fig. 12).

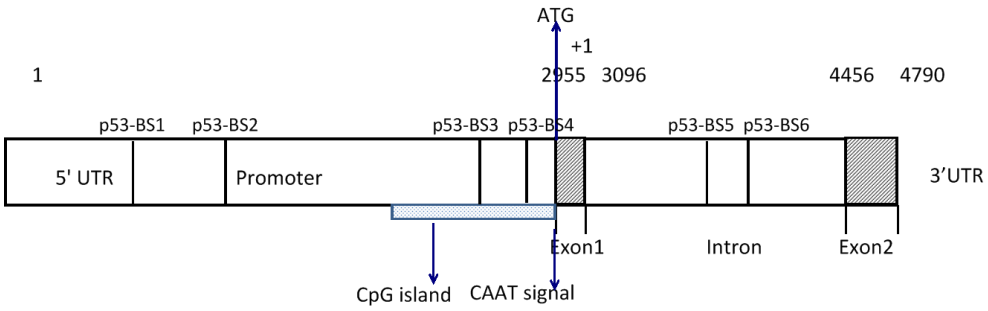

Figure 12. Diagrammatic representation of the human BTG2 gene.

ATG is the translation initiation site and a CCATT box is indicated by arrows; the transcription factors binding sites are indicated by Sp1; P53 binding sites are indicated by p53 BS1-6, CpG

island is showed as a strip rectangle. Sequence TGCCT element, p53 binding motif, can be bonded by the p53 consensus binding site consisting of four pentameric repeats of RRRCW, in which R is a purine, C is Cysteine and W represents either an Alanine or Threonine residue. Four p53 binding sites present in the promoter region and two in the intron. BTG2 appears to be the p53 target gene. In other words, p53 binds to sequence-specific DNA elements of BTG2 and induces the transcription of BTG2 genes (65). Especially the DNA of mammalian cells is damaged. So that BTG2 gene expression can go p53 dependent pathway. Expression of the BTG2 gene can also be up-regulated by a p53 independent pathway by 12-*O*-tetradecanoylphorbol-13-acetate (TPA), a potent tumor promoter. Stimulation is through the activation of PKC-δ pathway in tumor cells in which p53 is inactive (66). The protein product of BTG2 gene, has 158 amino acids, is present in the nuclei of epithelial cells in many tissues, and is an anti-proliferate protein. BTG2 protein contains three highly conserved domains among various species; Box A (50–71), Box B (96–115) and Box C (116-127) (67). The conserved N-terminal domain Box A of BTG2 is a protein–protein interaction module, which is capable of binding to DNA-binding transcription factors such as Caf1. which is also named GR (for growth regulator binding site), and Box B respectively appear to play key roles in anti-proliferative function and in binding to a number of molecular targets such as a protein-arginine N-methyl transferase (PRMT1) (68). There are two copies of LXXLL motifs in BTG2, one near box A, and one in box B, known as the nuclear receptor box (NR box) that is related to regulate estrogen-related receptor A1 (ERRA1) (69-71) and the androgen receptor (AR) (72, 73) in the breast cancer and prostate cancer. The C-terminal regions of Box are less conserved and appear to mediate protein–protein interactions.

The activity of BTG2 can be regulated by phosphorylation of serine 147 of BTG2. BTG2 plays multiple roles in cellular processes; it is as an anti-proliferation regulator and a transcription factor.

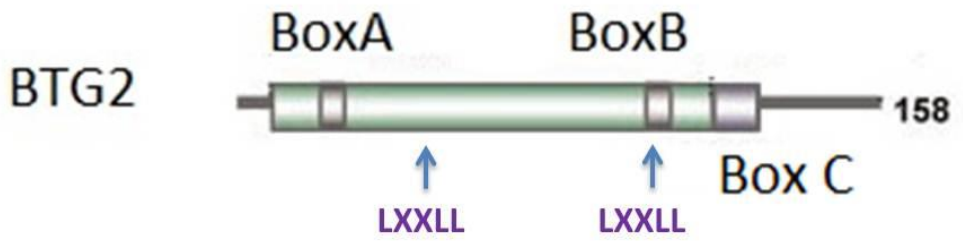

Figure 13. The structure of BTG2 protein

5.2 BTG2 inhibit G1/S phase transition by both a pRb dependent and a pRb independent manner

BTG2 expression is induced in response to genotoxic stress through a p53-dependent mechanism (74). When cells were damaged, the BTG2 expression increases with p53 (75). Overexpression of BTG2 down regulates the expression of cyclin D1 which leads to pRb hypo phosphorylation (76) (Figure 14); the growth-inhibitory activity of pRb is regulated by phosphorylation. Phosphorylation of pRb is activated by the cyclin-cdk complexes, whose activity, in turn, depends on cyclin level. When cyclin D1 mRNA levels were significantly reduced by BTG2, pRb is less phosphorylated and increased its binding to E2F, E2F is not able to activate the transcription of G1/ S-phase genes. The result is that G1 phase of cell cycle is arrested and there is a reduction in cell proliferation in a variety of cell types. S phase progression can be regulated by cyclin E instead of cyclin D in pRb inactive cell line derived from tumor cells (77). BTG2 expressed in the 293 cell line, (in the 293 cell line both pRb and p53 proteins are inactive due to

the infection of adenovirus type 5) inhibits G1/S phase transition by delayed biosynthesis cyclin E and CDK4 (65). The result is a decrease cyclin E associated CDK activity. Cyclin E expression can overcome a pRb-dependent block of the cell cycle (67, 76). Therefore, in the pRb independent pathway, BTG2 works as a tumor suppressor by causing arrest in the G1/S phase transition. Cellular senescence can appear in pRb defective tumor cells (78).

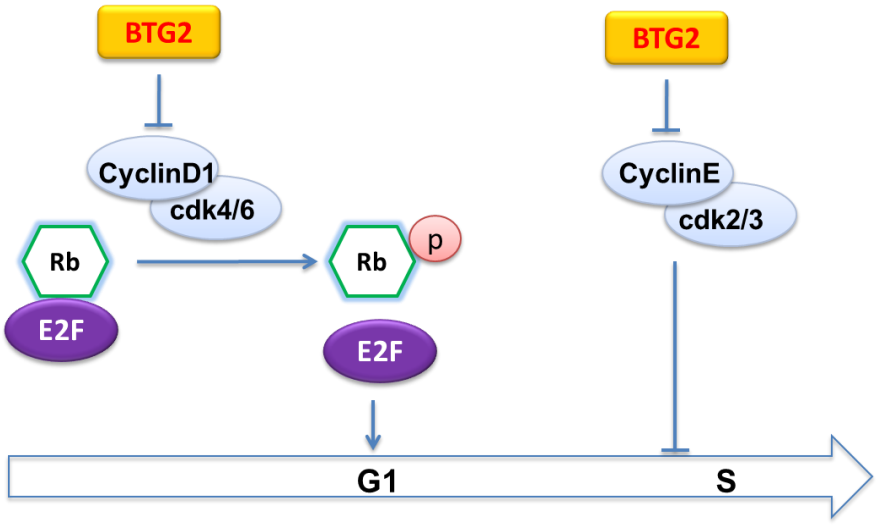

Figure14. BTG2 overcome of G1/S restriction point by Rb dependent or independent pathways

In a p53 null cell such as U937 cells, the potent tumor promoter TPA induced BTG2 expression by inhibition of PKC-δ (66, 79). Overexpression of BTG2 causes cell death via arrest at the G2/M interface (Figure 15). In tumor cells lacking p53, epidermal growth factor (EGF) induces activation of extracellular signal-regulated protein kinases 1 and 2 (ERK1/2), members of the mitogen-activated protein kinase super family that can mediate cell proliferation and apoptosis. ERK $_{1/2.}$ p-ERK, then phosphorylates S^{147} of BTG2 (80), which in turn binds to Pin-1 (peptidylprolyl cis/trans isomerase protein NIMA-interacting 1), which regulates mitosis, and translocates Pin-1 from the nucleus to the cytoplasm resulting in cell death instead of mitotic

progression. At the same time cyclin B1 expression is significantly decreased in BTG2 expressing cells. Here it was shown that Forkhead box protein M1 (Foxm1) upregulated cyclin B1 transcription. Foxm1 was phosphorylated by cyclin dependent kinase (cdk) and the transcriptional activity of Foxm1 was regulated by its phosphorylation. BTG2 inhibited Foxm1 phosphorylation *in vitro* and *in vivo* also via inhibition of cdk1 activity (cdk1 is known as M-phase promoting factor; MPF). BTG2 binds to the cyclin B1-cdk1 complex and inhibition of cdk1 activity. In summary, BTG2 has been shown to inhibit Foxm1 transcriptional activity by inhibition of Foxm1 phosphorylation which leads to inhibition of mitotic progression, decreased cell proliferation and tumorigenecity in p53 null cells. BTG2 therefore works as a tumor suppressor/anti-proliferation regulator.

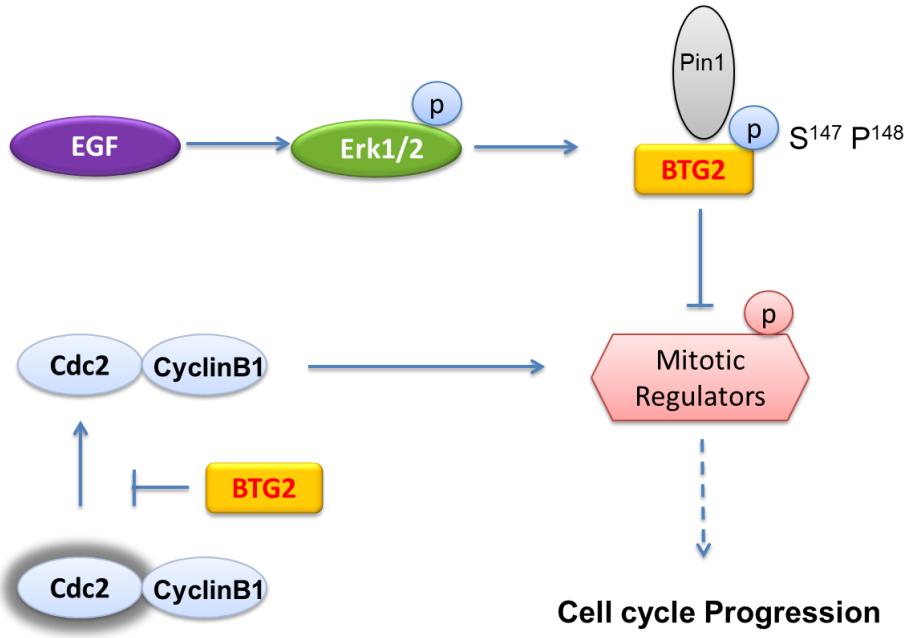

Figure 15. Overexpression of BTG2 causes cell death via arrested G2/M phase in p53 null cells

Binding of CCR4-Associated Factor 1 (CAF1) to BTG2 induces poly (A) degradation which requires Caf1 nuclease activity and deadenylase activities of Caf1 and its CCR4 partner for

efficient deadenylation in mammalian cells (81, 82). This is the major pathway of mRNA turnover in eukaryotes which mediates the initiation of shortening of the poly (A) tail.

MATERIAL and METHODS

1. Cell Culture

Derivation and culture of SV40-immortalized lines of human epidermal keratinocytes from keratinocyte primary cultures have been described previously (Ian Freshney (1996) Culture of Immortalized Cells p95-120 (A John Wiley &Sons, Inc. Press, New York)). Immortalization and expression of various markers of SV40-induced transformation in vitro has been extensively characterized(83). Cell lines were routinely passaged at a split ratio of 1:3 in Dulbecco's Minimal Essential Medium (DMEM; Life Technologies/GIBCO, Grand Island, NY) supplemented with 10% fetal calf serum, and hydrocortisone (0.5µg/ml). Bacteriophage libraries (see below) were created from both cell lines 22 and 130 at serial passages greater than 111 and 141. However, for the gene silencing experiments described line 130 cells were employed as previous Southern blot analyses had indicated that the viral sequences in this cell line were present in low copy number and appeared to be contained within a single Xba I restriction fragment(84).

Normal human epidermal keratinocytes (NHEK), (Lonza, Walkersville, MD) were grown in EpiLife medium supplemented with human keratinocyte growth supplement and penicillin-streptomicin-amphotericin B (Invitrogen), and incubated at 37°C under a humidified atmosphere of 5% CO_2.

2. Preparation of genomic DNA for sequence analysis of viral integrants

Genomic DNA was prepared for use either to be used as a template for the polymerase chain reaction (PCR) or for the creation of lambda phage genomic libraries. For PCR, genomic templates were prepared using a spin column-based kit (DNeasy; Qiagen, Valencia, CA). For large scale preparation of highly purified native DNA to be used for phage libraries, a phenol extraction procedure was used.

3. Preparation of high molecular weight genomic DNA by phenol-chloroform extraction

The extraction of cells grown in T75 cell culture flasks was initiated by pouring off the growth medium and rinsing the cell monolayer with 1x phosphate buffered saline (PBS; 137 mM NaCl, 2.7 mM KCl, 10 mM Na_2HPO_4, 2 mM KH_2PO_4, pH 7.4) twice followed by the addition of 5 ml of extraction buffer, (100 mM Tris-HCl, pH 7.9; 10 mM EDTA, 10 mM NaCl, and 0.5% sodium dodecyl sulfate (SDS)) containing 0.5 mg of proteinase K. The slurry was incubated at 37°C overnight and then extracted with phenol-chloroform. The flasks were scraped gently and the DNA mixture was placed into a 50 ml conical centrifuge tube(s). Equal volumes of phenol/chloroform-isoamyl alcohol, (24:1), in a ratio of 1:1 were then added to each tube. The tubes were then placed on a rotator and mixed gently for 10 minutes. The tubes were then centrifuged at 3,000 rpm in a tabletop centrifuge for 10 minutes. The aqueous upper phase was removed with a pipette and saved for phenol extraction; care was taken not to suction the white precipitate at the phase interface. The last steps starting with the phenol/chloroform-alcohol extraction were repeated. Two volumes of 95% ethanol were added to the saved aqueous phase and after gentle agitation it was placed at -70°C for 30 minutes. Precipitated DNA was pelleted by centrifugation for 10 minutes at 3,000 rpm on a tabletop centrifuge. The supernatant was poured off and the pellet was washed twice by centrifugation in 70% ethanol. The DNA pellet was then dried for 15 minutes under vacuum. Two ml of TE buffer was added to the dried

residue and DNA was dissolved at 37°C during overnight incubation. RNase A stock solution (10 mg/ml) was added to a final concentration of 10 µg/ml. Phenol/chloroform extraction followed by ethanol precipitation as described above was performed twice. The air dried pellet resulting from this extraction step was then dissolved in 0.5 ml of TE buffer at 37°C overnight. The DNA suspension was then dialyzed extensively (sample volume to dialysant volume ratio 1:2000) over a period of 3 days against several changes of TE buffer at 4°C to remove residual phenol. The purity of the DNA was checked by comparison of absorption at 260 and 280 nm. A value of 0.5 (OD_{280}/OD_{260}) considered to represent highly purified DNA.

4. RNA isolation and cDNA synthesis

4.1 Extraction of Total RNA

Cellular RNA was extracted from 1 $x10^6$ to 3 x 10^6 cells by RNeasy Mini kit (Qiagen, Valencia, CA) according to the manufacturer's instructions. Total RNA integrity was verified by visualization of well-defined ribosomal 28S and 18S RNA bands in 1% ethidium bromide-stained agraose gel. The concentration of total RNA was determined using a Nanodrop Spectrophotometer ND-1000 (NanoDrop Technologies, Inc. Wilmington DE, USA.) Nucleic acid purity was determined by the ratio of absorbances at 260 and 280nm. A ratio of 2.0 is generally accepted as "pure" for RNA. A second nucleic ratio measurement was taken at 260 and 230nm. At these wavelengths a ratio of 1.8-2.2 is accepted as pure.

4.2 Reverse transcription (RT) reaction

cDNA synthesis was carried out by reverse transcription an oligo dT primer, reverse transcriptase, dNTPs and buffer provided in a Protoscript First Strand cDNA Synthesis Kit (New England BioLabs) in a 20 µl reaction mixture with 2µg of total RNA as template.

5. Synthesis of siRNAs

We designed silencing RNA oligonucleotides (siRNAs) targeting sequences within the SV40 early gene region (nt 5163-2691). Complementary siRNA strands for 3 different siRNAs were synthesized (Stealth RNAi; Invitrogen, Carlsbad, CA). The sequence of a non-silencing oligonucleotide (E03) was chosen by Invitrogen technical services constrained only by the requirement of lack of homology to either the virus or any known human gene. This oligo was used as a control in the experiments described.

Table 1. siRNA oligonucleotides

RNA oligonucleotide	Nucleotide sequence (upper strand)	SV40 early gene nucleotides
E01	GAGGCUACUGCUGACUCUCAACAUU	4475-4451 (exon 2)
E03	GAGAUUCCGGUCACUCUAACCGAUU	NA
E05	GAACUCUUGCUUGCUUUGCUAUUUA	4357-4333 (exon 2)
D11	GAGAGGAAUCUUUGCAGCUAAUGGA	5144-5120 (exon 1)

5.1 Stealth RNAi Transfection using Lipofectomine™; determination of transfection efficiency using a fluorescent oligonucleotide probe

Block-It™ fluorescent oligo (Invitrogen) was used to test for RNA oligonucleotide transfection efficiency. One day before transfection, the cells were plated in a cell culture tray containing glass cover slide. When the cells reach 50-70% confluence, the fluorescent oligomer was

transfected into cell by Lipofectamine-2000 (Invitrogen). The plates were further incubated at 37^{o}C in a CO_2 incubator for 6 to 24 hours post-transfection. The glass cover slide was washed with 1x PBS buffer three times and then cells were fixed with ice cold 70% acetone 30% methanol. The fluorescent signal can be detected by Fluorescence microscopy.

5.2 Transfection of Stealth RNAi into 130 cells

Once efficient transfection of 130 cells was established we employed the same procedure is used to optimize transfection. Here transfection was carried out essentially as described for the preliminary experiments to determine transfection efficiency using the fluorescent probe except that we tested the effects of varying amounts of siRNA on silencing activity of SV40 T antigen. Cells were cultured to a density of $3 \text{ X } 10^5$ cells per well. One day before transfection, cells were cultured in Dulbecco's modified minimal essential medium (DMEM) in 24-well plates. Twenty-four hours after incubation, cells were 50-70% confluent (approximately $3x10^5$ cells per well). We then washed the cells with Opti-MEM reduced serum medium x3, and then added different volumes of Lipofectamine 2000 in a well containing Opti-MEM reduced serum medium. Triplicate sets containing 0.0, 0.5, 1.0, 1.5, 2.0 and 2.5µl of Lipofectamine-siRNA suspensions were made and mixed on a rocking plate. The cells were incubated at 37^{o}C in a 5% CO_2 incubator. Every twenty four hours for a total of three days the medium was changed and then the cells were collected and examined for T antigen expression by western blotting**.**

6. Determination of cell viability after transfection

Cells were transfected with varying amounts of lipofectamine-oligonucleotide as described above and then tested for viability by trypan blue dye exclusion. When the cells were confluent,

the medium was removed via aspiration and the cells were washed with 2 ml of 1xPBS and aspirated again. Eight hundred microliters of trypsin/EDTA was added to cover the monolayer of cells. Each plate was then incubated for a few minutes at 37^{o}C after which the cells are removed and checked under a microscope to ensure that all the cells were dislodged. The collected cells were then centrifuged in a tabletop centrifuge at 2000 rpm for 5 minutes, collected and diluted in 0.1 ml of medium without serum. Two tenths mililiter of 0.4% trypan blue stain was added and the cells were left standing for 5 min at room temperature. A hemocytometer was used to determine the fraction of viable cells as unstained/total cell number.

7. Cloning of a segment of the SV40 early gene region for absolute quantitation of LT gene expression

For our initial experiments where real time PCR was used to quantitate silencing of the SV40 early genes we created a plasmid containing a segment of the SV40 early gene region to derive a standard curve for absolute quantitation of LT gene expression. For this purpose cDNA templates were prepared from line 130. Then SV40 sequences within the LT segment targeted by our siRNAs were amplified by standard PCR using primers QSV63 (nt 4403→ 4422) and QSV79 (nt 5040→ 5017) and Expand Taq polymerase (Expand High Fidelity PCR System; Roche Applied Science). The PCR product was run on a 2% agarose gel and the expected 292 bp band was excised from the gel and extracted using the Q1Aquick gel extraction kit (Qiagen, Germany). The PCR product was sequenced to confirm its identity and then cloned into the T vector PCR 2.1-TOPO supplied in a T vector cloning kit (TOPO XL; Invitrogen). For creation of standards to be used for real-time PCR, the recombinant plasmid was isolated from bacteria using QIAprep Miniprep kit (Qiagen, Germany). Absorbance of the extracted plasmid DNA at

260 nm determined using a Nanodrop Spectrophotometer ND-1000 (Thermo Scientific, Wilmington, Delaware). Nucleic acid purity was measured by A_{260}/A_{280}. According to the absorbance of each solution, we calculated the plasmid copy numbers based on the conversion: absorbance at 260nm x 50 (DNA**) =** µg/ml of DNA (or µg/ml of DNA x dilution factor = original concentration as µg/ml of DNA). Then the copy number/µl = 6.02 x 10^{17} x original conc./MW (330) of each nucleotide x bps x 2 (for double stranded DNA) taking into account 3931 bp for the vector sequences. The stock standard solution was diluted to make standards with copies /µl= 10, 10^2, 10^3, 10^4, 10^5,10^6 and 10^8.

8. Stable Expression of an SV40-specific Interference RNA (RNAi) using a microRNA (miRNA)

8.1 Design of the Engineered Pre-miRNA

For long term expression of silencing RNAs we designed oligonucleotides for expression using Invitrogen's pcDNA™6.2-GW/miR plasmid (figure 11) using RNAi Designer (www.invitrogen.com/rnai), an online tool. Three target sequences were selected using Simian virus 40 strain776 complete genome:

Start at SV40 nucleotide 5028: CTTTATCAGGATGAAACTCCT
Start at SV40 nucleotide 4924: TGCATCCCAGAAGCCTCCAAA
Start at SV40 nucleotide 4762: CACAAGTGGATCTTTCCTGTA

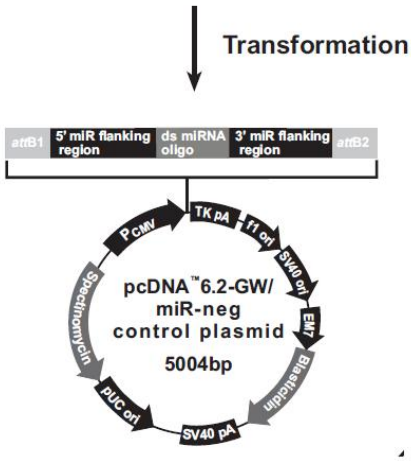

- Explanation of Features of pcDNA™6.2-GW/miR Explanation of Features
- pcDNA™6.2-GW/miR vectors contain the following elements.
- miRNA forward sequencing primer site
- CMV promoter
- *att* B1 site
- 5'miR flanking region
- 5' overhang
- 3' miR flanking region
- *att*B2 site
- miRNA reverse sequencing primer site
- TK polyadenylation signal
- Fi origin
- SV40 early promoter and origin
- EM7 promoter
- Balsticidin resistance gene
- SV40 polyadenylation signal
- pUC origin
- Spectinomycin resistance gene
- Spectinomycin promoter

Figure 16. miRNA 1 Block-IT MIR RNA expression vector kit k4935-00 (Invitrogen)

8.2 Generation of double-stranded (ds) oligos

Using synthetic siRNA for RNAi analysis in mammalian cells is limited by their transient nature; the use of shRNA vectors for RNAi analysis requires the screening of large number of sequences to identify active sequences and the use of Pol II promoters limits application such as tissue-specific expression. In order to overcome the limitations of siRNA and shRNA, we tested an approach employing an miRNA for long term silencing of the integrated virus in line 130 keratinocytes. The pcDNA6.2-GW/miR expression vectors (Invitrogen Inc.) are able to express engineered miRNA sequences from PolII promoters and facilitate the generation of an expression clone containing a double stranded oligo encoding a pre-miRNA sequence. All features have been functionally tested and the vectors have been fully sequenced. As a result that expression construct can be introduced into mammalian cells by transfection and stable transfectants can be generated. Complementary DNA oligos with each containing 4 nucleotide overhangs necessary for directional cloning were designed and synthesized:

af316139.1_4762_top
TGCTGTACAGGAAAGATCCACTTGTGGTTTTGGCCACTGACTGACCACAAGTGTCTT
TCCTGTA

af316139.1_4762_bottom
CCTGTACAGGAAAGACACTTGTGGTCAGTCAGTGGCCAAAACCACAAGTGGATCTTT
CCTGTAC

af316139.1_4924_top
TGCTGTTTGGAGGCTTCTGGGATGCAGTTTTGGCCACTGACTGACTGCATCCCAAGC
CTCCAAA

af316139.1_4924_bottom
CCTGTTTGGAGGCTTGGGATGCAGTCAGTCAGTGGCCAAAACTGCATCCCAGAAGCC
TCCAAAC

af316139.1_5028_top
TGCTGAGGAGTTTCATCCTGATAAAGGTTTTGGCCACTGACTGACCTTTATCAATGA
AACTCCT

af316139.1_5028_bottom
CCTGAGGAGTTTCATTGATAAAGGTCAGTCAGTGGCCAAAACCTTTATCAGGATGAA
ACTCCTC

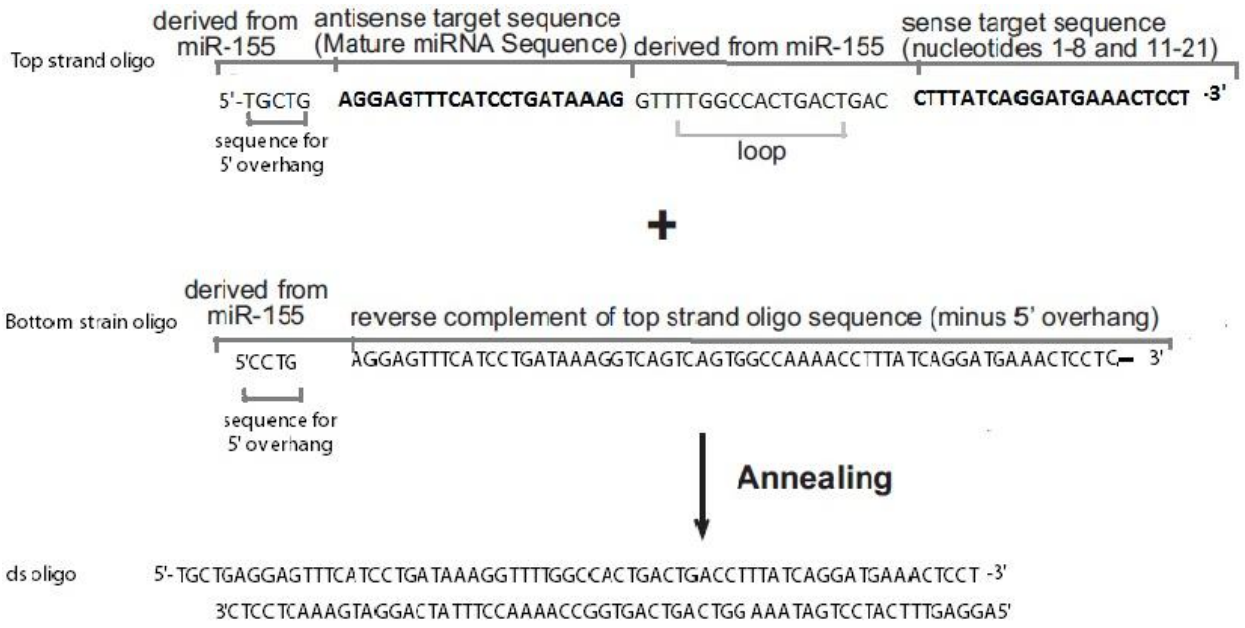

Figure 17. The diagram illustrates the required features of top strand and bottom strand single-stranded oligos. The example of starting at SV40 nucleotide 5028 miRNA lists the sequences of top and bottom strand oligos encoding an miRNA targeting Large T antigen gene

Five microliters of 200 µM each top and bottom strand DNA oligo were mixed with oligo annealing buffer (Invitrogen) incubated at 95^{o}C for 4 minutes, then cool to room temperature. The concentration of ds oligo was 50µM as a stock solution. The stock solution of ds oligo was diluted to 500nM with DNase/RNase-free water, and finally diluted to 10 nM with annealing buffer (Invitrogen). The annealing reactions of the negative control, the positive control (the miR-lacZ positive double-stranded oligo) and the miRNA sample were performed by the same assay.

8.3 Cloning the ds oligo into an expression vector

4 µl 5x Ligation buffer, 2 µl pcDNA 6.2-GW/miR, linearized (5ng/µl), 4 µl of 10nM double-stranded ds oligo of interest and 9 µl of DNase/RNase-Free were mixed in a 0.5 ml microfuge tube and 1 µl of T4 DNA ligase (1U/µl) was added. After 5 minutes incubation at room temperature, it was stored on ice.

8.4 Transformation of the ligation mixture into competent *E.Coli* cells

Two microliters of the ligation reaction was added into One Shot TOP 10 chemically competent *E.Coli*, and then incubated on ice for 30 minutes. The cells were heat-shocked for 30 seconds at 42^{o}C and then immediately transferred to ice. To the tubes 250 µl S.O.C medium was added and the tubes were shaken on a horizontal shaker (200 rpm) at 37^{o}C for one hour. Various volumes of each transformation sample were spread on LB agar plates containing 50 µg/ ml spectinomycin. The plates were incubated overnight at 37^{o}C. pUC 19 was used as a positive control was spread on an LB plate containing 100 µg/ml ampicillin. The spectinomycin-resistant colonies were picked and cultured at 37^{o}C on a shaker overnight in LB medium containing 50µg/ml spectinomycin. The plasmid DNAs were isolated with DNA purification kit (Promega). Sequencing of each pcDNA6.2-GW/miR expression construct was carried out to confirm the identity of each construct by miRNA forward (5'TCCCAAGCTGGCTAGTTAAG3') and reverse (5'CTCTAGATCAACCACTTTGT 3') sequencing primers.

8.5 Transfection of miR plasmids into 130 cells: selection of stable transfectants

Line 130 keratinocytes were transfected with the miR plasmids using lipofectamine 2000 as described above. Stable transfectants were selected in blasticidin, a selectable marker carried on

6.2-GW/miR (Figure 16). To determine the minimum concentration of blasticidin required for selection, DMEM medium was replaced by culture medium containing varying concentrations of blasticidin (0, 2, 4, 6, 8 and 10 µg/ ml). The selection medium was replenished every 3-4 days and the percentage of surviving cells was observed. The minimum concentration of blasticidin was determined within 14 days. By then, only blasticidin-resistant cells were selected. Clonal populations were derived by an end-point dilution process carried out immediately following antibiotic selection. In order to get colonies derived from single cells, the antibiotic-selected cells were diluted several times and replated into 24-well plates. Wells containing single cells were noted and grown to 70-90% confluence after which the cells were harvested for analysis of LT expression. Levels of LT mRNA in clonal populations were determined by RT-PCR.

9. Quantitation of gene expression by real time PCR

Relative quantification (RQ) of gene expression was carried out by real time PCR in an RealPlex 2 real-time thermal cycler (Eppendorf, Hauppage, NY). The Primer Bank of Massachusetts General Hospital (MGH) was used as a source of gene-specific primers (http://pga.mgh.harvard.edu/primerbank/) and the selected primers were synthesized at the MGH DNA synthesis core facility (table 2). For the gene expression studies, cDNA templates were synthesized from total RNA derived from the siRNA transfected 130 cells and a SYBR green PCR master mix from Applied Biosystems, Carlsbad, CA) was used to complete the reaction mixture. We also used pathway specific qPCR arrays from SABiosciences/Qiagen) which were supplied in a 96 well PCR plate format with gene specific primers distributed in each well. Relative changes in gene expression were compared with housekeeping gene expression using primers for either actin or GAPDH:

ActinF (FZ-1) ACACTGTGCCCATCTACGAGG

ActinR (FZ-2) AGGGGCCGGACTCGTCATACT

GAPDHF CTCAGACACCATGGGGAAGGTGA

GAPDHR ATGATCTTGAGGCTGTTGTCATA

RQ values were calculated from the Ct values ($RQ = 2^{-Ct}$) and normalized to undeleted genomes (RQ_{del}/RQ_{total}). Data analysis was performed using the web-based PCR array data analysis software (http://www.sabiosciences.com/pcr/arrayanalysis.php).

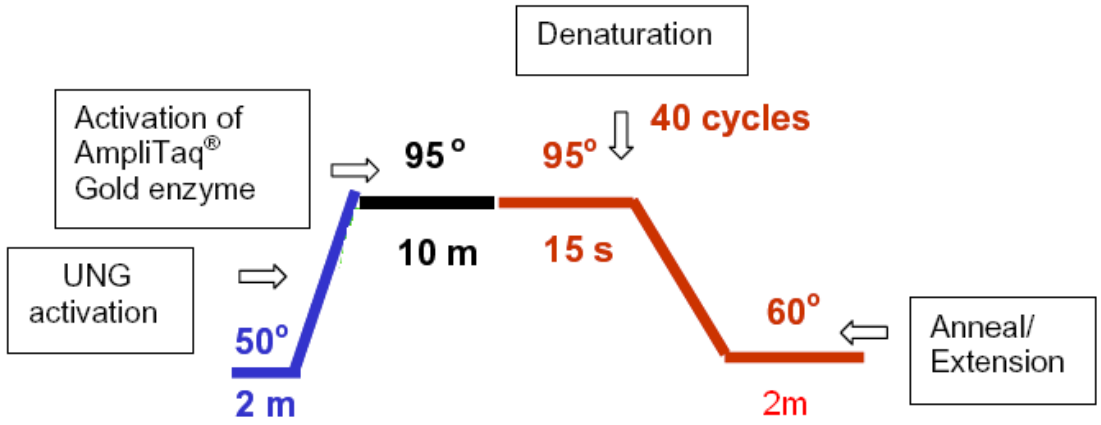

Figure 18. Real Time-PCR operating parameters

Table 2. Gene specific primers for Real Time-PCR

Transformation Related Gene	Forward primer	Reverse primer
CCND1	5'GAACAAACAGATCATCCGCAAAC3'	5'GCGGTAGTAGGACAGGAAGTTG3'
EGF	5'TGGATGTGCTTGATAAGCGG3'	5'TGTCCTTTCCAGTGTGTTTGTTG3'
PRMT1	5'CCACCTTGGCTAATGGGATGA3'	5'AGTGTGCGTAGGAGTCAAAGT3'
HOXB9	5'AGTGTGCGTAGGAGTCAAAGT3'	5'ACGCCCGAGTACAGTTTGG3'
Caf1	5'GTTCCCGAGAGGAGGAAGTTT3'	5'TGAGTGCCGTCTTCTTATTCCA3'
TGF	5'GCCAGCCCAAAAAGTGTGC3'	5'CAGTTGAGGGACACCTGTCTC3'
E2F3	5'GCAGCCTCCTCTACACCAC3'	5'AGGTACTGATGACCGCTTTCT3'
SOX17	5'GTGGACCGCACGGAATTTG3'	5'GAGGCCCATCTCAGGCTTG3'
WNT1	5'CAACCGAGGCTGTCGAGAAA3'	5'GTGCAGGATTCGATGGAACCT3'
FRZB	5'ACCCCTGTAAGTCTGTGTGC3'	5'CCCTGTCGTACACTGGCAG3'
HTERT	5'TGACACCTCACCTCACCCAC3'	5'CACTGTCTTCCGCAAGTTCAC3'

Myc	5’ACCACCAGCAGCGACTCTGA3’	5’TCCAGCAGAAGGTGATCCAGACT3’
GAPDH	5’CTCAGACACCATGGGGAAGGTGA3’	5’ATGATCTTGAGGCTGTTGTCATA3’
CD13	5’CTGGCATTTTGGAGAGGAAG3’	5’CCCTCGGTGTCCTACTTCAA3’
BTG2	5’CAGAGCACTACAAACACCACTG3’	5’CTGAGTCCGATCTGGCTGG3’
CDKN1A	5’CCTGTCACTGTCTTGTACCCT3’	5’GCGTTTGGAGTGGTAGAAATCT3’
MDM2	5’AGCCTGGCTCTGTGTGTAATA3’	5’CCTGATCCAACCAATCACCTGA3’
FAS	5’TATCACCACTATTGCTGGAGTCA3’	5’ACGAAGCAGTTGAACTTTCTGTT3’
TNFSF10	5’TGCGTGCTGATCGTGATCTTC3’	5’GGGGTCCCAATAACTGTCATCTT3’
TRAF4	5’GGTGCCCTAAGCTGGCAAT3’	5’GGCTGAAGCACTCAAGGTTG3’
GADD45A	5’GAGAGCAGAAGACCGAAAGGA3’	5’CACAACACCACGTTATCGGG3’
BIK	5’AGACCCTCCTGTATGAGCAG3’	5’GCATTCCAAAGAATCGAAGTCCT3’
CASP10	5’GAGGCTGACTTCCTACTTGGT3’	5’GCCCCTGATTTCCATTGTCTTT3’
CASP8	5’AGAGCCAGGGTGGTTATTGAA3’	5’GCAGTCTCCGAGTCCCCTA3’
CD70	5’CACTTGGGTGGGACGTAGC3’	5’CTGGTCCATGCAGGAAGGAG3’
APAF1	5’TGTCTGTCACCAGGGTACAGT3’	5’CGTTGTGGCCCCTCAATTCA3’
TP53	5’TGCTGTCCCCGGACGATATT3’	5’GTAGCTGCCCTGGTAGGTT3’
CFLAR	5’CTCTTTTTGTGCCGGGATGTT3’	5’GGTCAAATCGCCTCACTCTGT3’
PKNOX1	5’ATAGACAGCTATCAAGATGGGCA3’	5’AAATGGCCTGCTTGTCCACAT3’
Senescence genes		
Rb1	5’GCCTCTCGTCAGGCTTGAG3’	5’TCATCTAGGTCAACTCGTGCAA3’
RBL2	5’TCTCTCAAGGTGTCTGAACGC3’	5’GAGTCACACAAGGGCTATTCTC3’
ABL1	5’GCCCTGCATTTTATCAAAGGAGC3	5’CGAGCGGCTTCACTCAGAC3’
AKT1	5’GTGGACCAACGTGAGGCTC3’	5’GAAGGTGCGTTCGATGACAG3’
ALDH1A3	5’GCCCTGGAGACGATGGATAC3’	5’CCCTGGATTTTGTCTGCCC3’
CCNA2	5’CGCTGGCGGTACTGAAGTC3’	5’AAGGAGGAACGGTGACATGC3’
CDC25C	5’CCCGTCGATGCCAGAGAAC3’	5’CCCTGGTTAGAATCTTCCTCCA3’
CDKN1C	5’ACATCCACGATGGAGCGTC3’	5’GGAAGTCGTAATCCCAGCGG3’
CDKN2C	5’GGAAATCCCGAGATTGCCAGG3’	5’CAGCAAAGTCTGTAAAGTGTCCA3’
CITED2	5’GGGCGAGCACATACACTACG3’	5’ACCCATGAACTGGGAGTTGTTA3’
CREG1	5’GTGCCCTATTTCTACCTGAGCC3’	5’AGCATTATGTGAACACAAAGGGG3’
GSK3B	5’ATTTCCAGGGGATAGTGGTGT3’	5’TCCTGACGAATCCTTAGTCCAAG3’
ID1	5’ACGAGCAGCAGGTAAACGTG3’	5’GAAGGTCCCTGATGTAGTCGAT3’
IGF1R	5’AGGATATTGGGCTTTACAACCTG3’	5’GGCTTATTCCCCACAATGTAGTT3’
IGFBP3	5’TCTGCGTCAACGCTAGTGC3’	5’GCTCTGAGACTCGTAGTCAACT3’
ING1	5’CGGGCCTAGCGCAATAACT3’	5’GACCCGAAGACGTTCAAATCAA3’
MAP2K6	5’CTCTCGGTCAAGTGAAGATGTG3’	5’ACACTGTATCCCTTCTGGTTGAG3’

MAPK14	5’TGCCGAAGATGAACTTTGCGA3’	5’TCATAGGTCAGGCTTTTCCACT3’
MORC3	5’ATTCACCGACAATGGGAATGG3’	5’CGCATAGAACCCGACTTGAAG3’
PCNA	5’TCCCACGTCTCTTTGGTGC3’	5’TCTTCGGCCCTTAGTGTAATGAT3’
PIK3CA	5’ACCAGTAGGCAACCGTGAAG3’	5’TGGCGGATAGACATACATTGCT3’
PLAU	5’TCAAAAACCTGCTATGAGGGGA3’	5’GGGCATGGTACGTTTGCTG3’
RBL1	5’ATCCGAGGCAACTACAGCCTA3’	5’CCTTTCCAACCGTGGGAATAAT3’
SERPINB2	5’CAGCACCGAAGACCAGATGG3’	5’CCTGCAAAATCGCATCAGGATAA3’
SERPINE1	5’ATTCAAGCAGCTATGGGATTCAA3’	5’CTGGACGAAGATCGCGTCTG3’
SIRT1	5’CGCTGGCCGACAACTTGTA3’	5’CATGTGAGGCTCTATCCTCCT3’
SPARC	5’AGCACCCCATTGACGGGTA3’	5’GGTCACAGGTCTCGAAAAAGC3’
TGFB1	5’GGCCAGATCCTGTCCAAGC3’	5’GTGGGTTTCCACCATTAGCAC3’
HRAS	5’ACAACACCAAGTCTTTTGAGGAC3’	5’GCCTGCCGAGATTCCACAG3’
MAP2K1	5’CAATGGCGGTGTGGTGTTC3’	5’AGCTCCCTTATGATCTGGTTCC3’
MAP2K3	5’ATTGATGTCAAGGGATAGCCAGA3’	5’GTGATGAAGGTCCGGGAGT3’
NBN	5’TCTGTAACCAACCTGAGTCAAAC3’	5’TCAAAGTTCGGGAAAAGCCATT3’
TERF2	5’AGGCAGCTACGGAATCCTC3’	5’GGGCTGAACTTTCGTTTTCATCT3’
TERT	5’AACCTTCCTCAGCTATGCCC3’	5’GCGTGAAACCTGTACGCCT3’
TP53BP1	5’CTCCAGACGCACAAAGAAAATCC3’	5’GACCTGACTGATGGAACCACA3’
CALR	5’CCCGCCGTCTACTTCAAGG3’	5’GAACTTGCCGGAACTGAGAAC3’
TBX2	5’CATCTGCGCTCCCTCAAGAG3’	5’CGTGCCTAGCTTGTGGAACT3’
TBX3	5’TAAGGCCGACCCCGAAATG3’	5’CACTTGGGAAGGCCAAAGTAAAT3’
GLB1	5’CGCCATCCAGACGTATGTG3’	5’CATGAGCCAGCCGAAGAAAAT3’
TWIST1	5’GTCCGCAGTCTTACGAGGAG3’	5’GTCCGCAGTCTTACGAGGAG3’
PKNOX1-711	5’CAGATTCAAAGTGCCATCACA3’	5’GCGACAATGTCTGTGTGACC3’

10. Cloning of Integrated SV40 Sequences from Genomic Libraries Using the Lambda Bacteriophage Vector λGEM11

10.1 Restriction digestion of the genomic DNA

For purposes of cloning restriction fragments containing integrated SV40 virus, genomic DNA was cut with Xba I, an enzyme without cut sites in SV40 DNA. It was therefore anticipated that any SV40-bearing Xba I restriction fragments would contain integrated virus with the human DNA flanking the viral integration site. A typical restriction digest was carried out anywhere

from 2-8 hrs. at 100 units of enzyme per 1 microgram of genomic DNA. The restriction digests were checked for completion by agarose gel electrophoresis. The restriction digest was heated for 10 minutes at 70°C to inactivate the restriction enzyme prior to ligation to the bacteriophage arms.Ligation of restriction fragments to the Lambda bacteriophage arms and in vitro packaging of the recombinant DNA For genomic libraries the bacteriophage vector lambda GEM-11 (Promega, Madison, WI) was used (figure 19). For the creation of recombinant bacteriophage Xba I digested bacteriophage DNA was mixed with the Xba I digested genomic DNA in a ratio of 1:3 (genomic DNA; GEM 11 DNA) and ligated overnight at 15°C using 10 units of T4 ligase (New England Biolabs, Ipswich, MA) and buffer supplied by the manufacturer. Ligation was monitored by running aliquots of the ligation mixture (ligated sample as compared to unligated) on an agarose gel. A typical ligation reaction contained about 1 µg of DNA in a total volume of 10 µl. For *in vitro* packaging of the recombinant DNA 4 µL of the ligation mix was mixed with 100 µl of packaging extract (Gigapack, Stratagene, La Jolla, CA) and incubated at 22°C for 90 minutes after which 400 µl of suspension medium (SM; per liter: 0.1 M NaCl, 10 mM $MgSO_4$, 50 mM Tris-Cl (pH 7.5), 0.1% gelatin) was added. Two hundred microliters of chloroform was added to the packaging mixture which was then vortexed and stored at 4°C.

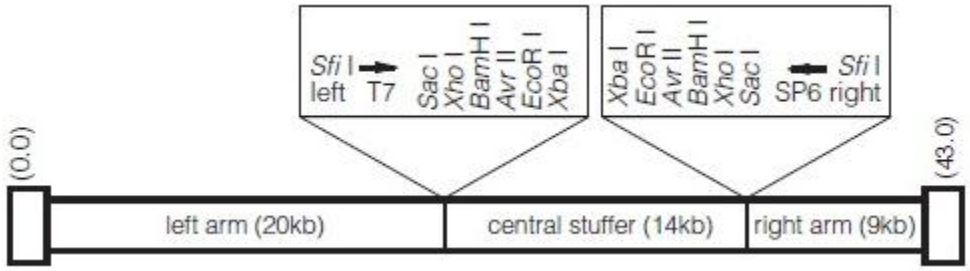

Figure 19. Schematic line map of Lambda GEM-11 genomic cloning vector (promega)

10.2 Bacterial culture

For growth of bacteriophage E. Coli host bacterial strains NM538 and NM539 (Promega, Madison, WI) were used. NM538 grows both the wild type and recombinant bacteriophage while NM539 which carries a lambda prophage and therefore expressed the spi+ phenotype, grows only the recombinant bacteriophage. Bacteria were grown to stationary phase in overnight culture in NZCYM bacterial growth medium, (10 g NZ amine (Difco; Becton-Dickinson, Franklin Lakes, NJ), 5g NaCl, 5g yeast extract (Difco; Becton-Dickinson, Franklin Lakes, NJ), 2g $MgSO_4 \cdot 7H_2O$ (pH 7.5) per liter). The bacteria were recovered by centrifugation and then re-suspended in 0.4 volumes of sterile 10 mM $MgSO_4$ and stored at 4°C. The bacterial suspension was viable for a period of up to 14 days.

10.3 Library screening for recombinant bacteriophage containing SV40 sequences

10.3.1 Plaque assay for determining bacteriophage titer

For determination of bacteriophage titer, various amounts of the bacteriophage suspension resulting either from packaging of recombinant genomes *in vitro* or from isolates derived from screening (described below) were mixed with 200 µl of NM539 bacterial host suspension and incubated for 15 minutes at 37°C to allow adsorption of bacteriophage to the bacterial host. This mixture was then suspended in 3 ml of 0.7% bacterial agar in NZCYM medium (top agar) and the top agar was spread evenly on top of a layer of bottom agar (1.5% bacterial agar in NZCYM medium) in plastic petri dishes and then incubated overnight at 37°C. In the morning plaques which were clearly visible within the top agar were counted to give a measure of the titer of the original bacteriophage inoculum.

10.3.2 Screening libraries for recombinant bacteriophage containing SV40-bearing inserts

For screening of libraries approximately 10,000 plaque forming units (PFU) of recombinant bacteriophage were plated onto NM539 host in 150 mm petri dishes essentially as described for plaque assay. To transfer the clear plaques which were produced overnight the following procedure was used. The plates were placed on a flat surface. A sterile nitrocellulose filter marked with a pencil was placed on top of the plaque-containing top agar layer. The filter's position was marked by making 3 asymmetrically placed holes using a 18 gauge needle and then the plate was marked with a pen at the positions corresponding to the holes on the filter. After the plaques were completely blotted onto the filter as indicated by uniform wetting, the filter was peeled off using a pair of forceps. Several pieces of Whatman 3 MM paper were cut so that the nitrocellulose filters would fit and have about one inch between each filter and then saturated with denaturing solution, (0.5 M NaOH and 1.5 M NaCl). Each nitrocellulose filter was placed onto the denaturant-saturated 3 MM paper and then left for 5 minutes at room temperature to denature the bacteriophage DNA present in the adherent bacteriophage. The nitorocellulose filters were then transferred to a second 3 MM sheet of paper that had been saturated with neutralizing solution, (1.5 M NaCl, 0.5 M Tris-HCl pH 8.0). This was allowed to stand for 5 minutes at room temperature after which they were transferred to a dry 3 MM paper and allowed to dry at room temperature for 30 to 60 minutes. After the drying period another two pieces of 3 MM Whatman paper was used to sandwich each filter. The filters were then baked for 2 hours at 80°C in a vacuum oven.

10.3.3 Hybridization Procedure

SV40 DNA probes were prepared with 3µl each of ^{32}P-labeled dATP, dGTP, dTTP and dCTP (10 mCi/ml; 3000 Ci/mmole). The reaction mixture was created by the addition of 1µl of SV40 DNA (1 µg/µl), 2 µl of nick translation buffer (500 mM tris-HCl, pH 7.5), and 2µl of H_2O. The reaction mixture was preincubated for 10 minutes at 37 °C followed by the addition of 2 µl of DNA polymerase (Pol I, 1 U/µl; Roche Diagnostics, Indianapolis, IN) and 1 µl of DNase I stock solution (0.1 µg/ml). The probe was then incubated in a 15°C water bath for a period of one hour after which 10 µl of EDTA (500 mM, pH 8.0) was added and mixed, then placed in a 68°C water bath for 15 minutes followed by the addition of 400 µL of TE buffer. The nitrocellulose filters were then placed in a prehybridization solution of the following composition (per 10 ml):

Formamide	5 ml
2% polyvinypyrrolidone, (PVP).	0.5 ml
2% ficoll	0.5 ml
20X SSPE*	2.5 ml
2% Bovine Serum Albumin (BSA).	0.5 ml
100 µg/ml non-specific DNA	0.2 ml
H_2O	0.8 ml

*per liter: 175.3g NaC , 27.6g NaH_2PO_4, 9.4g EDTA, pH 7.4

Filters underwent prehybridization for 1 hour at 42°C after which radiolabeled SV40 probe was added and hybridization was carried out overnight at 42°C. After hybridization the filters were washed twice in a solution of 0.1% sodium dodecyl sulfate and 0.1 X SSC (0.1 X SSC is prepared from a stock solution of 20 X SSC which contains 178.3 g of NaCl and 88.2 g of sodium citrate, pH 7.0 per liter), 20 minutes at 50 °C. Finally the filters were washed in 0.1 X SSC for another 20 minutes at 50°C. The filters were then ready for autoradiography. For autoradiography the filters were taped onto 3 MM paper, covered with clear plastic wrap and placed in an x-ray film cassette for 24 hours (or longer as needed) at -70°C. The exposed x-ray

films were then developed in Kodak x-ray developer the positive signals were aligned with the original plates for determination of the location of the probe-hybridizing plaques.

Figure 20. Plaques image of Southern blotting

The positive plaques were recovered by excision of the agar plug containing the target plaque(s) in a sterile environment. The bacteriophage on the agar plugs were eluted in 500 µl of sterile SM. The eluted bacteriophage were replated at low multiplicity of infection (MOI) and rescreened several times until isolation of pure clones was achieved as demonstrated by the hybridization of probe to 100% of the PFU plated.

10.3.4 Isolation of recombinant bacteriophage

Recombinant bacteriophage grown in small scale culture was incubated in 5 ml of NM539 bacterial host (prepared as described above) for 10 minutes at 37°C. The lysate was then added to fresh NZCYM medium and placed in a shaker overnight. This mix was then poured into 500 ml of sterile NZCYM medium and allowed to incubate at 37°C overnight. To the lysed bacterial suspension were added 10 ml of chloroform; the mixture was vortexed and allowed to stand for 10 minutes at room temperature after which the mix was centrifuge at 8,000xg at 4°C for 10

minutes. The aqueous phase was decanted and filtered through cheese cloth. The pellet containing bacterial debris and chloroform were then discarded. To the bacteriophage suspension RNase and DNase were added to a final concentration of 10 mg/ml and incubated at 37°C for 1 hour. For each 500 ml of bacteriophage 29.2 g of NaCl and 50g of polyethylene glycol (PEG 8000) were added and dissolved at room temperature. The preparation was then placed in ice for 1 hour to precipitate the bacteriophage. The precipitate was recovered by centrifugation at 4°C for 10 minutes at 8000xg. The pellet was recovered and resuspended in 8 ml of SM. Six ml of SM was used to resuspend the pellet. An equal volume of chloroform was then added to the resuspended pellet. The mixture was vortexes for 30 seconds and phase separation was achieved by centrifugation at 10,000xg for 15 minutes. The aqueous phase was poured off and the PEG-containing chloroform phase was discarded. The volume of the aqueous phase containing the bacteriophage was then measured accurately and a volume of CsCl was added according to the formula:

(Final Volume x 67)/82 = grams of CsCl to be added.

The CsCl added was then completely dissolved and the resulting mix was centrifuged at 40,000 rpm for 24 hours at 22°C in a TST60.4 ultracentrifuge rotor. The following day the small plastic tubes which contained the centrifuged mix were removed from the rotor with a set of special forceps. A beam of light was used to visualize the milky light-scattering bacteriophage band. Each centrifuge tube was punctured with a 20 gauge needle and fractions containing the flocculent bands were collected dropwise. The collected bands were pooled and placed in dialysis bags (Spectrum Inc.) and were dialyzed against 1000 ml of TE for 1 hour to remove most of the CsCl. The bacteriophage were then transferred into a fresh 50 ml conical centrifuge tubes EDTA was added from a 500 ml stock solution (500 mM, pH 8.0) to a final concentration

of 20 mM. Proteinase K was then added from a stock solution of 20 mg/ml to a final concentration of 50µg/ml. For isolation of DNA from bacteriophage preparation, powdered sodium dodecyl sulfate (SDS) was added to a final concentration of 5% and each tube was mixed several times by inversion. Each sample was incubated for one hour at 68°C followed by extraction with an equal volume of TE-saturated phenol, centrifuged and the aqueous phase recovered. The aqueous phase was then extracted twice with an equal volume of chloroform. The extracted aqueous phase was pooled and dialyzed against 1 liter of TE buffer at 4°C overnight. Dialysis was then repeated in the morning with a fresh change of TE buffer for 1 hour. A 5 µl sample of the dialyzed solution was checked for DNA concentration and purity by agarose gel electrophoresis. The isolated bacteriophage DNA was then used for restriction digestion for various purposes as described in the Results section.

11. Southern Blotting

Analytic Southern blotting of restriction digested genomic or recombinant bacteriophage was carried out essentially as described previously (85, 86).

12. Western Blotting

12.1 Preparation of lysate from cell culture

Cells in 6- well plate were washed with 1X PBS three times, then lysed with 250 µl of sample Lysis buffer (63 mM Tris HCl,2% SDS, pH 6.8). Constant agitation was maintained until the cells were completely visibly lysed. Lysates were then transferred into 1.5 ml microfuge and then heated for 5 min in a boiling water bath. The lysates were cleared by centrifugation for 5 minutes in a microcentrifuge.

12.2 Determination of protein concentration

Protein concentration was determined by a DC protein assay as described by the manufacturer (Bio-Rad, Melville, NY) with Bovine Serum Albumin (BSA) used for protein standards.

12.3 SDS polyacrylamide gel electrophoresis

10-30 ug of the protein sample was mixed with 2x Laemmli buffer (126 mM Tris HCl,20% Glycerol,4% SDS, 2% β-mercaptoethanol and 0.005% Bromophenol Blue, pH 6.8) in 1:1 ratio and heated in a boiling water bath for 5minutes after which the samples were chilled in ice for 5 minutes and then centrifuged briefly. 10µg of protein samples and 5µl of Protein standards (marker) were loaded with gel loading pipet tips into the wells of a 4-20% gradient gel (Bio-Rad). For gel electrophoresis the gel was submerged in 1x Tris-glycine running buffer (25 mM Tris, 192 mM glycine, 0.1% SDS, pH8.3) and run for 55 minutes at 110 volts.

12.4 Transfer of protein to a PVDF membrane

Using wet transfer, the gel and membrane were sandwiched between sponge and paper (sponge/paper/gel/membrane/paper/sponge) and all are clamped tightly together after ensuring no air bubbles have formed between the gel and membrane. The sandwich was submerged in 1x Tris-glycine transfer buffer with 20% methanol. Under a 20 volts electrical field, the proteins are transferred to a PVDF membrane overnight. The negatively-charged proteins travel towards the positively-charged electrode, where they are bound by the membrane.

12.5 Primary antibody binding

PVDF membrane was pre-wet in 100% methanol, and wetted in 1X PBS for 2 minutes. The membrane was incubated in Odyssey Blocking Buffer for one hour. Primary antibody was

diluted by Odyssey Blocking Buffer (Li-Cor) with 0.2% Tween 20. The dilution range is from 1:200 – 1:5000, depending on the primary antibody. The blot was incubated in the diluted primary antibody a Western Blot Incubation Box overnight at 4°C with gentle shaking. The primary antibody solution was poured off carefully. The membrane was rinsed and covered with 1x PBS-T (0.1% Tween 20), Shaking on a platform shaker at room temperature for 5 minutes. The wash procedure was repeated 2 additional times.

12.6 Probing the membrane with infrared dye labeled secondary antibodies

Infrared dyes labeled secondary antibodies were purchased from Li-Cor. The secondary antibody was diluted in Odyssey Blocking buffer (Li-cor) with 0.2%Tween 20 and 0.01% SDS. The IRDye® 800CW secondary (Li-Cor) was used ay dilutions between 1:5,000 and 1:25,000; the IRDye 680LT secondary (Li-Cor) was diluted from1:20,000 to 1:50,000. The blot was incubated in diluted secondary antibody for 30-60 minutes at room temperature with gentle shaking. The membrane was washed for 5 minutes with 1x PBS-T (0.1% Tween 20), on a shaker platform at room temperature. The wash was repeated 3 additional times after which the membrane was rinsed with 1x PBS to remove residual Tween 20. The membrane was scanned to an image file with the Odyssey Fc Imaging System

13. Sequences analyses

13.1 Sequence analysis of PCR products

For sequence analysis of PCR products, the PCR reaction mixture was run an agarose gel to determine the size(s) and number of bands to be analyzed. For PCR reactions containing multiple products for analysis the gel bands were excised with a scalpel and the DNA was extracted using a gel extraction kit (Qiagen). For PCR reactions that contained only one product the EXOsapit

reagent (US Biochemicals,) was added to the reaction mix to destroy residual primers and deoxyribonucleotides (dNTPs) and used directly for sequence analysis. In some cases PCR products were cloned into a T-vector for sequence analysis as described below.

13.2 PCR methods

PCR thermal cycling: 95^{o}C 3 minutes, 94^{o}C 30 seconds, 59^{o}C 20 seconds, 72^{o}C 3 minutes 35 cycles.

Segments of integrated SV40 were amplified by conventional PCR using both genomic DNA templates and cassette-ligated restriction fragment templates. For cassette ligation, genomic DNAs were digested with XbaI or BamHI and ligated to either an M13 primer sequence adaptor (5´GTAAAACGACGGCCAGCCGAT 3´) or the cassette primer described by Wang et al. (CP cassette, ACGCGTAATACGACTCACTATAGGGAGATC; (87). Amplification was carried out using the cassette adaptor sequence primer and various SV40 primers as indicated in the figures shown in the Results.

13.3 Inverse PCR

130 DNA (100 ng) was digested with XbaI and the resulting restriction fragments were circularized by overnight incubation at 16^{o}C in a reaction buffer containing 6 units of T4 DNA ligase (Fisher Scientific). The circularized DNA was used as a template for PCR amplification using primer pairs specific to SV40 sequences potentially joined to the human genomic DNA. The amplification was performed in a 50 µl reaction mixture containing 5µl of DNA template, 2 mM $MgCl_2$, 250 µM each of deoxynucleotide triphosphates, 300 nM of each primer, and 5.2 units of Expand polymerase (Roche Applied Science). The cycling protocol was: initial

denaturation at 95^{o}C for 5 min followed by 35 repetitions of the following 3 segment cycle: 1 min at 94^{o}C, 1 min at 58^{o}C, and 2 min at 72^{o}C. The amplified products were fractionated by electrophoresis in a 1% agarose gel, visualized by ethidium bromide staining, and purified from the gel for cloning in the TOPO XL T vector or for direct sequencing.

13.4 Cloning methods

We cloned the PCR product using the cloning kit PCR 2.1-TOPO vector (Invitrogen). Four µl of PCR product was used for the transfection reaction. After the transfection reaction the PCR product is introduced into a competent *E.Coli* cell. PCR 2.1-TOPO vector carries a copy of *lacZ* reporter gene. Insertion of the PCR product into this gene inactivates β-galactosidase synthesis in order to isolate recombinants. The cells are plated onto X-gal agar plates and incubated overnight at 37^{o}C. The recombinant plaques are clear compared to the non-recombinant blue plaques. A few of clear plaques were chosen from the plate and individually transferred to a 15 ml tube with LB broth and incubated overnight at 37^{o}C in a shaker.

13.5 pUC18 subcloning

The insert is ligated with pUC18 vector in ratio 1:1 and 1:3

	Vector: Insert = 1:1	Vector: Insert = 1:3
Vector (pUC18/*Bam*HI)	3 µl	3 µl
Insert (Phage DNA/*Bam*HI)	7µl	21µl
Buffer (10X)	2µl	3 µl
Water	7µl	2 µl
T4 Ligase	1µl	1 µl
Total	20µl	30 µl

The reaction was taking place at 15°C in water bath for overnight and the final ligated product was examined by agarose gel electrophoresis.

Table 3. Primers for SV40 and Human Chromosomes

Primer Name	DNA Sequence	Primer Name	DNA sequence
GV-2	5'-GAG GAT GTA AAG GGC ACT GG-3'	GV-3	5'-TGGGGATCCAGACATGATAAG-3'
GV-4	5'-TTAATTTGCCCTTGGACAGG-3'	QSV16	5'-TCCACACAGGCATAGAGTGTCT-'3
ET-2	5'-GGC AGC CTA TGA TTG GAA TG-3'	QSV18	5'-GGAACTGATGAATGGGAGCA-'3
QSV28	5'GAGGATGTAAAGGGCACTGG 3'	QSV46	5'TTGAGGAAAGTTTGCCAGGT-3'
QSV51	5'-CCAGAAGCCTCCAAAGTCAG-3'	QSV71	5'-TTGGTCCTTTAAACAGCCAGT
QSV53	5'-TTTTACTCCATCTTCCATTTTCTT G-3'	QSV73	5'-CCCCCACATAATTCAAGCAA-'3
QSV55	5'-TTCTTCATCTCCTCCTTTATCAGG-3'	QSV75	5'-TTAACCCACCTGGCAAACTT-'3
QSV57	5'-TTGCTGCAATTTTGTGAAGG-3'	QSV77	5'-ACCTGGCAAACTTTCCTCAA-'3
QSV59	5'-TTTGGGCCTAAAATCTATTTGTTT-3'	QSV81	5'AGCTCAACGCCTTTTTGTGT-3'
QSV61	5'-GCT CAA AGT TCA GCC TGT CC-3'	QSV83	5'CAACTCCAGCCATCCATTCT-3'
QSV63	5'-CATCCTGATAAAGGAGGAGATGA-'3	QSV85	5'CCTGCAGTGTTTTAGGCACA-3'
QSV65	5'-CCTCAGTGGATGTTGCCTTT-3'	QSV87	5'TTGCTGCAATTTTGTGAAGG-3'
QSV91	5'TGGGCAACAAACAGTGTGC-3'	QSV89	5'CCTGAAGGCAAATCTCTGGA-3'
P21	5'-CCT CAT CAT CAC TAG AT-3'		

Table 4. Primers for Chromosomes21, 10 and 6

Primer Name	DNA Sequence	Primer Name	DNA sequence
ZZ-2	5'- TCA CAC CTG TAA TCC CAG CA-3'	Chr 6-1	5'-AATTTGCCCACAAAAGGAAA-3'
ZZ-3	5'-CTG TGC CTG GCC TTT TTA AG-3'	Chr 6-2	5'-ATTTTCCTTTTGTGGGCAAAT-3'
ZZ-5	5'-TTC TAA CAG GCT GGG GTC TG-3'	Chr 6-3	5'-CAGGAAGTCTGGGGGATGTGT-3'
ZZ-6	5'-CCT CTG TTG GGT GAA AAT GC-3'	Chr 6-4	5'-ACACATCCCCAGACTTCCTG-'3
Chr21-3	5'-TGACCTGTGTCTGTCCTTGG-3'	Chr10-1	5'-GGGAGGAACTTCCCATCTGT-3'
Chr21-4	5'-AGCCAAGGACAGACACAGGT-3'	Chr10-2	5'-CCCTTCAGGGCCACTTTATT-3'
Chr21-5	5'-CCCGAGTAGCTGGGACTACA-3'	Chr-10-3	5'-GGAGTTTCATGGGGAGGAAC-3'
Chr21-6	5'-AAATTAGCCGGGCGTGGT-3'		

14. qPCR array

In our PCR array analysis, 102 µl of diluted first-strand cDNA was added into 1248 µl of H_2O, and then mixed with 1350 µl of 2 X SABiosciences RT2q PCR master mixes (SABiosciences). We added 25 µl of the experimental cocktail into each well on a 96-well plate. The RT_PCR was performed on the Applied Biosystems 7500 standard Real–Time PCR System. The parameters were set up as shown in Fig 5. Data analysis was performed u

sing the web-based PCR array data analysis software

(http://www.sabiosciences.com/pcr/arrayanalysis.php).

15. Flow cytometric (FACS) analysis of cell cycle parameters

Cells grown to approximately 70% confluence in monolayer culture were harvested with trypsin-EDTA, washed twice with phosphate buffered saline (PBS) by centrifugation and then fixed by resuspension in 3% formaldehyde in PBS for 1 h at 4 °C. The fixed cells were washed twice with PBS and resuspended in permeabilization buffer (5 mM HEPES, pH 7.5, 150 mM NaCl, 4% fetal bovine serum, 0.1% Triton X-100) at 4 °C. After 10 min, the cell suspension was diluted with one volume of PBS, pelleted by centrifugation and then stained with propidium iodide in PBS containing 0.5 mg/ml RNase for 2 h at room temperature. Cells were washed three times in PBS and used for flow cytometry on a Becton Dickinson LSRII cell sorter. In order to generate histograms, FCS files were translated into Excel spreadsheets using FCS Express software from Flowjo software (Tree Star Inc. CA) allows graphical display of frequency as a linear function of PI fluorescence. Gaussian approximations of the G1, S and G2 subpopulations from which their fractional parts were estimated

16. Fluorescence Activated Cell Sorting (FACS) for Apoptosis

APO-BRDUTM Kit (The Phoenix Flow Systems, Inc.) is a two color TUNEL (Terminal deoxynucleotide transferase dUTP Nick End Labeling) assay for labeling DNA breaks and total cellular DNA to detect apoptotic cells by flow cytometry. One of the most easily measured features of apoptotic cells is the break-up of the genomic DNA by cellular nucleases. These DNA fragments can be extracted from apoptotic cells. The large number of DNA fragments appearing in apoptotic cells results in a multitude of 3’-hydroxyl group ends in the DNA. This property can be used to identify apoptotic cells by labeling the 3’-hydroxyl ends with bromolated deoxyuridine triphosphate nucleotides (BrdUTP). The enzyme terminal deoxynucleotidyl

transferase (TdT) catalyzes a template independent addition of deoxyribonucleoside triphosphates to the 3'-hydroxyl ends of double- or single-stranded DNA with either blunt, recessed or overhanging ends(88). A substantial number of these sites are available in apoptotic cells providing the basis for the method utilized in the APO-BRDUTM Kit. The Br-dUTP is more readily incorporated into the genome of apoptotic cells than are the deoxynucleotide triphosphates complexed to larger ligands like fluorescein, biotin or digoxigenin. This greater incorporation gives rise to a stronger flow cytometry signal when the Br-dUTP sites are identified by a fluorescein labeled antiBrdU monoclonal antibody. Non-apoptotic cells do not incorporate significant amounts of the Br-dUTP owing to the lack of exposed 3'-hydroxyl DNA ends.

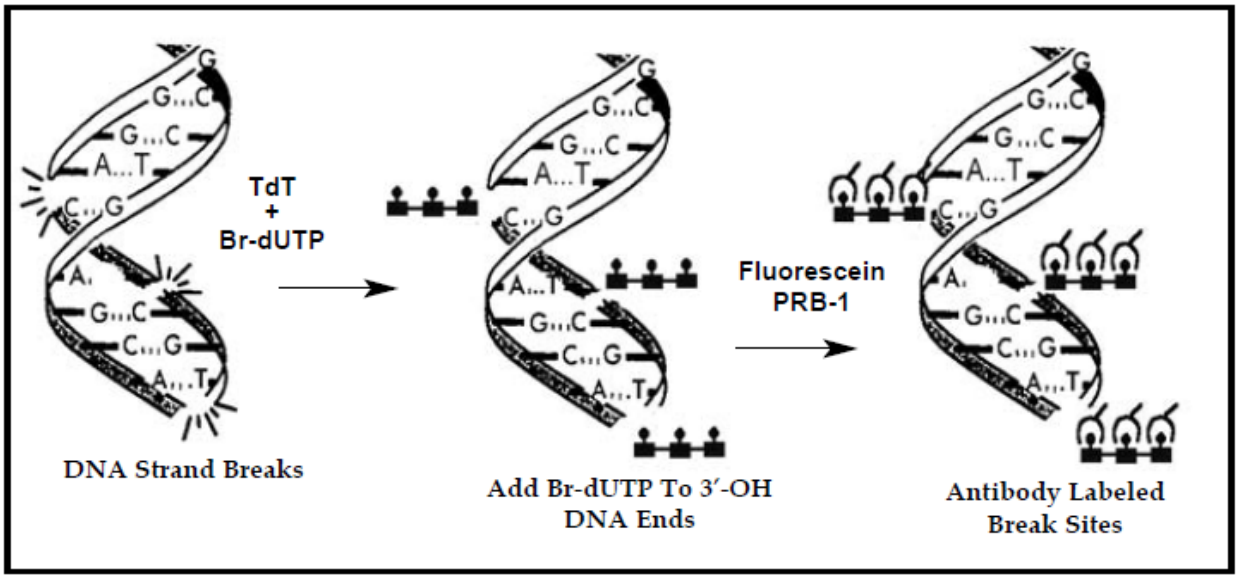

Figure 21. Diagrammatic representation of the addition of bromodeoxyuridine triphosphate (Br-dUTP) catalyzed by terminal deoxynucleotidyl transferase (TdT) to the 3'-OH sites of DNA strand breaks induced in the genome of apoptotic cells. Source: APO-BRDUTM Kit manual (The Phoenix Flow Systems, Inc.)

The kit contains positive and negative control cells for assessing reagent performance. The labeling assay was performed according to the manufacturer's instructions.

17. Caspase-Glo 3/7 Assay

The Caspase –Gol 3/7 assay is a luminescent assay that measures caspase-3 and -7 activities. These enzymes belong to the cysteine aspartic acid-specific protease family and play key roles in apoptosis in mammalian cells. Caspases are proteases that have a cysteine at their active site and cleave their target protein at specific aspartic acids. The assay provides a luminogenic caspase-3/7 substrate, which contains the tetrapeptide sequence DEVD (Aspartyl -Glutamatyl –Valinyl-Aspartyl)or (Asp-Glu-Val-Asp). In cell lysis, the caspases cleave the tetrapeptide of substrate at specific aspartic acid and generates a "glow-type" luminescent signal produced by luciferase. Luminescence is proportional to the amount of caspase activity present. (Figure 22).

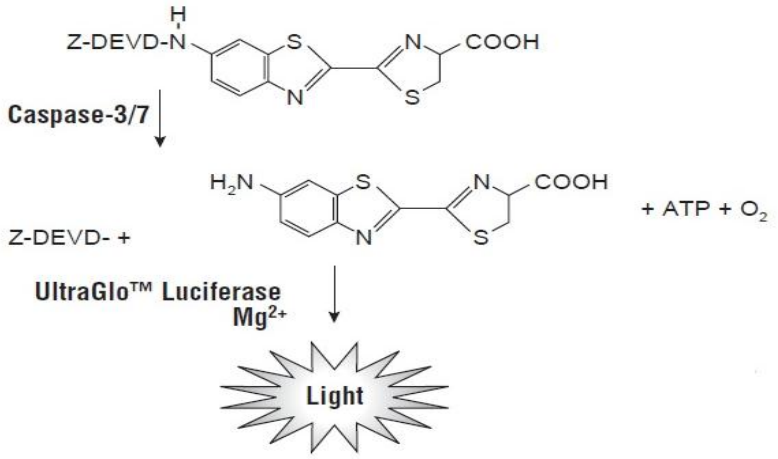

Figure 22, Caspase-3/7 cleavage of the luminogenic substrate containing the DEVD peptide

Following caspase cleavage, a substrate, aminoluciferin, for luciferase is released; luminescence is produced by the luciferase reaction. The quantity of Caspase- 3/7 is proportional to intensity of luminescence signal.

Cells were grown in 6-well plate and harvest with typsin-EDTA, and wash the cells three times with DMEM medium. Then Cells were counted using a hemacytometer. One hundred microliter samples with equal numbers of cells (~10^3 cells) were loaded into the wells of white-walled 96-well plate. Caspase-gole 3/7 reagent was added in a 1:1 ratio and placed on a plate shaker for mixing and incubating for one hour at room temperature and luminescence was read using a GloMax 96 Microplate reader using the instrument luminescence module (Promega Biotec, WI).

18. Senescence associated β-galactosidase assay

ß-galactosidase (SA-ß-Gal) activity is common biochemical marker of senescent cells. An increase of β-galactosidase activity is associated with senescence in tissue culture cells. β-galactosidase activity was measured using an *in situ* method developed by Dimri et al(89). After siRNA transfection into the 130 cells, cells were collected at 1, 2, 3, 4, and 5 days. Cells were then washed with 1X PBS and fixed for 3-5 min (room temperature) in 4% paraformaldehyde, β-galactosidase activity was detected via histo-chemical staining after incubation at 37°C (no $C0_2$) with fresh senescence associated β-Gal (SA-,β-Gal) stain solution (1 mg of 5-bromo-4-chloro-3-indolyl β-D-galactosidase (X-Gal) per ml/40 mM citric acid/sodium phosphate, pH 6.0/5 mM potassium ferrocyanide/5 mM potassium ferricyanide/150 mM NaCl/2 mM MgCl2) for 12-16 hr.

RESULTS AND DISCUSSION

1. Cloning and sequence analysis of the unique SV40 integrant

Previous work in Dr. Steinberg's laboratory has shown (90) that, following viral infection of keratinocytes, there is a rapid increase in SV40 DNA copy number as the cells are passaged. However, over time, viral DNA copy number gradually decreases and cells in long term culture are invariably found to contain integrated viral DNA only in low copy number (84). Our Southern blot analyses of the viral DNA in the 130 cell line indicated that the viral sequences were completely contained on a unique XbaI fragment of about 12-14 kb (84). Since XbaI has no restriction sites in SV40, we created genomic libraries in the bacteriophage vector GEM11 with the idea that any cloned restriction fragments would necessarily also contain human sequences flanking the integration site. From these libraries five independent bacteriophage clones were isolated. Restriction patterns and subsequent sequence analyses of portions of the inserts of the different clones indicated, they were identical. The cloned virus-containing XbaI fragment was sequenced by: 1) subcloning BamHI subfragments of the insert into pUC18 and 2) sequencing of PCR products derived from the cloned insert as PCR template. A contiguous sequence was assembled by matching overlapping sequences by routine "primer walking" along the various subclones or PCR products. Identity of individual sequences was determined by BLAST alignment against the GenBank sequence databank. The coding derived from the assembled sequences is shown in Figure 23. From the alignments of the BamHI restriction fragments in pUC18, we found a linear viral genomic segment in which SV40 nt 3511 was joined to chromosome 21q in the intronic region between the 3rd and 4th exons (GenBank

accession no. AP001748; nt 166939). Interestingly, sequence analysis of the viral integrant in a second, independently derived line of SV40-immortalized cells (line 22) also showed the virus to be integrated within an intronic region of the PKNOX gene (Figure 23). Although we sequenced more than 25 clones from130 cell line, our screen failed to find any clones containing viral sequences in the part of the SV40 early region between the viral BamHI site (nt 2530) and nt 3511. In order to continue sequencing past the viral BamHI site, we continued primer walking by a PCR-based approach using both genomic and bacteriophage cloned DNA templates. Using the PCR products derived from these templates and primer sets targeting various segments of the early region, we were able to obtain additional sequence spanning the early region segment that was missing from the BamHI fragment containing the leftward human chromosome 21 sequences. This method proved to be relatively straightforward and we were able to obtain additional sequence covering the entire early region up to nt 4068 (blue segment shown in Figure 23). From this point, sequencing by traditional PCR yielded inconclusive sequence results, and so we employed several other approaches including: 1) inverse PCR (circularized restriction fragments), 2) random primer, and 3) cassette-ligated restriction fragments. Using these approaches we were able to obtain additional sequence covering the remainder of the early region, the origin/promoter and the late region up to nt 1267 (green segment in Figure 18). Attempts at further sequencing past this point yielded conflicting results and a number of repeated sequencing runs using the same primer sets were required before we ultimately found that this portion of the late region contained numerous rearrangements and inversions and we found a putative rightward viral integration junction with human chromosome 10 joining the integrated virus at nt 3052. Sequence data for the viral portion of the cloned XbaI fragment appear to represent the entire complement of viral sequences contained on the restriction

fragment as seen in our previous Southern blots. However, sequence analyses using the genomic templates also showed that there were several small viral segments derived from various sites along the viral genome and integrated at multiple chromosomal locations (Table 5). Taken together these findings indicate that the integration process involved chromosomal breakage and/or translocation.

Table 5. SV40 integration site and flanking sequence

SV40 nt	**integration site/flanking sequences**
2460 ->2631	Unidentified
3388 -> 3556	Unidentified
357 -> 636	chromosome 6
4918 -> 5041	Unidentified
2460 -> 2631	Unidentified

With regard to the early region target of our siRNA, our sequence data shows that there is, in fact, only a single intact copy of the SV40 early region. We had also carried out sequence analyses of cDNAs using primers mapping within the viral early region. These experiments are consistent with this finding since all of the cDNAs sequenced showed only the presence of the normal early region transcript encoding the large T and small (t) antigens.

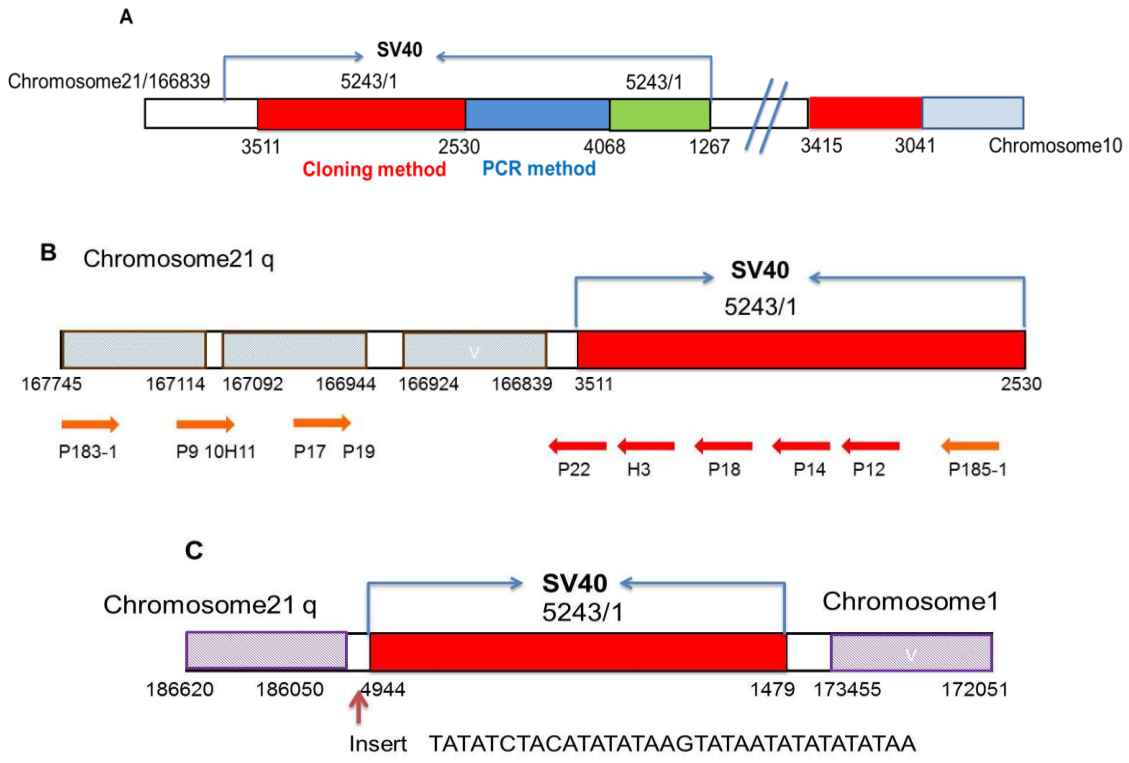

Figure 23. DNA sequence results. A. Total sequence analysis of integrated SV40 in 130 cell line. B. Sequence of integrated SV40 from previous year in 130 cell line. C. Sequence of integrated SV40 in 22 cell line.

2. Integration of SV40 into an intronic region of the PKNOX1 homeobox gene

It is known that integration of SV40 DNA is accompanied by human chromosomal changes involving a variety of chromosomal aberrations and especially disrupted human chromosomes. In this study, therefore, we analyzed SV40 integrated DNA sequence of 130 and 22 cell lines. It can be seen from the results in Figure 23. A, more than one copy of the SV40 DNA-integrated fragment were integrated into human chromosome 21. Furthermore, we found that a segment of about 21kb spanning chromosome nucleotides 168179 and 186050 of chromosome 21 was replaced by SV40 DNA (Figure 23.C). The missing fragment is within the homeobox-

containing protein gene PKNOX1 region (160243 to 185959). The insertion site for both cell lines is located at human chromosome 21.q22.3. PKNOX1, a gene encoding PREP1, is a transcription factor and a regulator of Pbx activity that map on human chromosome 21q22.3. This gene regulates PF4 (platelet factor 4) gene expression. PKNOX1 gene-dosage imbalance is associated with overexpression of FABP7 (fatty acid binding protein 7 in Down syndrome fetal brains). PKNOX1 also plays a role in F9 teratocarcinoma cells; it causes an increase of PBX-2 by preventing its degradation (91). The finding that viral integration occurred in Chromosome 21 at the PKNOX1 locus is of some interest as it suggests that an integration event in this region of PKNOX1 may have a functional significance with regard to immortalization. We therefore wondered whether expression of PKNOX1 gene is regulated by the integrated viral early genes. The results showed that expression of mRNA of PKNOX1 was down-regulated by 1.5 fold (Figure40.A) but the PREP1 protein encoded by PKNOX1 did not exhibit any significant change in expression by western blotting (Figure 24).

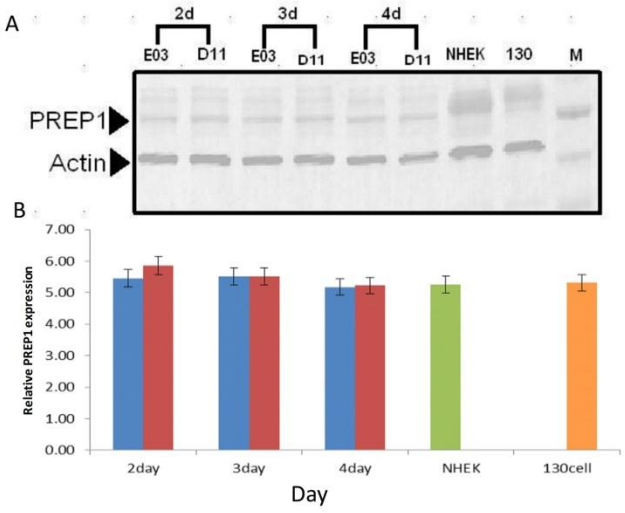

Figure 24. 130 cells were transfected with E03 and D11 siRNAs and protein expression of PREP1 was analyzed by western blotting at various days following transfection. A) Western

blots were probed with a rabbit anti-PREP1 antibody (Santa Cruz Biotechnology), Actin was used as an internal control. For actin, blots were probed with a mouse anti-actin antibody from Licor, Inc. For visualization of the bands, IRDye 800CW goat anti-mouse secondary antibody and IRDye 680LT goat anti-rabbit secondary antibody (Licor) were used as secondary antibodies. B) The expression of p53 is related to the expression of actin in each sample; (blue bars: negative siRNA controls, red bars: siRNA targeting T antigen. NHEK: normal human epidermal keratinocytes; 130: SV40 transformed epidermal keratinocytes 130 cell lines.

The PKNOX1 gene has eleven exons (nucleotide ends according to the numbering in GenBank locus AF316139.1: 160180..160290, 163349..163476, 165911..166082, 168926..169096, 172766..172865,173991..174088, 177161..177289, 180729..180805, 184560..184732,185748..187814, 293803..293981) and ten introns. The SV 40 binding site is between exon four and exon nine of PKNOX1 gene, which is far from the promoter region which probably explains why the expression of PKNOX1 was not downregulated effectively. Our results showed that the translation of PKNOX1 was not changed as well.

3. Establishment of experimental system

The approach we used to silence T antigen in SV 40 transfected cells has to meet the following requirements:

1) The amount of delivery reagent (Lipofectamin 2000) with positive change should not significantly affect cell viability

2) The efficiency of siRNA transfection in line 130 cells should be over 90%;

3) The primers for RT-PCR should only generate a single product.

4) The material for standard curve in absolute qRT- PCR must be stable at the storage, and the curve must be highly accurate for calculation of T antigen copy number.

Furthermore we need to know:

1) Which siRNA has the highest efficiency in silencing T antigen

2) The optimum concentration of siRNA for knock-down of over 70% mRNA of T antigen

3) The time post transfection when T antigen mRNA is reduced to a minimum

4) When does the T antigen protein level reach the minimum concentration

Therefore we performed a series of tests to find out the optimum experimental conditions.

3.1 Viability of Cell Transfection

Cell viability determination by Trypan blue exclusion Assay

Since lipofectamine 2000 is known to be toxic to cells and the degree of toxicity varies widely with cell type, we tested the effects of various amounts of lipofectamine-RNA on viability of 130 cells. For this purpose **c**ell viability determination by Trypan blue exclusion assay.

Trypan blue is a dye that is used to determine the viability of a cell. Living cells exclude the dye, whereas dead cells will take up the blue dye. The blue stain is easily visible, and cells can be counted using a light microscope. Lipofectamin 2000 reagent is a proprietary formulation that facilitates highly efficient delivery of Stealth RNA molecules including sh RNA (siRNA or plasmid DNA) to mammalian cells for RNAi analysis. However, there is a problem caused by cation liposome, which damages the living cells. In order to establish optimal Lipofectamine concentration for RNAi transfection, samples with different amounts of Lipofectaminw 2000

were added into 24-well plate and collected after three days following transfection. Figure 25. shows the results of the viability assay using trypan blue dye exclusion.

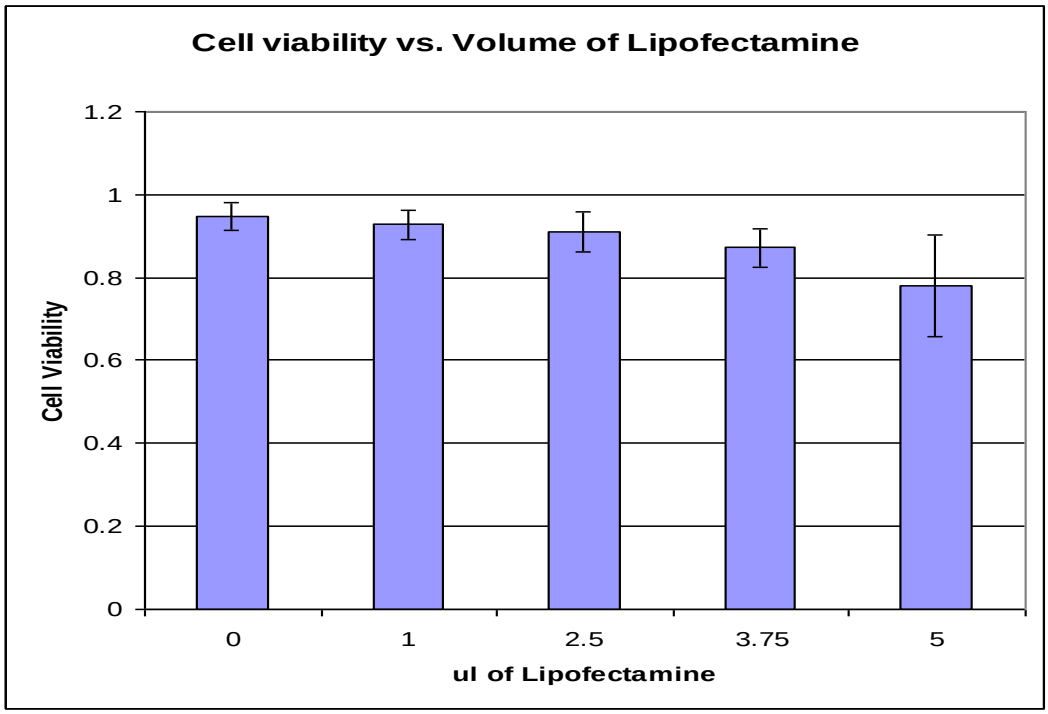

Figure 25. Viability of cell transfected by Lipofectamin 2000. Cells were treated for three days by various amount of Lipofectamin 2000. Use of less than 2.5µl of Lipofectamin 2000 does not affect cell viability significantly under the conditions designed for transfection in a 24-well plate.

3.2 Transfection Efficiency

Fluorescent Oligo (Invitrogen) is a fluorescein-labeled ds RNA oligomer designed for use in RNAi analysis to facilitate assessment and optimization of cationic lipid-mediated delivery ds oligonucleotides into mammalian cells. The concentration of Fluorescent Oligo is 100nM of for transfection in 130 cells. The superimposed contract image over the final fluorescent image (Figure 26).

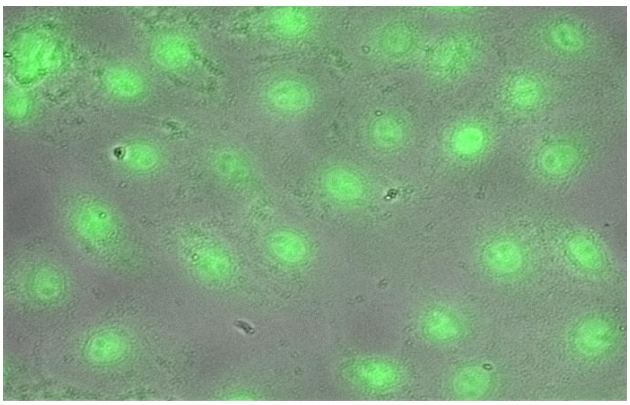

Figure 26. 130 cells uptake fluorescent Oligomers

Under the conditions of transfection used it can be seen that dsRNA is seen localized to the nucleus. The transfection efficiency of ds oligomer was seen to be well over 90%. Since sequence of the fluorescent oligomer is not homologous to any known human gene there are no artifacts of gene expression due to the presence of the fluorescent oligo

.

3.3 Selection of Primers for Real-Time PCR

Cloned recombinant SV40 standard template contains target sequences of SV40 (nt 5040-4917 and nt 4572-4403). Many different primers can be used in this target region. It is, therefore, important to select and use a proper pair of primers since SYBR green dye was used for real-time PCR. It is also necessary to mention that SYBR green can bind to any double stranded DNA, thus, if more double stranded amplicons are produced, the intensity of the fluorescent will increase. Four pairs of primers were selected and tested with PCR and real-time PCR. The products of PCR appear on the 1% agarose gel as described in table 6 and fig. 20. It was observed that the selected QSV63 and p21 primer pair produces a unique band (product) on the gel. This finding is important in establishing guideline in selection of primer pairs to be used for the experiments described.

Table 6. Selection of a pair of primers

A Pair of primers	Region of primer	Band No. of PCR products on the gel
P21 QSV 14	4472-→ 4489 5052-→ 5033 (R)	N/A
P21 QSV 63	4472-→4489 5040-→ 5017 (R)	one
QSV79 QSV 63	4403-→ 4422 5040-→ 5017(R)	three
QSV 79 QSV 14	4403-→4422 5052-→5033 (R)	N/A

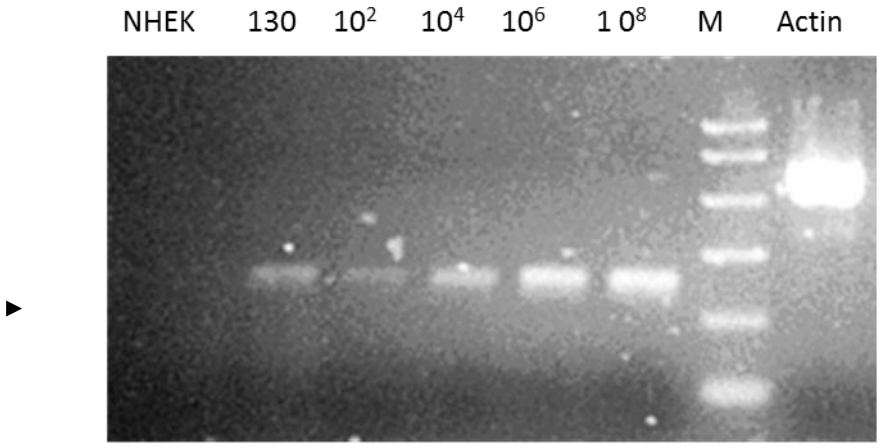

Figure 27. Image of RT-PCR products on 1% Agarose gel. Primers: p21 and QSV63; Template: NHEK: normal human epidermal keratinocytes, 10^2, 10^4,10^6 and 10^8 copies of the recombinant SV40 DNA in each standard solution. M: DNA maker, 130: SV40 transfected 130 cells, Actin: a positive control

3.4 Efficiency of LT antigen transcriptional silencing by different siRNAs

We designed three siRNAs for interfering expression of mRNA of T antigen and a negative control using the STEALTH siRNAs (Invitrogen). In order to find out which one has the most powerful silencing efficiency for T antigen, cells were transfected with the same amount of each

siRNA to cells grown in a 6-well culture tray. Four days transfection cells were harvested for western blotting (Figure 24).

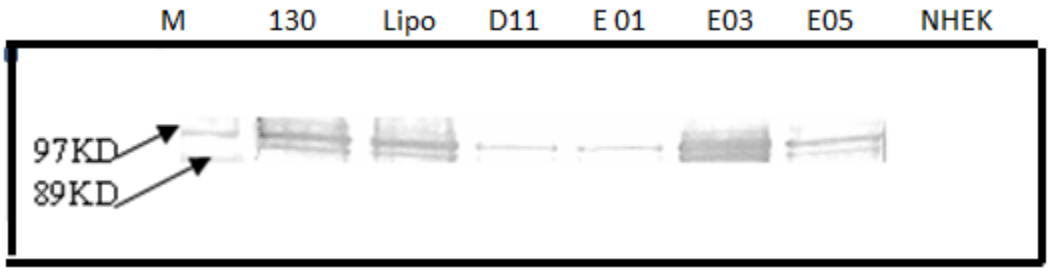

Figure 28. The analysis of silence efficiency of four different siRNAs for targeting T antigen by Western blot. M: Protein Marker; 130: 130 cells as a positive control; Lipo: 130 cell grown in Lipofectamine 2000; D11, E01, E03, and E05: Four Stealth RNAis were tested (E01, E03, E05 and D11); NHEK: normal human epidermal keratinocytes. The molecular weight of LT antigen is 94 KD; there is another one normally around 91KD in human cells.

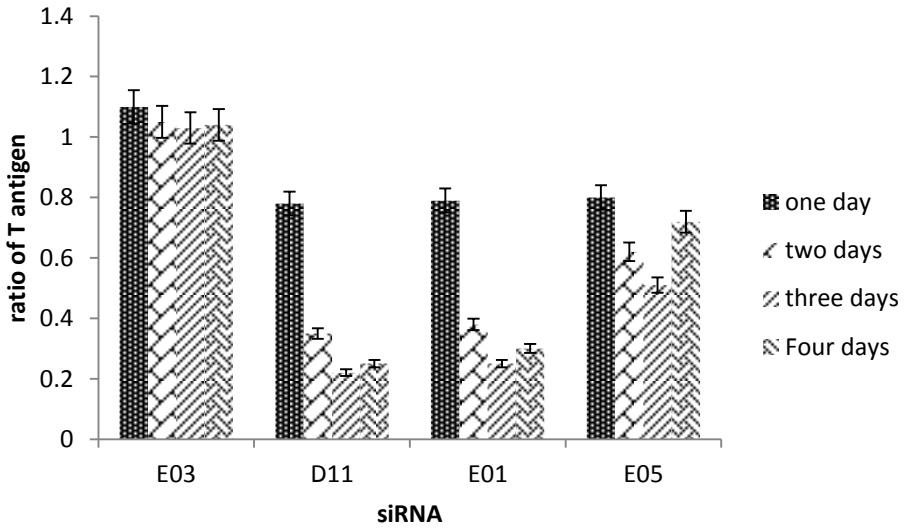

Figure 29. The suppression of LT antigen by four different siRNAs was determined by Western blot for 4 days. The ration of T antigen silenced was compared with T antigen in 130 cells.

The results showed the D11 and E01 have the highest silencing efficiency for T antigen; E05 has less efficiency, and E03 does not silence the T antigen at all. Based on the sequence of E03, E03 should be a negative control siRNA. According to siRNA design rules, the target sequence of siRNA should be approximately 50-100 nt downstream from the start codon (ATG) to achieve the highest efficiency of silencing (92).We selected D11 as the most efficient siRNA for later application because its targeting sequence is located at 50-80 nt downstream of the T antigen ATG initiation codon.

3.5 siRNA silenced expression of mRNA of T antigen

The number of copies of T antigen mRNA was determined by absolute quantification using the RT-PCR method, which can generate highly sensitive and reproducible results using calibration curves; the accuracy of the method depends on the use of reliable standards. Cloned the recombinant plasmid DNAs for use as standards (recDNA) are very stable and generate highly reproducible standard curves even after a long storage time, in comparison to freshly synthesized RNA. We cloned recDNA of T antigen covering the primer region used in our knockdown experiments. For our experiment we isolated the recombinant plasmid DNA and confirmed the presence of the SV40 sequence. For use as standards we measured the concentraion of isolated plasmid DNA and created standards representing 10^1 to 10^8 plasmid copies in each reaction mixture. The R^2 of Calibration curve was 0.967 (Figure.30).

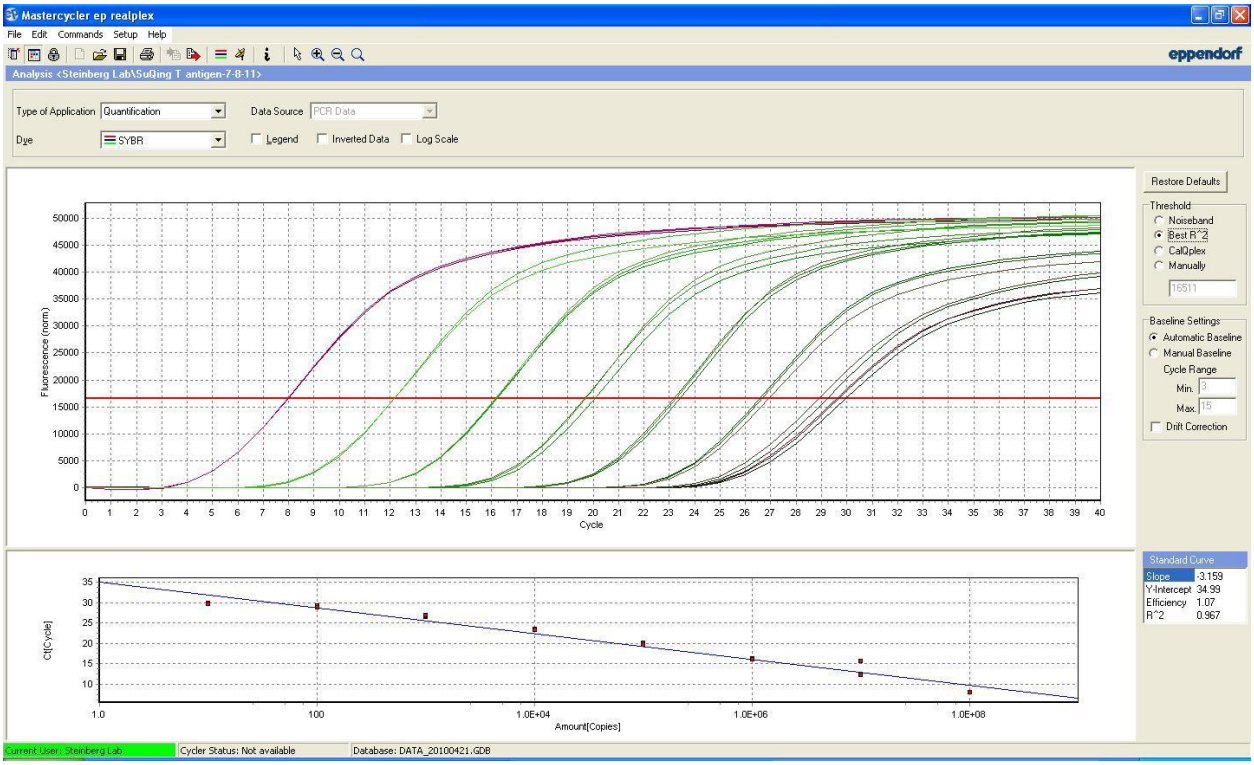

Figure 30. Calibration curve of Absolute RT-PCR . The curve covers a range of 10^1 to 10^8 T antigen DNA copies.

The quantity of siRNA to be used in each experiment was determined by adding various pmols of siRNA in cell transfection (Figure.31A). The figure shows that 100 pmols has the strongest silencing effect. In the following experiments, 100 pmols of siRNA was used for transfection. Maximal knockdown (>80%) was seen on day 2 post-transfection and knockdown persisted at >70% through days 5–7(Invitrogen). Significant knockdown was still observed at day 10 with all but one siRNA the target mRNA of T antigen was knocked down to 20 to 30% of the E03 negative control (Figure. 31 B).

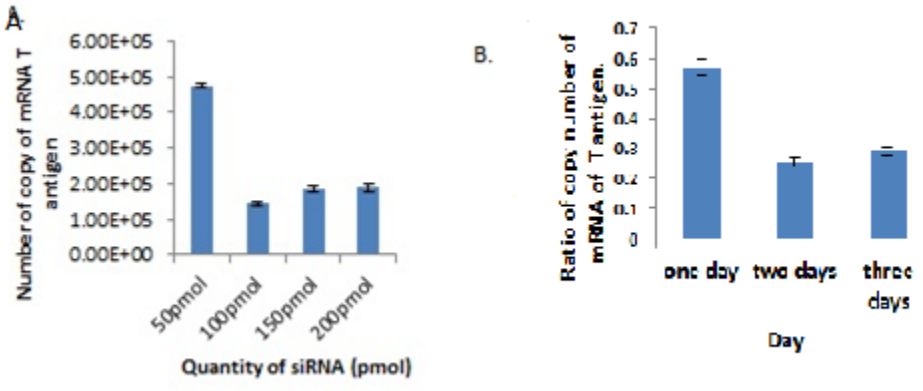

Figure 31. Inhibition of siRNA D11 in Line 130 cells. A. Silencing effect of different amount of siRNA. B. Expression of T antigen mRNA varied at different days after transfection of D11 in Line 130 cells.

4. Alteration of growth properties of 130 Cells related after silencing of T antigen

130 line cells are human epidermal cells immortalized by SV40 virus. Immortalization and transformation involves binding of the viral T antigen inactivation of numerous host proteins, including tumor suppressor p53 and pRb, and transactivates several cellular promoters. Therefore, it is expected that in viral transformed cells, various cell cycle check points may be abrogated, pathways of cellular senescence may be bypassed and form these reason cells can come to acquire an infinite lifespan. We hypothesize that after T antigen mRNA of 130 line cells was silenced by siRNA, the loss of these functions of T antigen would be diminished and cells would exhibit changes in the cell cycle of 130 line cells in which normal checkpoints at the G1/S interface would be partially restored. We also expect that the siRNA transfected cells would undergo either senescence or apoptosis. We therefore examined the cell cycle in 130 cells collected from one day to five days after siRNA transfection.

4.1 Cell cycle was changed by siRNA transfection

FACS analysis performed at different times after siRNA transfection 130 line cells. The percentage of cells in G1, S and G2/M phase of cell cycle is shown with each histogram in Figure. 33. Flow cytometry data were acquired on the LSRII (BD Immunocytometry Systems) and analyzed using FlowJo software (Treestar, Inc., San Carlos, CA) on indicated days.

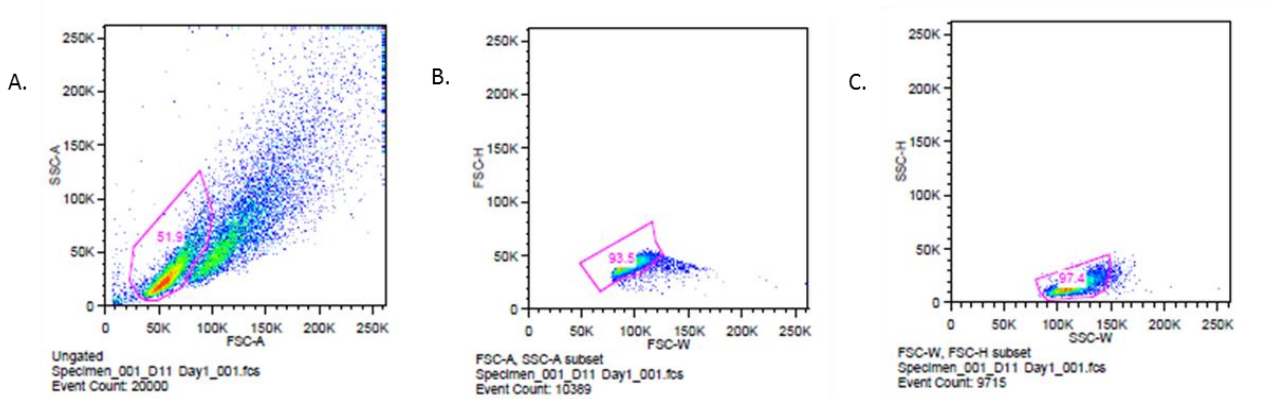

Figure 32. Two dimensional FACS scattergrams showing the gating used for cell cycle analyses

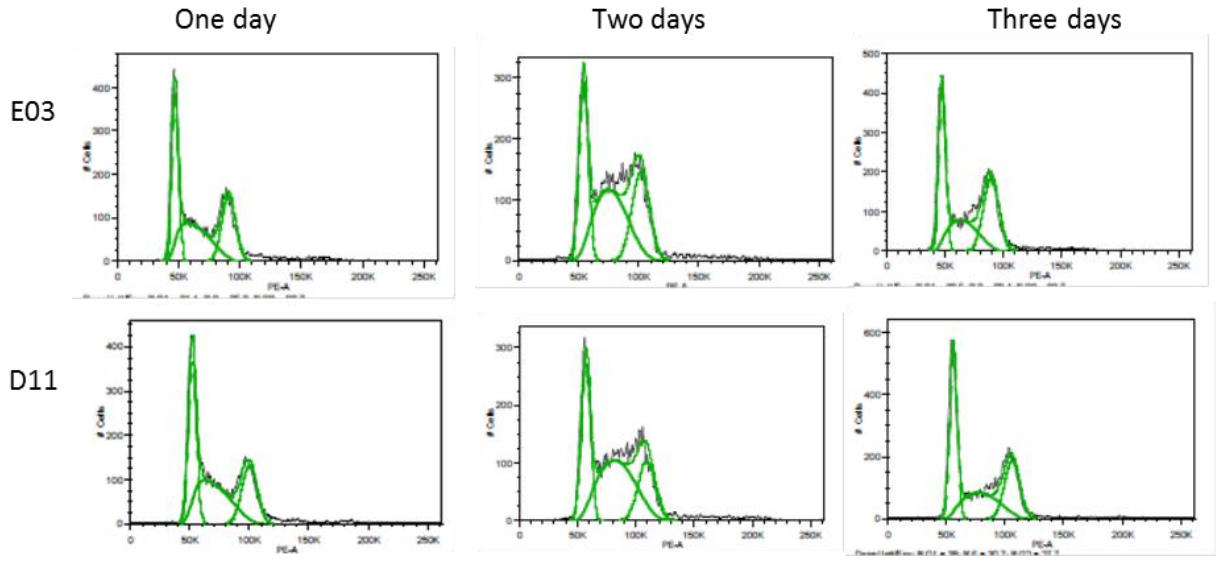

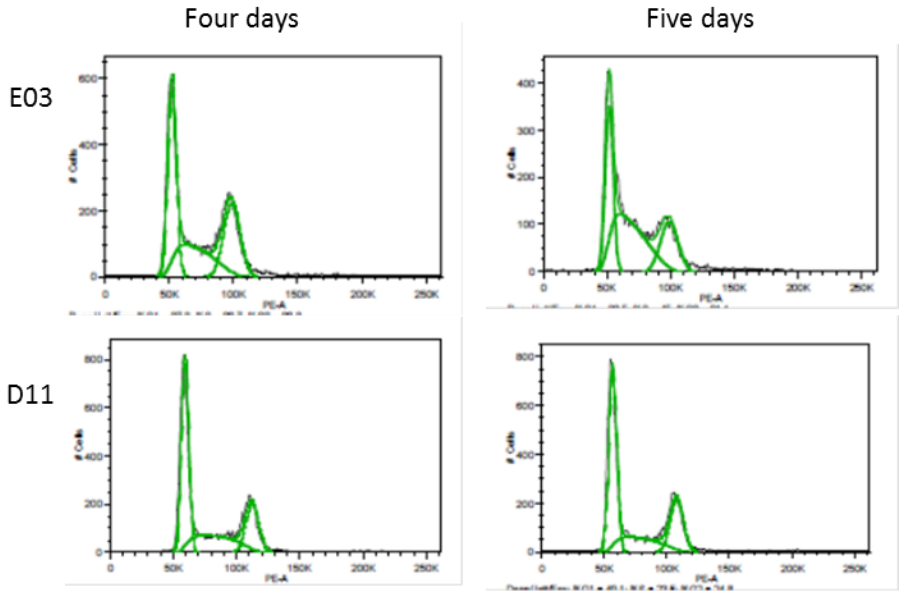

Figure 33. FACS analysis of cell cycle progression and Silenced T antigen induce growth arrest of 130 cells. Fluorescence intensity representing the cellular DNA content is shown on the X axis, and cell count is shown on the Y axis. A total of 20,000 events were collected in FACS analysis. The left-hand peak in each panel represents G_1 cells, the right-hand peak represent G_2 cells and the points in between, represent S-phase cells. E03 is a negative siRNA control, D11 is siRNA targeting T antigen. Cells were treated with the 100pmols of siRNAs. Cells were collected at each day point, and DNA content was analyzed.

The results of flow cytometry analyses indicated that the relative number of cells in G1 phase decreased while conversely, the relative number of cells in S phases increased in cells transfected with either E03 or D11 siRNAs on the second day after transfection. During exponential growth it seems likely that autocrine stimulation promotes cell proliferation after siRNA delivery in the cells as they grow, even the negative control. Also there might be a stimulation of growth causes by the change from OptiMEM medium to DMEM medium after 24 hours following siRNA transfection inasmuch as there are growth factors present in the DMEM which contains a higher

amount of FBS than in the Optimum medium. However, after the second day, the majority of cells began to gradually accumulate the G1 phase of cell cycle gradually. The fraction of cells reached the highest in the G1 phase on the fifth day post transfection (Table 7). The results clearly show accumulation of cells in G1 specifically related to T antigen silencing (D11 compared E03 transfection). However, it is not proportional to amount of T antigen, but, may be proportional to the cellular levels of BTG2 protein. (see Figure 40). BTG2 inhibits the proliferation of cells and has been shown to block the cell cycle transition at G1-S phase by inhibition of cyclin D1 expression.

Table 7. The summary of the fractions of cells in each cell cycle phase

	D11/E03		
Day	G1	S	G2
1	1.03	0.86	1.22
2	0.96	1.00	1.04
3	1.15	0.93	0.91
4	1.17	0.85	0.93
5	**1.44**	**0.59**	1.00

4.2 Induction of cellular senescence after T antigen silencing

Normal somatic cells proliferate for a limited number of doubling in culture and then enter an irreversible growth-arrested stage called replicative senescence. The key phenotypes of senescence include enlarged and flat cell morphology. β- galactosidase activity is used as a biomarker of senescent cells. We used senescence-associated β –galactosidase assay (SA-β-gal) to detect the senescent cells. Activity of β –galactosidase is detected using X-gal (5-bromo-4-chloro-indolyl-β-D-galactopyranoside), which forms an intense blue product (5-bromo-4-chloro-3-hydroxyindole), one of products of X-gal cleaved by the β- galactosidase. Thus the blue color can be used to identify the senescent cells. As seen in figure 34, senescent cells were detected 48

hours after transfection of the silencing siRNA, D11 but not in cells transfected with the nonsilencing control siRNA E03, in line 130 cells.

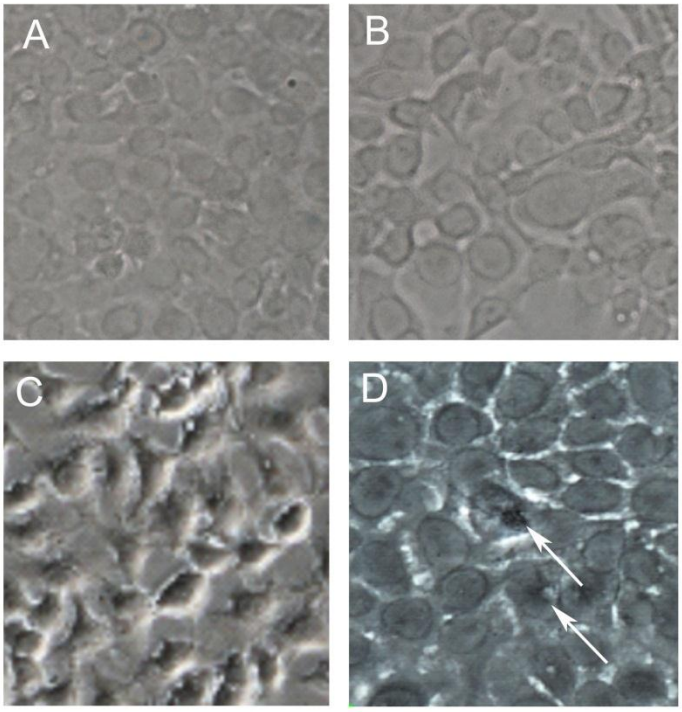

Figure 34. Induction of cellular senescence after T antigen silencing in line 130 cells. The β-galactosidase assay was performed by cytochemistry at pH 6.0. A. Line 130 cells treated by a negative siRNA (E03) for 24 hours. B. Line 130 cells treated by siRNA (D11) targeting T antigen for 24 hours. C. 130 cell lines treated by a negative siRNA (E03) for 48 hours. D. 130 cells treated by siRNA (D11) targeting T antigen for 48 hours. The arrows indicate blue color.

4.3 siRNA transfection induces activity of caspase 3/7 without apoptosis

The caspases are a family of cysteine-dependent aspartate-directed protease that are prominent among the programmed cell death proteases. Caspases recognize tetra-peptide sequences on their substrates and hydrolyze peptide bonds on the C-terminal end of aspartic acid residues. Caspase

3 and caspase 7 share similar substrate specificity by recognizing tetra-peptide motif Asp-x-x-Asp.(93) The C-terminal Asp is absolutely required while variations at other three positions can be tolerated. Caspase 3 is present in cytosol and nuclei, whereas active caspase 7 is localized in the microsomal compartment (94). Caspase-3 is the primary executioner caspase in the caspase system (95). It is necessary for the cytochrome *c*/dATP-inducible cleavage of fodrin and gelsolin. In addition, caspase 3 is required for internucleosomal DNA degradation and chromatin condensation as well (96, 97). Proteins such as the retinoblastoma protein (pRb) and p21 activated kinases (PAK2) that mediates genomic DNA degradation are all cleaved by caspase 3 during cell death. Caspase -7 cannot substitute for caspase-3 for the majority of the substrate cleavage events. So far only PARP as a substrate of caspase -7 has been identified (98). The activity of Caspase 3/7 was determined by a luminescent assay. Cell samples were collected over a five day period after siRNA transfection. The results showed that the Caspase 3 /7 activities increased more than four folds at the third day after siRNA transfection, which corresponds to the day of the lowest concentration of T antigen. However, the activity of Caspase 3/7 rapidly returned to normal level on the fourth day (Figure 35). To find out whether the apoptosis occurred when caspase 3/7 activity increases after siRNA transfection, flow cytometry was performed to determine DNA strand decomposition. The histographs of FACS are showed in Figure 33. Samples after siRNA transfection were compared with apoptosis-positive cells (Figure 36.B) and apoptosis-negative cells (Figure.36.A). No peak corresponding to apoptotic DNA degradation appeared in D11 siRNA transfected 130 cells, even when caspase 3/7 activity increased on the third day after siRNA transfection (Figure. 35). It means that caspase 3/7 activity is not correlated with DNA decomposition. Thus, it

appears that T antigen knock-down in this system induces senescence but not apoptosis. This has been observed in other studies (99-101) .

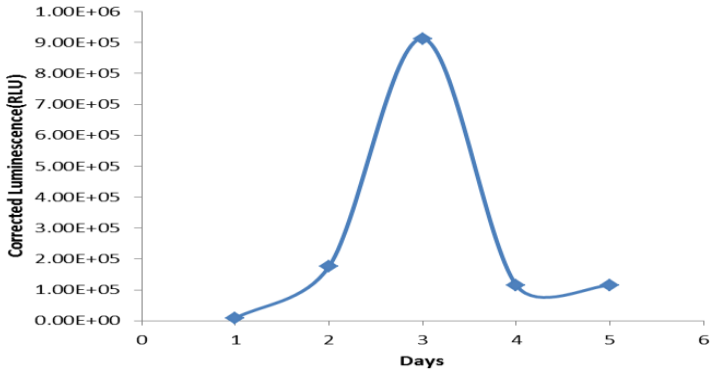

Figure35. Activity of Caspase 3/7 after siRNA transfection from one to five days.siRNA E03 is a negative control, Luminescence of D11 was corrected with E03

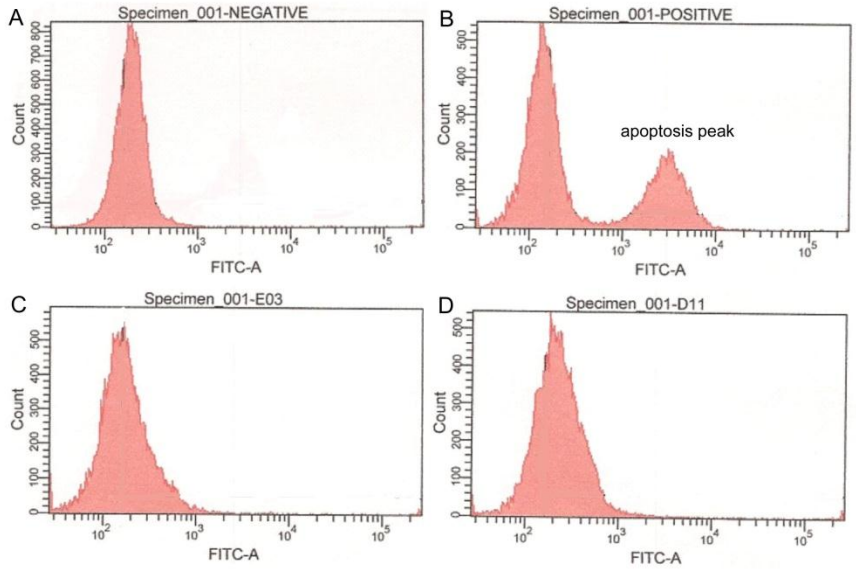

Figure 36. Apoptosis of Line 130 cells after three days siRNA transfection. Apoptosis was determined by flow cytometric analysis as described in Materials and Methods. A. Apoptosis in negative control cells (The Phoenix Inc.). B. Apoptosis in positive control cells (The Phoenix Inc.). C. Line 130 cells transfected with E03. D. Line 130 cells transfected with D11.

5. Signaling pathway regulation by knock-down mRNA of T antigen in SV40 transfected human keratinocyte cells

5.1 General outline of screen to identify genes that mediate T oncogene activity of SV40 virus

130 cells have been carried in culture over many years after the initial infection by SV40 that resulted in immortalization and transformation. Immortalization of cells by SV40 stems from the formation of a complex between the T antigen oncoprotein and the tumor suppressors p53 and Rb which inactivates them. This allows cells to overcome p53-mediated growth arrest and become immortalized. Since these tumor suppressors are known to affect a number of downstream pathways involving altered gene expression we sought to identify candidate genes that might mediate properties of transformation whose expression is directly modulated by T antigen. For this purpose we studied gene expression in 130 cells after T antigen silencing by siRNA knockdown using qPCR arrays with the idea that some of the genes identified in this screen might represent critical targets of T antigen responsible for T antigen mediated transformation in 130 cells. Using the qPCR expression array method, the regulation of cellular genes by knock-down of mRNA of T antigen were first examined with human signaling transduction pathways finder arrays in a 96 well plate format (SABiosciences) which contains eighty four genes related to eighteen signaling transduction pathways, including the Mitogenic Pathway, Wnt Pathway, Hedgehog Pathway, TGF-β Pathway, p53 Pathway, Stress Pathway, NFκB Pathway, NFAT Pathway, CREB Pathway, Jak-Stat Pathway, Estrogen Pathway, Androgen Pathway, Calcium and Protein Kinase C Pathway, Phospholipase C Pathway, Insulin Pathway, LDL Pathway, and Retinoic acid (RA) pathways. Ct values for the individual genes expressed in E03 vs D11 transfected cells were analyzed using the web based utility provided by

SABiociences. Table 8 shows the results of the qPCR array screen for the genes provided in the qPCR arrays.

Table 8. Altered expression of cellular genes in the human signaling transduction pathways finder array after T antigen silencing

	PAHS-014 Human Signaling Transduction Pathway Finder	Up-Down Regulation (comparing to control group)	
Symbol	Description	Fold Regulation	p-Value
ATF2	Activating transcription factor 2	-1.0253	0.984995
BAX	BCL2-associated X protein	2.0524	0.660662
BCL2	B-cell CLL/lymphoma 2	-1.0348	0.938379
BCL2A1	BCL2-related protein A1	-1.3623	0.858434
BCL2L1	BCL2-like 1	1.8626	0.603289
NAIP	NLR family, apoptosis inhibitory protein	1.0074	0.923245
BIRC2	Baculoviral IAP repeat containing 2	-1.0837	0.907558
BIRC3	Baculoviral IAP repeat containing 3	1.7867	0.592847
BMP2	Bone morphogenetic protein 2	-1.1804	0.949016
BMP4	Bone morphogenetic protein 4	-1.3098	0.899145
BRCA1	Breast cancer 1, early onset	-1.2249	0.910712
CCL2	Chemokine (C-C motif) ligand 2	1.475	0.854982
CCL20	Chemokine (C-C motif) ligand 20	-1.3781	0.814867
CCND1	Cyclin D1	1.0478	0.933682
CD5	CD5 molecule	1.8626	0.500854
CDK2	Cyclin-dependent kinase 2	-1.1832	0.935323
CDKN1A	Cyclin-dependent kinase inhibitor 1A (p21, Cip1)	7.2133	0.428499
CDKN1B	Cyclin-dependent kinase inhibitor 1B (p27, Kip1)	1.0772	0.841883
CDKN2A	Cyclin-dependent kinase inhibitor 2A (melanoma, p16, inhibits CDK4)	-1.2623	0.837396
CDKN2B	Cyclin-dependent kinase inhibitor 2B (p15, inhibits CDK4)	1.2634	0.812881
CEBPB	CCAAT/enhancer binding protein (C/EBP), beta	1.123	0.727662
CSF2	Colony stimulating factor 2 (granulocyte-macrophage)	1.8201	0.833467
CXCL9	Chemokine (C-X-C motif) ligand 9	-1.848	0.516767
CYP19A1	Cytochrome P450, family 19, subfamily A, polypeptide 1	1.7299	0.817511
EGR1	Early growth response 1	-1.0205	0.871414
EN1	Engrailed homeobox 1	-1.1669	0.939894
FAS	Fas (TNF receptor superfamily, member 6)	3.2959	0.526241
FASLG	Fas ligand (TNF superfamily, member 6)	1.1653	0.959686
FASN	Fatty acid synthase	1.0649	0.830945
FN1	Fibronectin 1	1.0168	0.940831
FOS	FBJ murine osteosarcoma viral oncogene homolog	2.0524	0.646739

PRKCE	Protein kinase C, epsilon	1.1282	0.886374
PTCH1	Patched 1	-1.1168	0.941748
PTGS2	Prostaglandin-endoperoxide synthase 2 (prostaglandin G/H synthase and cyclooxygenase)	1.3794	0.835897
RBP1	Retinol binding protein 1, cellular	-1.2108	0.849952
SELE	Selectin E	1.0624	0.961991
SELPLG	Selectin P ligand	-1.0713	0.837774
TANK	TRAF family member-associated NFKB activator	-1.0112	0.726609
TCF7	Transcription factor 7 (T-cell specific, HMG-box)	-1.0182	0.843766
TERT	Telomerase reverse transcriptase	-1.477	0.659535
TFRC	Transferrin receptor (p90, CD71)	-1.1219	0.939273
PMEPA1	Prostate transmembrane protein, androgen induced 1	-1.2136	0.942952
TNF	Tumor necrosis factor	-1.7851	0.485705
TP53	Tumor protein p53	-1.0963	0.957371
TP53I3	Tumor protein p53 inducible protein 3	3.9376	0.482273
VCAM1	Vascular cell adhesion molecule 1	1.373	0.723704
VEGFA	Vascular endothelial growth factor A	1.3572	0.695805
WISP1	WNT1 inducible signaling pathway protein 1	8.799	0.417367
WNT1	Wingless-type MMTV integration site family, member 1	-1.0565	0.554272
WNT2	Wingless-type MMTV integration site family member 2	-1.9354	0.705002
B2M	Beta-2-microglobulin	1.4784	0.575775
HPRT1	Hypoxanthine phosphoribosyltransferase 1	-1.1271	0.774093
RPL13A	Ribosomal protein L13a	1.0262	0.992017
GAPDH	Glyceraldehyde-3-phosphate dehydrogenase	-1.1376	0.921256
ACTB	Actin, beta	-1.1832	0.990048

FOXA2	Forkhead box A2	1.1653	0.959686
GADD45A	Growth arrest and DNA-damage-inducible, alpha	1.8117	0.584206
GREB1	Growth regulation by estrogen in breast cancer 1	3.7685	0.55505
GYS1	Glycogen synthase 1 (muscle)	-1.175	0.964109
HK2	Hexokinase 2	1.5627	0.614137
HOXA1	Homeobox A1	-1.0444	0.989447
HSF1	Heat shock transcription factor 1	-1.1887	0.933207
HSPB1	Heat shock 27kDa protein 1	-1.0205	0.963474
HSP90AA2	Heat shock protein 90kDa alpha (cytosolic), class A member 2	-1.1832	0.801242
ICAM1	Intercellular adhesion molecule 1	1.0168	0.974079
IGFBP3	Insulin-like growth factor binding protein 3	1.6709	0.698585
IKBKB	Inhibitor of kappa light polypeptide gene enhancer in B-cells, kinase beta	1.1256	0.867358
IL1A	Interleukin 1, alpha	1.1519	0.833568
IL2	Interleukin 2	1.1653	0.959686
IL4	Interleukin 4	1.1256	0.984286
IL4R	Interleukin 4 receptor	1.3262	0.776825
IL8	Interleukin 8	1.2374	0.83841
IRF1	Interferon regulatory factor 1	1.1439	0.876683
JUN	Jun proto-oncogene	1.3986	0.688825
KLK2	Kallikrein-related peptidase 2	-1.0276	0.901683
LEF1	Lymphoid enhancer-binding factor 1	-1.3007	0.902172
LEP	Leptin	-1.8912	0.972531
LTA	Lymphotoxin alpha (TNF superfamily, member 1)	-1.3007	0.71154
MDM2	Mdm2 p53 binding protein homolog (mouse)	5.1718	0.458491
MMP10	Matrix metallopeptidase 10 (stromelysin 2)	1.3922	0.691529
MMP7	Matrix metallopeptidase 7 (matrilysin, uterine)	1.0999	0.861372
MYC	V-myc myelocytomatosis viral oncogene homolog (avian)	1.1178	0.759229
NFKB1	Nuclear factor of kappa light polypeptide gene enhancer in B-cells 1	-1.1887	0.959204
NOS2	Nitric oxide synthase 2, inducible	1.3479	0.740005
NRIP1	Nuclear receptor interacting protein 1	1.123	0.907448
ODC1	Ornithine decarboxylase 1	-1.7934	0.774181
PECAM1	Platelet/endothelial cell adhesion molecule	1.1734	0.976264
PPARG	Peroxisome proliferator-activated receptor gamma	-1.1588	0.945246
PRKCA	Protein kinase C, alpha	1.0872	0.94422

The RT-PCR array assay was repeated for three times. We compared gene regulation of the SV40 transformed human keratinocyte with that of LT antigen silenced SV40 transformed human keratinocyte. After carefully examining the patterns of gene regulation, our results showed that three out of eighty four genes in the LT silenced the SV40 transformed human keratinocyte cells were upregulated over four fold. None of eighty four genes were under-expressed at the 4-fold cutoff level. Among the three genes, CDKN1A and MDM2 of them are related to the P53 signaling transduction pathway and WISP1 was involved the Wnt signaling transduction pathway. The affected genes and the related pathways are summarized in Table 9.

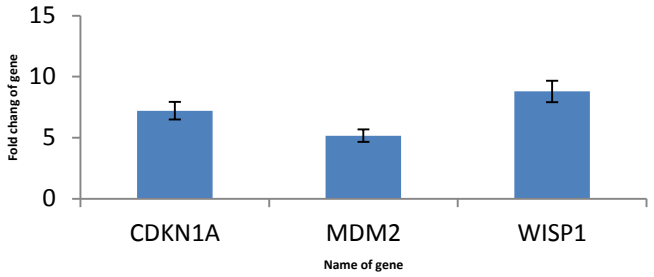

Figure 37. The expression of genes were up- regulated with T antigen inhibition using RT-PCR array of Human Signaling pathway finer (SABioscientific).

Table 9.Over –expressed genes and their functions from human signaling transduction pathway finer

Gene Symbol	Official name	Mean of Fold Regulation	Related pathway
CDKN1A	cyclin-dependent kinase inhibitor 1A (p21, Cip1)	7.21	P53 pathway
MDM2	Mdm2 p53 binding protein homolog	5.17	P53 pathway
WISP1	WNT1 inducible signaling pathway protein 1	8.8	Wnt pathway

5.2 BTG2 and GDD45A were up-regulated by knock-down mRNA of T antigen

In our PCR array studies, the CDKN1A and MDM2 genes which are in the p53 pathway were found to be upregulated. The p53 Pathway is related to the transcription factor p53 that responds to diverse stresses (including DNA damage, overexpressed oncogenes and various metabolic limitations) to regulate many target genes that induce cell-cycle arrest, apoptosis, senescence, and DNA repair. The Human P53 Signaling pathway RT-PCR array (PAHS-0277, SABiosciences) was utilized to find gene regulation dependent on knock-down mRNA of T antigen (Table. 10). This array contains 84 genes related to p53 mediated signal transduction. The array contains primers for genes involved in the processes of apoptosis, the cell cycle, cell growth, proliferation, differentiation, and DNA repair. After data analysis of PCR array, Four out of eighty four genes were found to be upregulated including MDM2 and CDKN1A. The most interesting gene was BTG2, which is an anti-proliferation gene that has not previously been implicated in the immortalization process by PaPoVa viruses. GDD45A, a growth arrest and DNA damage-inducible gene, is related to p53-resposive stress gene. The important functions of these genes are listed in table 11.

Table 10. Altered expression of cellular genes in human p53 signaling transduction pathway array after T antigen silencing.

	PAHS-027 P53 pathway	Fold Change (comparing to control group)	
Symbol	Description	Fold Change	p-value
APAF1	Apoptotic peptidase activating factor 1	2.1675	0.032842
ATM	Ataxia telangiectasia mutated	1.1429	0.666
ATR	Ataxia telangiectasia and Rad3 related	0.9262	0.012959
BAI1	Brain-specific angiogenesis inhibitor 1	1.0913	0.611563
BAX	BCL2-associated X protein	2.1228	0.001596
BCL2	B-cell CLL/lymphoma 2	0.8464	0.276424
BCL2A1	BCL2-related protein A1	0.8905	0.047838
BID	BH3 interacting domain death agonist	1.1669	0.055867
BIRC5	Baculoviral IAP repeat containing 5	0.5649	0.002321
BRCA1	Breast cancer 1, early onset	0.8044	0.040339
BRCA2	Breast cancer 2, early onset	0.7419	0.258954
BTG2	BTG family, member 2	4.305	0.161474
CASP2	Caspase 2, apoptosis-related cysteine peptidase	0.9835	0.954224
CASP9	Caspase 9, apoptosis-related cysteine peptidase	1.0492	0.450638
CCNB2	Cyclin B2	0.7402	0.007878
CCNE2	Cyclin E2	0.8843	0.493061
CCNG2	Cyclin G2	1.831	0.055529
CCNH	Cyclin H	0.9283	0.203473
CDK1	Cyclin-dependent kinase 1	0.7593	0.002698
CDC25A	Cell division cycle 25 homolog A (S. pombe)	0.8864	0.523965
CDC25C	Cell division cycle 25 homolog C (S. pombe)	0.8582	0.011574
CDK4	Cyclin-dependent kinase 4	0.777	0.072777
CDKN1A	Cyclin-dependent kinase inhibitor 1A (p21, Cip1)	8.0892	0.000233
CDKN2A	Cyclin-dependent kinase inhibitor 2A (melanoma, p16, inhibits CDK4)	0.9029	0.199457
CHEK1	CHK1 checkpoint homolog (S. pombe)	0.8405	0.132554
CHEK2	CHK2 checkpoint homolog (S. pombe)	1.059	0.687105
CRADD	CASP2 and RIPK1 domain containing adaptor with death domain	1.0938	0.029563
DNMT1	DNA (cytosine-5-)-methyltransferase 1	0.8503	0.185989
E2F1	E2F transcription factor 1	0.8701	0.528112
E2F3	E2F transcription factor 3	1.3497	0.930632
EGR1	Early growth response 1	0.7233	0.384341
EI24	Etoposide induced 2.4 mRNA	1.0492	0.641133
ESR1	Estrogen receptor 1	1.0963	0.442912
FADD	Fas (TNFRSF6)-associated via death domain	0.7663	0.163278
FASLG	Fas ligand (TNF superfamily, member 6)	1.4136	0.011748
FOXO3	Forkhead box O3	0.8967	0.699097
GADD45A	Growth arrest and DNA-damage-inducible, alpha	4.877	0.180735

GML	Glycosylphosphatidylinositol anchored molecule like protein	1.4136	0.011748
HDAC1	Histone deacetylase 1	0.9903	0.898983
HK2	Hexokinase 2	1.5721	0.259111
IFNB1	Interferon, beta 1, fibroblast	0.8641	0.002927
IGF1R	Insulin-like growth factor 1 receptor	1.2769	0.008047
IL6	Interleukin 6 (interferon, beta 2)	0.8503	0.038204
JUN	Jun proto-oncogene	1.274	0.27111
KRAS	V-Ki-ras2 Kirsten rat sarcoma viral oncogene homolog	0.8762	0.437879
PIDD	P53-induced death domain protein	3.2325	0.000251
MCL1	Myeloid cell leukemia sequence 1 (BCL2-related)	1.1942	0.115689
MDM2	Mdm2 p53 binding protein homolog (mouse)	6.3908	0.004738
MDM4	Mdm4 p53 binding protein homolog (mouse)	1.0396	0.816007
MLH1	MutL homolog 1, colon cancer, nonpolyposis type 2 (E. coli)	1.0468	0.560574
MSH2	MutS homolog 2, colon cancer, nonpolyposis type 1 (E. coli)	0.8742	0.073504
MYC	V-myc myelocytomatosis viral oncogene homolog (avian)	1.1914	0.495429
MYOD1	Myogenic differentiation 1	1.4136	0.011748
NF1	Neurofibromin 1	0.9633	0.986494
NFKB1	Nuclear factor of kappa light polypeptide gene enhancer in B-cells 1	0.9262	0.416779
TP53AIP1	Tumor protein p53 regulated apoptosis inducing protein 1	1.0989	0.578773
KAT2B	K(lysine) acetyltransferase 2B	0.689	0.31456
PCBP4	Poly(rC) binding protein 4	1.3435	0.310746
PCNA	Proliferating cell nuclear antigen	1.2334	0.203752
PPM1D	Protein phosphatase, Mg2+/Mn2+ dependent, 1D	1.6163	0.051096
PRC1	Protein regulator of cytokinesis 1	0.797	0.658366
PRKCA	Protein kinase C, alpha	0.9655	0.987455
PTEN	Phosphatase and tensin homolog	1.0468	0.555756
PTTG1	Pituitary tumor-transforming 1	0.8522	0.092994
RB1	Retinoblastoma 1	0.9588	0.896406
RELA	V-rel reticuloendotheliosis viral oncogene homolog A (avian)	1.1376	0.550801
RPRM	Reprimo, TP53 dependent G2 arrest mediator candidate	1.4136	0.011748
SESN1	Sestrin 1	3.3854	0.044986
SESN2	Sestrin 2	3.03	0.001025
SIAH1	Seven in absentia homolog 1 (Drosophila)	0.5861	0.058605
SIRT1	Sirtuin 1	0.7575	0.058642
STAT1	Signal transducer and activator of transcription 1, 91kDa	1.0738	0.769018
TADA3	Transcriptional adaptor 3	0.9566	0.698367
TNF	Tumor necrosis factor	1.1723	0.316626
TNFRSF10B	Tumor necrosis factor receptor superfamily, member 10b	2.1525	0.071217
TNFRSF10D	Tumor necrosis factor receptor superfamily, member 10d, decoy with truncated death domain	1.4433	0.419979
TP53	Tumor protein p53	0.8701	0.719237

GML	Glycosylphosphatidylinositol anchored molecule like protein	1.4136	0.011748
HDAC1	Histone deacetylase 1	0.9903	0.898983
HK2	Hexokinase 2	1.5721	0.259111
IFNB1	Interferon, beta 1, fibroblast	0.8641	0.002927
IGF1R	Insulin-like growth factor 1 receptor	1.2769	0.008047
IL6	Interleukin 6 (interferon, beta 2)	0.8503	0.038204
JUN	Jun proto-oncogene	1.274	0.27111
KRAS	V-Ki-ras2 Kirsten rat sarcoma viral oncogene homolog	0.8762	0.437879
PIDD	P53-induced death domain protein	3.2325	0.000251
MCL1	Myeloid cell leukemia sequence 1 (BCL2-related)	1.1942	0.115689
MDM2	Mdm2 p53 binding protein homolog (mouse)	6.3908	0.004738
MDM4	Mdm4 p53 binding protein homolog (mouse)	1.0396	0.816007
MLH1	MutL homolog 1, colon cancer, nonpolyposis type 2 (E. coli)	1.0468	0.560574
MSH2	MutS homolog 2, colon cancer, nonpolyposis type 1 (E. coli)	0.8742	0.073504
MYC	V-myc myelocytomatosis viral oncogene homolog (avian)	1.1914	0.495429
MYOD1	Myogenic differentiation 1	1.4136	0.011748
NF1	Neurofibromin 1	0.9633	0.986494
NFKB1	Nuclear factor of kappa light polypeptide gene enhancer in B-cells 1	0.9262	0.416779
TP53AIP1	Tumor protein p53 regulated apoptosis inducing protein 1	1.0989	0.578773
KAT2B	K(lysine) acetyltransferase 2B	0.689	0.31456
PCBP4	Poly(rC) binding protein 4	1.3435	0.310746
PCNA	Proliferating cell nuclear antigen	1.2334	0.203752
PPM1D	Protein phosphatase, Mg2+/Mn2+ dependent, 1D	1.6163	0.051096
PRC1	Protein regulator of cytokinesis 1	0.797	0.658366
PRKCA	Protein kinase C, alpha	0.9655	0.987455
PTEN	Phosphatase and tensin homolog	1.0468	0.555756
PTTG1	Pituitary tumor-transforming 1	0.8522	0.092994
RB1	Retinoblastoma 1	0.9588	0.896406
RELA	V-rel reticuloendotheliosis viral oncogene homolog A (avian)	1.1376	0.550801
RPRM	Reprimo, TP53 dependent G2 arrest mediator candidate	1.4136	0.011748
SESN1	Sestrin 1	3.3854	0.044986
SESN2	Sestrin 2	3.03	0.001025
SIAH1	Seven in absentia homolog 1 (Drosophila)	0.5861	0.058605
SIRT1	Sirtuin 1	0.7575	0.058642
STAT1	Signal transducer and activator of transcription 1, 91kDa	1.0738	0.769018
TADA3	Transcriptional adaptor 3	0.9566	0.698367
TNF	Tumor necrosis factor	1.1723	0.316626
TNFRSF10B	Tumor necrosis factor receptor superfamily, member 10b	2.1525	0.071217
TNFRSF10D	Tumor necrosis factor receptor superfamily, member 10d, decoy with truncated death domain	1.4433	0.419979
TP53	Tumor protein p53	0.8701	0.719237

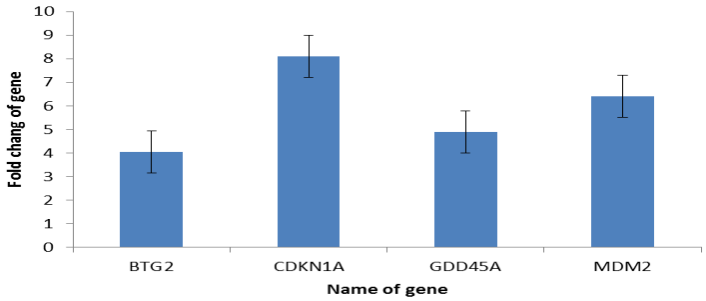

Figure 38. The expressions of genes were upregulated after T antigen silencing using RT-PCR array of human P53 signaling transduction pathway (SABioscientific).

Table - 11. Upregulated genes and their functions from RT-PCR array of P53 signaling transduction pathway

Gene Symbol	Official name	Mean of Fold Regulation	Related pathway
BTG2	BTG family, member 2	4.30	Negative Regulation of Cell Proliferation:
CDKN1A	cyclin-dependent kinase inhibitor 1A p21	8.09	Induction of Apoptosis Cell Cycle Arrest
GADD45A	growth arrest and DNA-damage-inducible, alpha	4.88	Cell Cycle Arrest DNA Repair Genes
MDM2	Mdm2 p53 binding protein homolog	6.39	Negative Regulation of Cell Proliferation:

5.3 FRZB, WNT2 were upregulated and SOX 17 was down regulated by know-down mRNA of T antigen

WISP1 overexpressed by LT antigen silenced in cell 130 line. WISP1 is related to Wnt pathway. Wnt signaling comprises three pathways: the canonical pathway and two non-canonical pathways, planar cell polarity (PCP) and a calcium ion-dependent pathway. The well-studied canonical Wnt pathway signals through ß-catenin and regulates the cell cycle, cell growth, and proliferation. The PCP pathway regulates cytoskeletal dynamics and cell motility, and the

WNT/calcium pathway promotes NFAT transcription, both independently of ß-catenin signaling. For further investigation, the Human Wnt Signaling Pathway PCR Array (PAHS-0432, SABioscientific) was used (Table.12). In which contains Wnt signaling ligands and receptors as well as other downstream signaling molecules for all three pathways. In addition, regulators of Wnt signaling are included as well as downstream target genes. The results showed in Figure. 39. The most important functions of these genes are listed in the table 13.

Table 12. The regulation of cellular genes of human Wnt signaling transduction pathway by inhibition of expression of T antigen.

	PAHS-043 Wnt pathway	Fold Change (comparing to control group)	
Symbol	**Description**	Fold Change	P-value
AES	Amino-terminal enhancer of split	0.9736	0.814466
APC	Adenomatous polyposis coli	0.7533	0.276048
AXIN1	Axin 1	0.8456	0.462703
BCL9	B-cell CLL/lymphoma 9	0.7691	0.105665
BTRC	Beta-transducin repeat containing	1.1313	0.280408
FZD5	Frizzled family receptor 5	1.3454	0.006799
CCND1	Cyclin D1	0.8301	0.214384
CCND2	Cyclin D2	1.0877	0.507379
CCND3	Cyclin D3	1.0434	0.91919
CSNK1A1	Casein kinase 1, alpha 1	0.8794	0.526148
CSNK1D	Casein kinase 1, delta	0.8554	0.189523
CSNK1G1	Casein kinase 1, gamma 1	1.2757	0.14834
CSNK2A1	Casein kinase 2, alpha 1 polypeptide	0.8979	0.459126
CTBP1	C-terminal binding protein 1	0.8835	0.619618
CTBP2	C-terminal binding protein 2	0.9274	0.370417
CTNNB1	Catenin (cadherin-associated protein), beta 1, 88kDa	0.9579	0.806474
CTNNBIP1	Catenin, beta interacting protein 1	1.7958	0.085245
CXXC4	CXXC finger protein 4	3.2671	0.004856
DAAM1	Dishevelled associated activator of morphogenesis 1	1.0678	0.502069
DIXDC1	DIX domain containing 1	1.4688	0.011022
DKK1	Dickkopf homolog 1 (Xenopus laevis)	0.921	0.588376
DVL1	Dishevelled, dsh homolog 1 (Drosophila)	0.9404	0.610385
DVL2	Dishevelled, dsh homolog 2 (Drosophila)	0.6696	0.28676
EP300	E1A binding protein p300	0.7799	0.26365
FBXW11	F-box and WD repeat domain containing 11	0.8714	0.203256
FBXW2	F-box and WD repeat domain containing 2	0.7327	0.18052
FGF4	Fibroblast growth factor 4	0.8856	0.590365
FOSL1	FOS-like antigen 1	1.4287	0.058238
FOXN1	Forkhead box N1	0.8244	0.663786
FRAT1	Frequently rearranged in advanced T-cell lymphomas	1.1055	0.640063
FRZB	Frizzled-related protein	4.1068	0.009518
FSHB	Follicle stimulating hormone, beta polypeptide	1.3177	0.013022
FZD1	Frizzled family receptor 1	1.1029	0.335541
FZD2	Frizzled family receptor 2	0.6948	0.147599
FZD3	Frizzled family receptor 3	0.7871	0.132591
FZD4	Frizzled family receptor 4	1.1366	0.568713
FZD6	Frizzled family receptor 6	0.6588	0.381856

FZD7	Frizzled family receptor 7	0.731	0.143696
FZD8	Frizzled family receptor 8	1.1313	0.146917
GSK3A	Glycogen synthase kinase 3 alpha	0.9189	0.547236
GSK3B	Glycogen synthase kinase 3 beta	1.1055	0.226638
JUN	Jun proto-oncogene	1.2935	0.211671
KREMEN1	Kringle containing transmembrane protein 1	1.2669	0.047232
LEF1	Lymphoid enhancer-binding factor 1	0.9317	0.679734
LRP5	Low density lipoprotein receptor-related protein 5	1.1287	0.768844
LRP6	Low density lipoprotein receptor-related protein 6	1.1418	0.451302
MYC	V-myc myelocytomatosis viral oncogene homolog (avian)	1.1029	0.676832
NKD1	Naked cuticle homolog 1 (Drosophila)	0.9253	0.555727
NLK	Nemo-like kinase	0.9042	0.571343
PITX2	Paired-like homeodomain 2	1.0531	0.745308
PORCN	Porcupine homolog (Drosophila)	1.2611	0.066773
PPP2CA	Protein phosphatase 2, catalytic subunit, alpha isozyme	0.7853	0.071824
PPP2R1A	Protein phosphatase 2, regulatory subunit A, alpha	0.9021	0.502404
PYGO1	Pygopus homolog 1 (Drosophila)	0.6727	0.086203
RHOU	Ras homolog gene family, member U	1.3454	0.135322
SENP2	SUMO1/sentrin/SMT3 specific peptidase 2	0.721	0.221993
SFRP1	Secreted frizzled-related protein 1	0.9339	0.747611
SFRP4	Secreted frizzled-related protein 4	1.0953	0.955221
FBXW4	F-box and WD repeat domain containing 4	0.9404	0.525951
SLC9A3R1	Solute carrier family 9 (sodium/hydrogen exchanger), member 3 regulator 1	1.0079	0.92893
SOX17	SRY (sex determining region Y)-box 17	-5.4101	0.35672
T	T, brachyury homolog (mouse)	0.7378	0.356909
TCF7	Transcription factor 7 (T-cell specific, HMG-box)	0.587	0.192686
TCF7L1	Transcription factor 7-like 1 (T-cell specific, HMG-box)	0.7656	0.347609
TLE1	Transducin-like enhancer of split 1 (E(sp1) homolog, Drosophila)	0.9469	0.770308
TLE2	Transducin-like enhancer of split 2 (E(sp1) homolog, Drosophila)	0.7908	0.003743
WIF1	WNT inhibitory factor 1	0.6964	0.263004
WISP1	WNT1 inducible signaling pathway protein 1	6.9259	0.036178
WNT1	Wingless-type MMTV integration site family, member 1	1.8764	0.216168
WNT10A	Wingless-type MMTV integration site family, member 10A	1.0243	0.825189
WNT11	Wingless-type MMTV integration site family, member 11	1.4025	0
WNT16	Wingless-type MMTV integration site family, member 16	1.0243	0.768579
WNT2	Wingless-type MMTV integration site family member 2	4.7371	0.09004
WNT2B	Wingless-type MMTV integration site family, member 2B	0.591	0.090018
WNT3	Wingless-type MMTV integration site family, member 3	0.8111	0.412396
WNT3A	Wingless-type MMTV integration site family, member 3A	0.4947	0.393557
WNT4	Wingless-type MMTV integration site family, member 4	1.6036	0.370778
WNT5A	Wingless-type MMTV integration site family, member 5A	0.4459	0.387805
WNT5B	Wingless-type MMTV integration site family, member 5B	0.8534	0.096859
WNT6	Wingless-type MMTV integration site family, member 6	0.8794	0.581683
WNT7A	Wingless-type MMTV integration site family, member 7A	1.6298	0.085628
WNT7B	Wingless-type MMTV integration site family, member 7B	1.0928	0.538995
WNT8A	Wingless-type MMTV integration site family, member 8A	0.6498	0.435133
WNT9A	Wingless-type MMTV integration site family, member 9A	1.988	0.054279
B2M	Beta-2-microglobulin	1.1739	0.11198
HPRT1	Hypoxanthine phosphoribosyltransferase 1	1.0126	0.787992
RPL13A	Ribosomal protein L13a	1.1106	0.113499
GAPDH	Glyceraldehyde-3-phosphate dehydrogenase	0.9535	0.726838

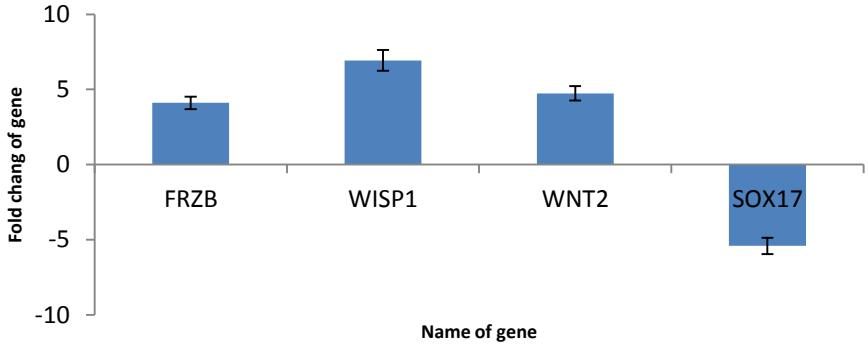

Figure 39. The expressions of genes were up- or down- regulated with T antigen inhibition using RT-PCR array of human Wnt signaling transduction pathway (SABioscientific).

Table13 .Over –expressed and under –expressed genes from the Wnt signaling transduction pathway

Gene Symbol	Official name	Mean of Fold Regulation	Related pathway
FRZB	frizzled-related protein	4.11	Negative Regulation Wnt pathway
WISP1	WNT1 inducible signaling pathway protein 1	6.92	Regulation of Growth
WNT2	Wnt oncogene analog 2	4.74	Frizzled-2 Signaling Pathway
SOX17	SRY (sex determining region Y)-box 17	-5.41	Other Regulators of Transcription

5.4 Regulation of cellular genes related to BTG2 gene signaling transduction pathway by silencing T antigen

Since blocking T antigen induced BTG2 expression, some genes interacting with BTG2 may be affected by T antigen as well. To investigate the regulation of these genes, thirty-one pairs of primers related to cell proliferation were designed. Expression of these genes in 130 cell line was determined by RT-PCR. The results showed that five genes (BTG2, Fas, CDKN1A, GADD45A and MDM2) out of the thirty one were up-regulated over two fold; and five genes (TGFβ2, Bbl, Ras, CCNA2 and CDKN2A) were down-regulated over two fold (Figure 40). In

addition, the gene of p53 was down-regulated 1.9 fold (Figure 40.A)

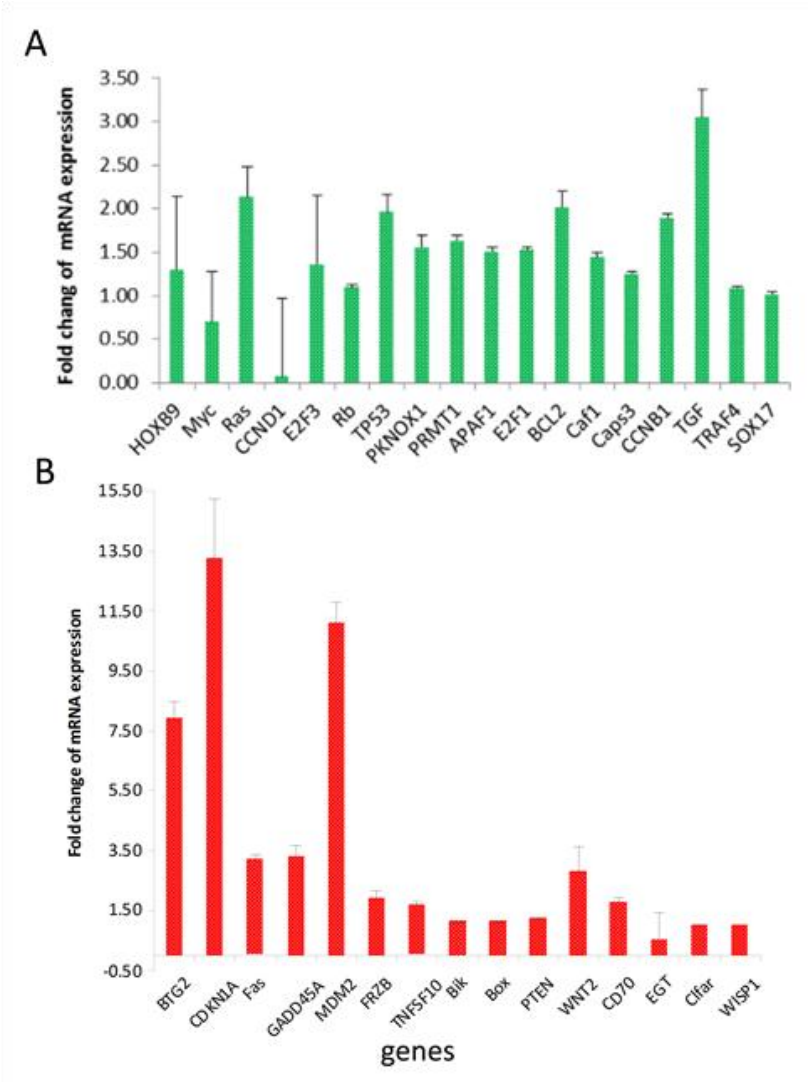

Figure 40. The expression of thirty- one genes after T antigen knock-down in 130 cells. GAPDH was used as internal standard. A. Down-regulated genes (green); TGF-β2, for example, was down-regulated 3 fold. B. Up-regulated genes (red).

The expression of genes related to senescence or apoptosis pathways was quantitated by RT-PCR. Eleven out of fifty-four senescence or apoptosis related genes were up-regulated but only two of them, SERPINE1 and TGFB2, were changed by more than two fold (Figure 41. C) and

B). Sixteen genes were down-regulated over two fold, which are NBN, ATM, CDK2, BM1, CCNE1, PPP1R15A, SIRT1, SERPINB2, RB1, PIK3CA, MAPK14, CDC25C, CHEK1, CDKN2D and CDKN2A (Figure 41. A and B). We investigated translation of some of these genes in the following studies.

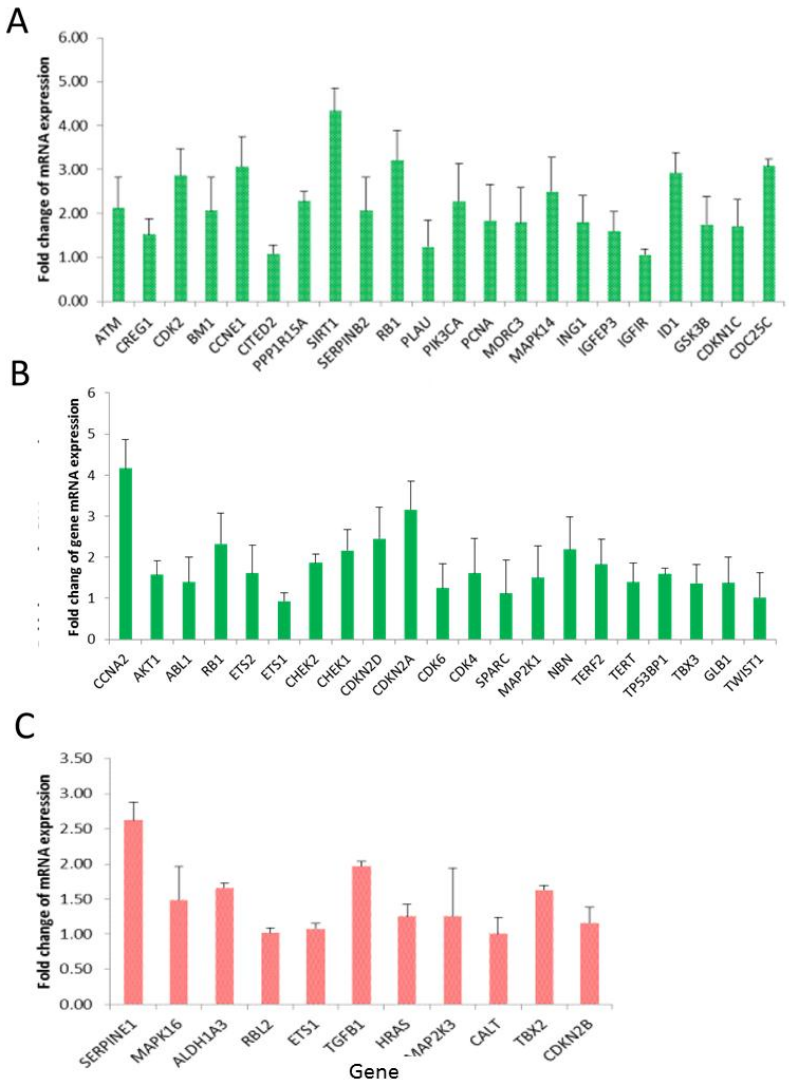

Figure 41. The regulation of fifty-four genes related to senescence or apoptosis pathways by T antigen mRNA in line 130 cells. GAPDH was the internal standard. A. and B. Forty-three genes were down-regulated. C. Eleven genes were up-regulated.

5.5 BTG2 expression is blocked by the SV40 Large T antigene.

As a focus for further studies we examined a possible role for BTG2 as a novel mediator of immortalization. In experiments in which D11 (vs. E03) was used to knock down T antigen expression, we found that BTG2 expression correlated with suppression of T antigen (Figure 42). BTG2 is a very labile protein with a short half-life of about 15 minutes (102) and is usually difficult to detect by immunoblotting at endogenous levels. Therefore, we first assessed possible alterations of *BTG2* expression at the mRNA level by quantitative RT-PCR. As shown in Figure 40. The amount of fusion protein of BTG2 was determined by western blot as shown in Figure 42. In Line 130 cells, the decrease in Large T antigen level is correlated with up-regulation of BTG2. In other words, T antigen blocks the expression of BTG2. No BTG2 fusion protein was detected from normal human epidermal cells (NHEK). In addition, the results showed that the expression of BTG2 mRNA is correlated with cell density, which was observed by (67, 103).

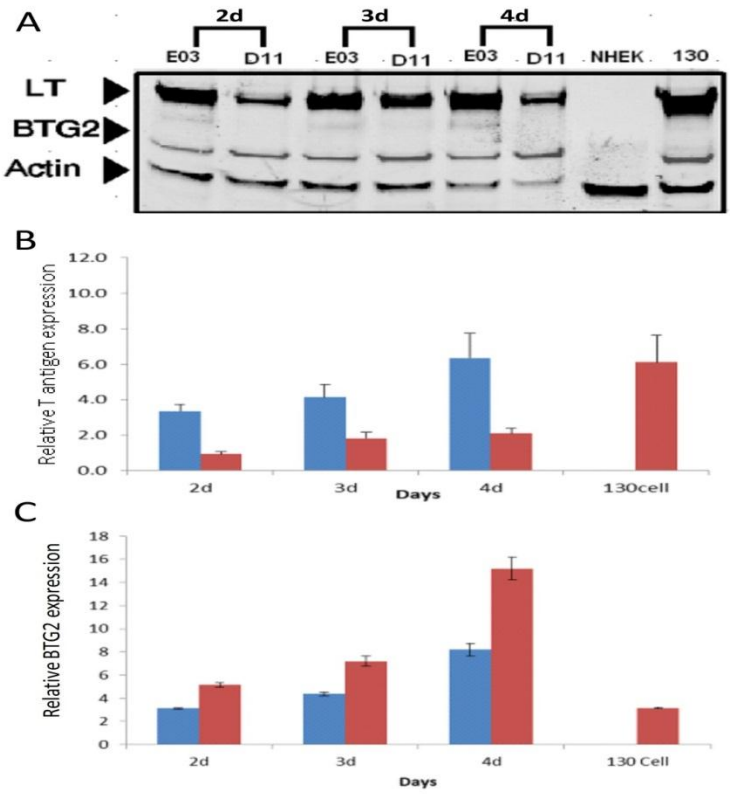

Figure 42. Protein expression of T antigen and BTG2 in Line 130 cells at various days.

A. western blot of T antigen and BTG2 protein. The T antigen was probed with a mouse anti-large T antibody (Santa Cruz), and BTG2 protein was probed with a rabbit anti-BTG2 antibody (GenWay). Actin was probed with a mouse anti-actin antibody (Licor). IRDye 800CW goat anti-mouse secondary antibody and IRDye 680LT goat anti-rabbit secondary antibody (Licor) were used. B. The expression of T antigen relative to the expression of actin. C. The expression of BTG2 relative to the expression of actin. (Blue bars are negative control of siRNA, red bars are siRNA targeting T antigen)

5.6 Inducing of BTG2 expression in SV40 transformed human epithelial cells is p53 dependent

The stimulation of BTG2 expression can be effect by both p53 –dependent and p53- independent pathways. Since T antigen can functionally antagonize p53, we wished to determine whether the observed BTG2 stimulation was p53-dependent. The results revealed that as the expression of T antigen was reduced by siRNA targeting, the expression of BTG2 was concomitantly increased. In contrast, p53 gene expression was repressed 1.8 fold (Figure 40A). p53 is normally highly mutated in many cancer and immortalized cell lines, but p53 is generally not mutated in human epithelial cells which have been immortalized by SV40 (104). In our western blots we found that wild type p53 is in normal human epidermal cells is expressed at low levels (Figure 40A, Figure 43).

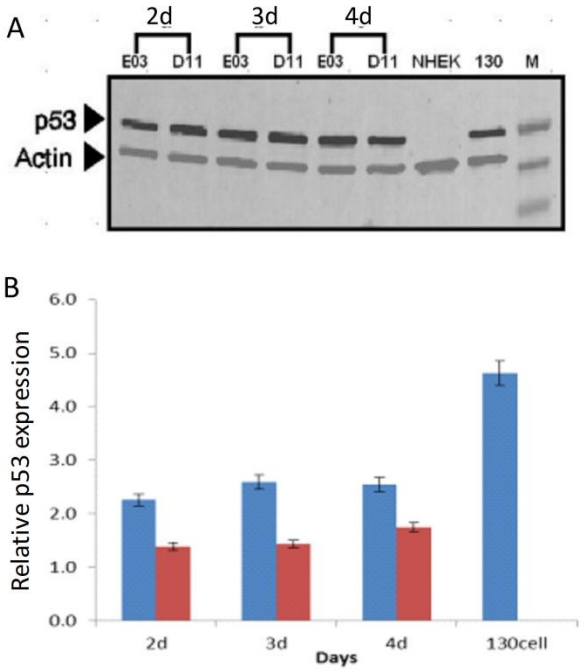

Figure. 43. Expression of p53 protein in Line 130 cells at various days. A. western blot was probed with a mouse anti-p53 antibody (Santa Cruz). Actin was visualized with a rabbit anti-actin antibody (Licor). IRDye 800CW goat anti-mouse secondary antibody and IRDye 680LT goat anti-rabbit secondary antibody (Licor) were used. B. The expression of p53 in relative to the

expression of actin in each sample; (blue is a negative control of siRNA, red is siRNA targeting T antigen)

When p53 protein concentration increased gradually day by day after siRNA transfection, which is correspond to T antigen concentration increase, since the siRNA targeting T antigen is only constant during short time, usually silencing function of siRNA persists about four to five days after transfection of siRNA.

Since T antigen binding to wild type p53 in SV40 transformed cells increases the stability of p53, the cellular levels of p53 protein (as well as levels of its mRNA transcripts) are high (Figure 40 and 43), but inactivated. Even as levels of p53 protein were reduced as the result of silencing of T antigen, expression of BTG2 was still greatly stimulated (Figure 40 and 43). This suggests that despite the fact that the concentration of p53 protein was decreased in D11 transfected cells, its overall activity was elevated. BTG2 levels are regulated by a feedback mechanism in that p53 protein binds to BTG2 and the p53-BTG2 complex gene induces BTG2 transcription. Thus, BTG2 regulation is p53-dependent in SV40 transformed human epithelial cells. (Figure 44)

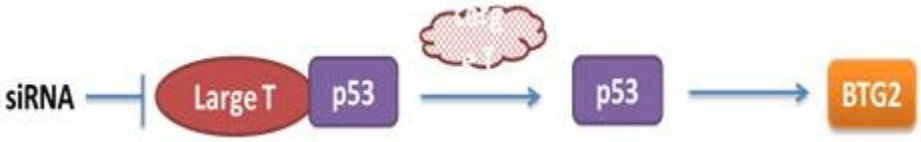

Figure 44. BTG2 regulation is p53-dependent

5.7 Mdm2 expression was induced enormously by Silence of the SV40 T antigen

Mdm2, a p53 binding protein homolog is a target gene of p53. The encoded protein is a nuclear phosphoprotein. Mdm2 functions as an ubiquitin E3 ligase and induces p53 protein degradation through ubiquitination-proteasome pathway, as part of an auto regulatory negative feedback loop for controlling cell proliferation. Overexpression of Mdm2 results in excessive inactivation of p53, diminishing its tumor suppressor function. Mdm2 also interacts with pRb and inhibits pRb functions in part by blocking Rb-E2F-DNA complex formation (105). In addition, Mdm2 promotes pRb interaction with the proteasome (106), leading to a proteasome-dependent ubiquitin-independent degradation of pRb (105). As a result Mdm2 affects the cell cycle, apoptosis, and tumorigenesis.

In our study system, T antigen affects Mdm2 expression and translation indirectly (Figure 46). T antigen binds to p53 and abolishes its functions by forming T antigen-p53 complex which leads to highly enhanced p53 level in SV40- transformed Line 130 cells. During cellular transformation, the increase in p53 levels correlates with an enhanced SV 40 transformation. Since the T antigen-p53 complex and free T antigen differ in their phosphorylation patterns (107), the phosphorylation of T antigen–p53 complex is significantly higher than free T antigen phosphorylation. Since the phosphorylation status of T antigen –p53 complex was changed by SV40 transformation, more T antigen-p53 complex can bind to Mdm2 and form a trimeric complex as well (108) (Figure 45).

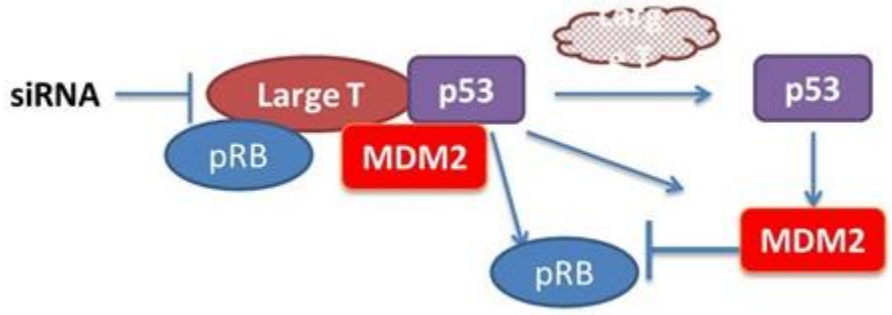

Figure 45. Large T antigen binds p53 and MDM2 forming a trimer complex

Mdm2 becomes metabolically stabilized during SV40 transformation in a similar pattern as for p53, but Mdm2 binding with T antigen was not as strong as p53 Binding to T antigen (Fig 43 and 46). Mdm2 also quantitatively binds the free p53 in SV40-transformed cells as well. In our studies, after T antigen was silenced in 130 cells, the expression of Mdm2 was up-regulated over tenfold determined by RT-PCR (Figure 40 B). Western blot assay revealed that the protein level of Mdm2 was significantly increased, compared with that of 130 cells (Figure 46). Also we observed that the highest protein concentration of MDM2 was at the second day after siRNA transfection (Figure. 46) and corresponded to the lowest concentration of T antigen, meaning that T antigen knock-down is a key point in p53 activation. In other words, p53 stimulates Mdm2 expression. Mdm2 protein was gradually decreased two days after siRNA transfection. We compared protein levels of p53 and MDM2 in Line 130 cells with those in T antigen silenced Line 130 cells. The protein level of p53 was much higher than that of Mdm2 in 130 cells, even higher than a negative control. Nevertheless, the Mdm2 protein level in 130 cells was the same as a siRNA negative control. This finding made it difficult to explain whether a negative control siRNA can interfere with the stability of the T antigen-p53 complex.

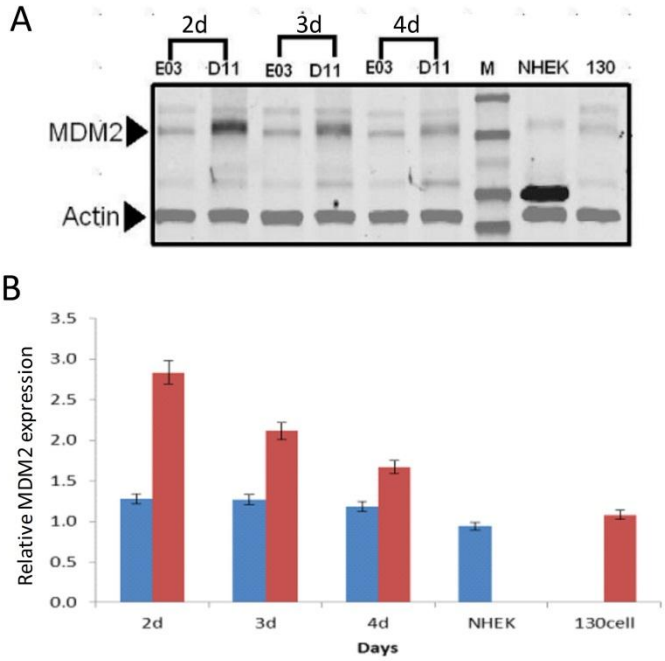

Figure. 46. 130 cells were transfected with siRNAs, Protein expression of Mdm2 (90KD) was analyzed by Western blot at various days. A. Mdm2 blot was probed with a mouse anti-Mdm2 antibody (Santa Cruz), Actin was probed with a rabbit anti-actin antibody (Licor). Two secondary antibodies were used, IRDye 800CW goat anti-mouse secondary antibody and IRDye 680LT goat anti-rabbit secondary antibody (Licor). B. The expression of Mdm2 is shown as relatove to the expression of actin in each sample; (blue is a negative control of siRNA, red is siRNA targeting T antigen.

5.8 Silencing of SV40 T antigen stimulates CDKN1A gene expression

As a transcriptional activator, p53 regulates more than one cell cycle checkpoint-related genes. Among the genes that were shown to be induced by p53 in cells are Mdm2, GADD45, and p21 (WAF1/CIP1) (109). We examined the transcription of these p53 regulated molecules, because it had been documented that T antigen binding to p53 may adversely affect its function.

The CDKN1A gene encodes a potent cyclin-dependent kinase inhibitor. The encoded protein binds to and inhibits the activity of cyclin-CDK2 or -CDK4 complexes, and thus functions as a regulator of cell cycle progression at the G1/S interface (110). The expression of this gene is tightly controlled by the tumor suppressor protein p53, through which this protein mediates the p53-dependent cell cycle G1/S phase arrest in response to a variety of stress stimuli. This protein can interact with proliferating cell nuclear antigen (PCNA), a DNA polymerase accessory factor, and plays a regulatory role in S phase DNA replication and DNA damage repair (111) (Figure 47).

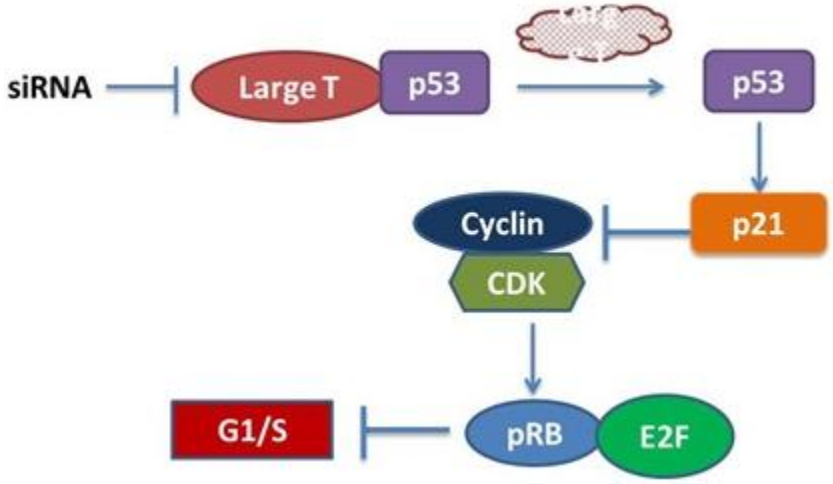

Figure 47. Expression of CDKN1A induces cell cycle G1/S phase arrest

In our studies, P53- induced p21 expression can be inhibited by T antigen binding. After T antigen was silenced, the expression of CDKN1A (the p21 gene) was up-regulated more than tenfold (Figure 40. B). More experiments of Western blot are required to determine whether p21 level is elevated. (Figure 48A and B) since the p21 antibody produced more than two bands on the membrane, there was not a significant change). It is well known that the expression of CDKN1A is transcriptionally regulated by p53 therefore, inactivation of the T antigen should

lead to activation of p53 and induction of CDKN1A in SV40 T antigen transformed immortalized cells.

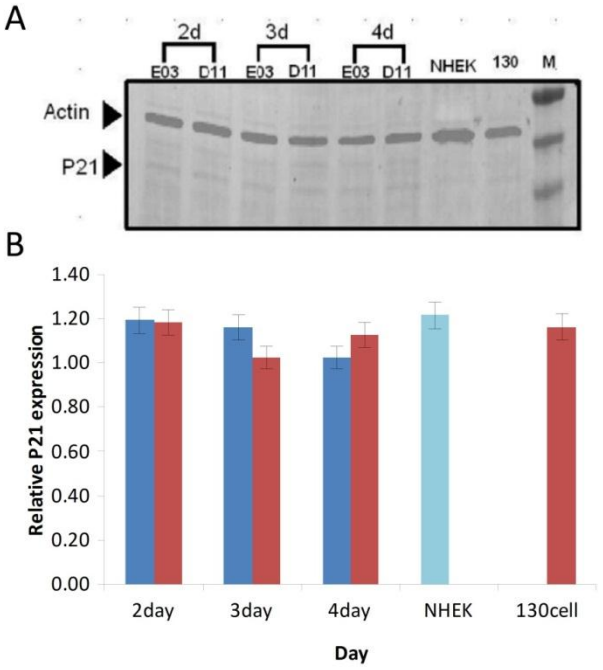

Figure 48. CDKN1A expression in Line 130 cells transfected with E03 and D11 siRNAs. p21 was analyzed by Western blot at various days. A. Western blot probed with a mouse anti-p21 antibody (Santa Cruz Biotech). Actin was visualized with a rabbit anti-actin antibody (Licor). IRDye 800CW goat anti-mouse antibody and IRDye 680LT goat anti-rabbit antibody (Licor) were used as secondary antibodies. B. The expression of p21 in relative to the expression of actin. Blue bars: negative control of siRNA, red bars: siRNA targeting T antigen.

5.9 Silencing of SV40 T antigen stimulates GDD45A gene expression

Growth arrest and DNA damage 45α (Gadd45), a p53- and BRCA1-regulated stress-inducible gene, has been characterized as one of the important players that participate in cellular response to a variety of DNA damage agents (112-114). GADD45A protein has been reported to interact

with multiple important cellular proteins, including Cdc2 protein kinase, proliferating cell nuclear antigen (PCNA), p21Waf1/Cip1 protein (115, 116), core histone protein and MTK/MEKK4, an up-stream activator of the JNK/SAPK pathway (113, 117), indicating that GADD45A may play important roles in the control of cell cycle checkpoint, DNA repair process, apoptosis and signaling transduction (118). Interestingly, the signaling machinery that regulates GADD45A induction by genotoxic stress and DNA damage involves both p53-dependent and -independent pathways; the latter may employ BRCA1-related or MAP kinase-mediated signals (119). The transcription and translation of GADD45A is known to be stimulated by the activated p53 (114, 120) (Figure 49).

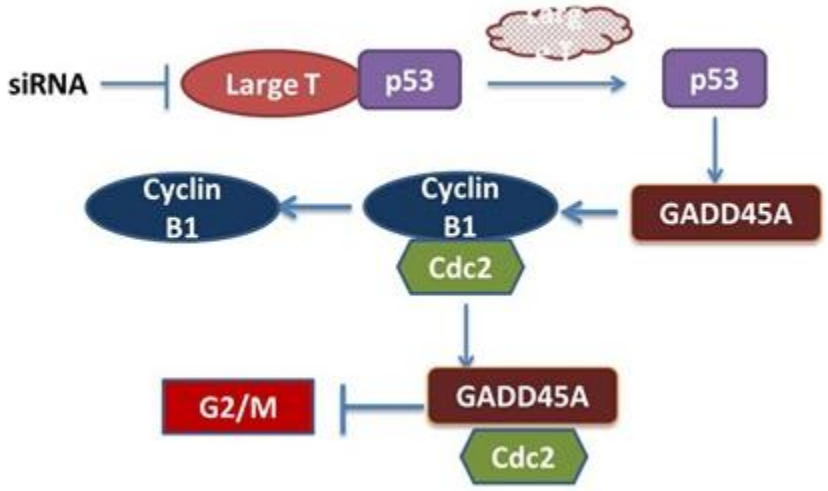

Figure 49. GADD45A inhibits cell cycle G2/M phase transition

In our studies, the expression of GADD45A was increased by over two fold after T antigen was silenced by siRNA (Figure 40.B). However, we did not detect any significant change in the protein level (Figure 50). Elevated GADD45A expression inhibits cell proliferation which is related to cell cycle arrest, senescence or apoptosis. On the other hand, decreased GADD45A expression is considered a survival mechanism as cancer cells can evade the apoptotic pathway without GADD45A leading to increased tumorigenesis.

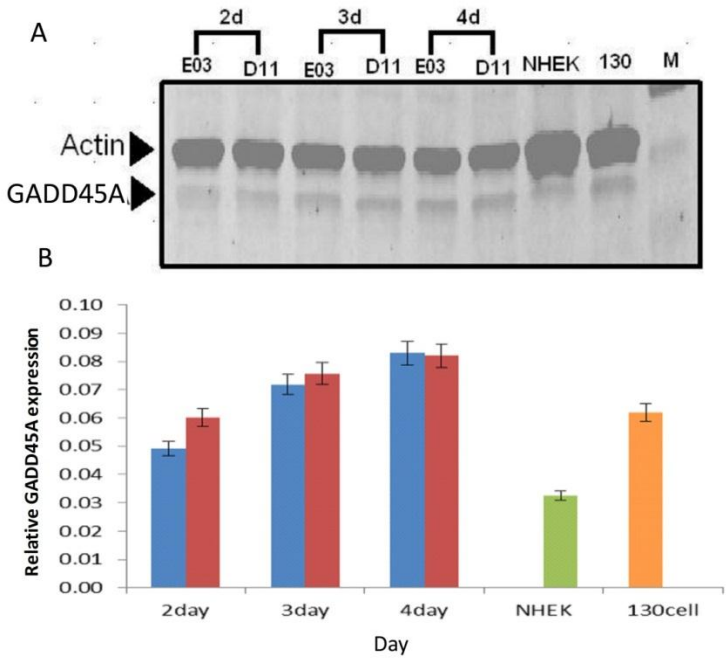

Figure. 50. Protein expression of GADD45A in Line 130 cells at various days. A. GADD45A western blot probed with a mouse anti-GADD45A antibody (Santa Cruz). Actin was probed with a rabbit anti-actin antibody (Licor). IRDye 800CW goat anti-mouse antibody and IRDye 680LT goat anti-rabbit antibody (Licor) were used as secondary antibodies. B. The expression of GADD45A in relative to expression of actin. Blue bars: negative control of siRNA, red bars: siRNA targeting T antigen.

5.10 Transcription of CCND1 was not changed by silenced T antigen

The CCND1 gene encodes the cyclin D1 protein that belongs to the highly conserved family of cyclins. Transcription of CCND1 is up-regulated by Rb (76, 121, 122). Cyclin D proteins are characterized by a periodicity in protein abundance throughout the cell cycle. Cyclin D1 is a regulator of Cdk kinases. The regulatory component of cyclin D1-Cdk4 complex phosphorylates

and inhibits members of retinoblastoma (pRb) protein family including pRb and regulates the cell-cycle during G(1)/S transition. Phosphorylation of pRb allows dissociation of the transcription factor E2F from the Rb/E2F complex and the subsequent transcription of E2F target genes which are responsible for the cell progression through the G1 phase (123). Mutations, amplification and overexpression of *CCND1* gene will alter cell cycle progression and may contribute to tumorigenesis.

We tested the expression of pRb and p53. The level of both of the proteins reduced after T antigen was silenced in Line 130 cells. However, the activity of p53 was increased by T antigen silencing as explained before. The activated p53 induces *BTG2* transcription, and expression of *BTG2* causes accumulation of hypophosphorylated, growth-inhibitory forms of pRb and leads to G1 arrest through impairment of DNA synthesis (76, 77, 124). As a result, inactivated pRb inhibits transcription of CCND1. Therefore, CCND1 transcription level does not change after T antigen silencing in Line 130 cells(Figure 51). This was also demonstrated in our studies (Figure 40A, and 41). It means that only p53 is activated after T antigen silencing in Line 130 cells, while pRb is still inactivate through BTG2 regulation.

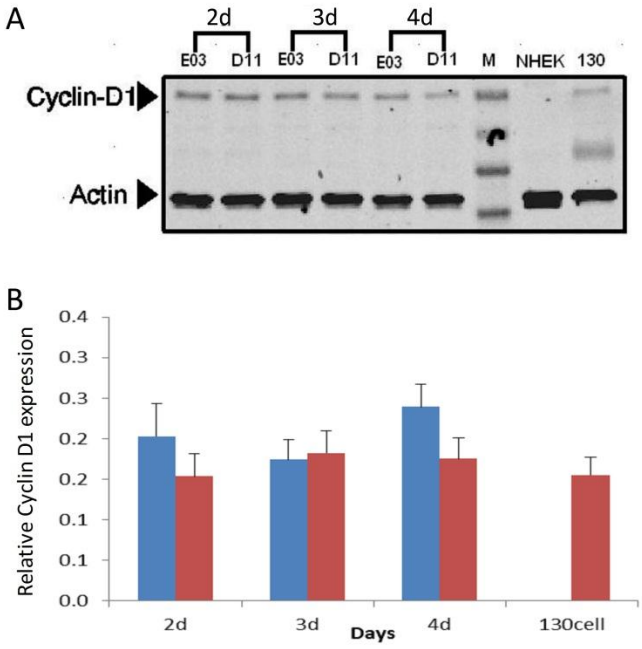

Figure 51. Protein expression of Cyclin D1 in Line 130 cells. A. Cyclin D1level at different days. Cyclin D1 was probed with a mouse anti-Cyclin D1 antibody (Santa Cruz). Actin was probed with a rabbit anti-actin antibody (Licor). IRDye 800CW goat anti-mouse antibody

5.11 Transcription of Cdc25c was down-regulated by silenced T antigen

Cdc25c (cell division cycle 25 homolog C) gene encodes a tyrosine phosphatase. The phosphatase removes phosphate groups from only selected phosphotyrosines on a substrate of tyrosine phosphorylated proteins. Cdc25C protein, which is an activator of CDC2 kinase, regulates the cell-division cycle and some signaling cytokine responses by dephosphorylating activated forms (125-127).

Mammalian cell division is controlled by a number of regulatory factors, including mitotic cyclins A, B1, and B2, mitotic kinase Cdc2 and mitotic phosphatase Cdc25C. During cell division, Cdc25c directs dephosphorylation of cyclin B-bound CDC2 and triggers entry into mitosis. In SV40 T antigen-expressing cells, cyclin B/CDC2 activity is constantly at elevated

level (128) and the protein level of Cdc25C increases more than two fold (129, 130). However, the overall level of cyclin B is not affected by expression of SV40 T antigen. Increased expression of this phosphatase contributes to the elevated mitotic kinase activities, which leads to mitotic initiation. Cdc25c activity can be regulated by its phosphorylation reaction (129). Phosphorylation of Cdc25C by Chk kinase creates a binding site for 14-3-3 protein that can anchor Cdc25C in the cytoplasm, thus preventing Cdc2 activation. The dual specificity phosphatase Cdc25C mediates cell cycle progression into mitosis and also serves as a checkpoint at G2 phase (Figure 52).

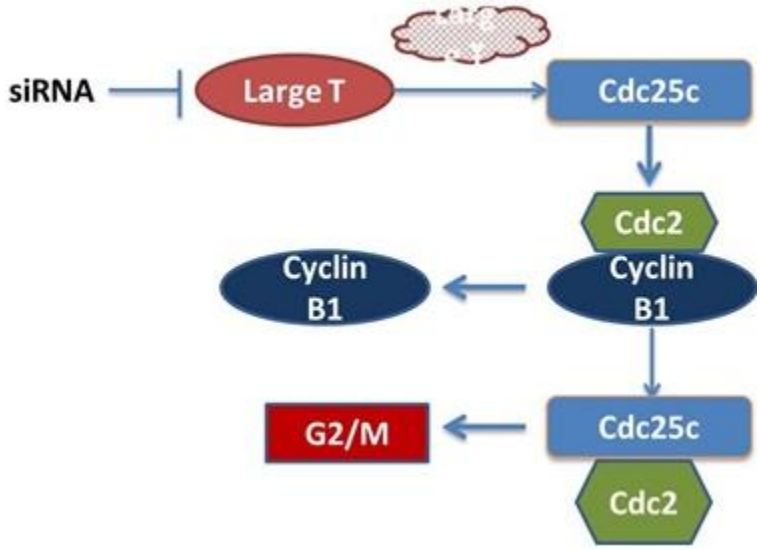

Figure 52. Cdc25c serves as a checkpoint at G2 phase

In our studies, contrary to Yuan L's study (119), Cdc25c transcription was down regulated more than two fold by silenced T antigen (Fig 40. A), and the protein of Cdc25c were inhibited as well (Figure 53). The cell transition from G2 to M phase may be arrested by low protein level of Cdc25c.

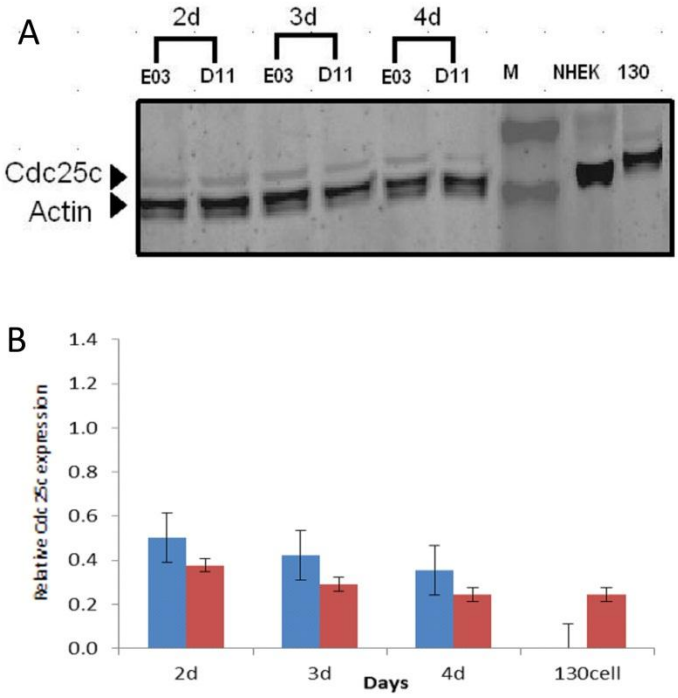

Figure. 53. Protein expression of Cdc25c in Line 130 cells at various days. A. Cdc25c level at various days. Cdc25c was probed with a mouse anti-Cdc25c antibody (Santa Cruz), Actin was probed with a rabbit anti-actin antibody (Licor). IRDye 800CW goat anti-mouse antibody and IRDye 680LT goat anti-rabbit antibody (Licor) were used as secondary antibodies. B. The expression of Cdc25c in relative to actin expression. Blue bars: negative control of siRNA, red bars: siRNA targeting T antigen.

5.12 Transcription of HOXB9 was regulation various by silenced T antigen

The p53-regulated protein BTG2 interacts with the homeoprotein HoxB9 and enhances its transcriptional activation. BTG2 enhance Hoxb9-mediated transcription with formation of a Hoxb9·BTG2 complex on a Hoxb9-responsive target to DNA. This interaction may mediate anti-proliferative functions (77, 131). Protein level of HOXB9 in our studies has not been changed by silencing LT antigen (Figure 54).

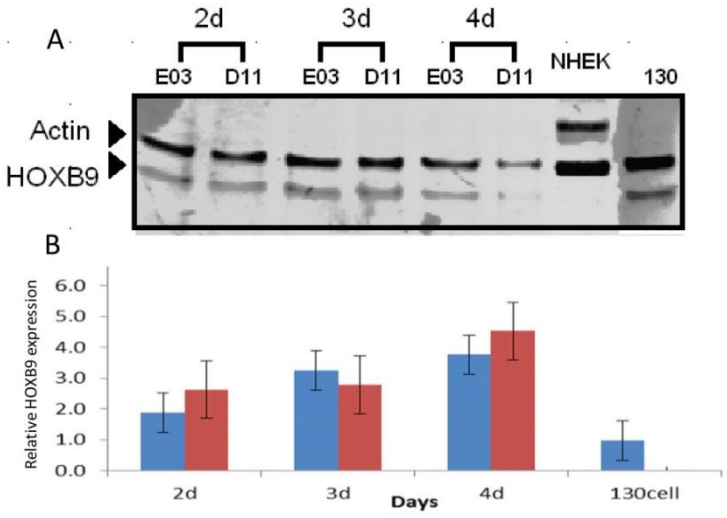

Figure 54. Protein expression of HOXB9 in Line 130 cells at various days. A. HOXB9 levels as seen in western blots over a 4 period following E03 and D11 transfection. HOXB9 was probed with a rabbit anti-HOXB9 antibody (Santa Cruz). Actin was probed with a mouse anti-actin antibody (Licor). IRDye 800CW goat anti-mouse antibody and IRDye 680LT goat anti-rabbit antibody (Licor) were used as secondary antibodies. B. Expression of HOXB9 at various days. Blue bars: negative control of siRNA, red bars: siRNA targeting T antigen.

5.13 Expression of CDKN2A was down-regulated by T antigen silencing in SV40 transformed cells

Cyclin-dependent kinase inhibitor 2A (CDKN2A) gene, also referred to as *INK4A*, *CDK4I*, and *MTS1*, is a putative tumor suppressor gene (132). CDKN2 encodes a 156-amino-acid protein, designated p16, which specifically binds to and inactivates the cyclin-dependent kinases (CDKs) Cdk4 and Cdk6, which function as regulators of cell cycle progression in G1 by contributing to the phosphorylation of the retinoblastoma protein (pRb) (133). The transcription of p16 is influenced by the status of pRb. Usually, p16 expression in pRb negative human tumor cell lines is much higher than that in pRb-positive lines. Cells that have become immortalized through the

loss of pRb therefore contain high levels of p16. Conversely, cells may be able to escape senescence by losing p16. In SV40 transformed cells, it was found that T antigen binds to pRb and inactivates pRb. Transcriptional regulation of p16 levels increased two to five fold. However, when T-antigen is completely inactivated, p16 RNA levels declined more slowly (48, 134-136).

Our data suggest that levels of Cdkn2A mRNA were down regulated 3 fold by T antigen silencing (Figure 41B). But the protein level of p16 was not changed significantly (Figure 55). If p16 decreases, the cells are not able to enter the senescence p16 pathway. It has been reported that p16 expression does not correlate with cellular proliferation or maturation (137, 138).

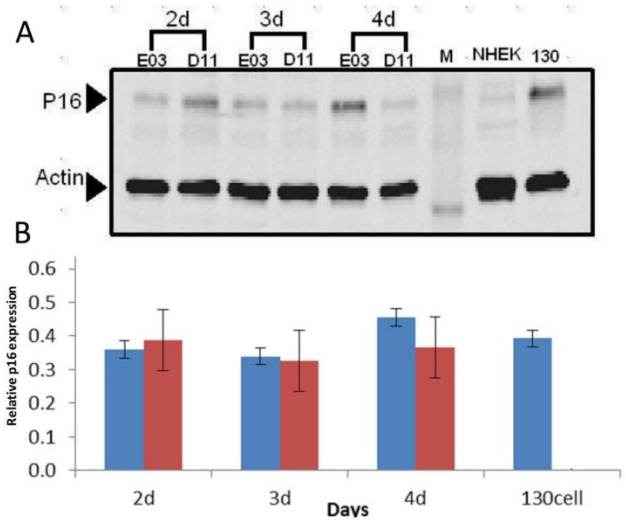

Figure 55. Protein expression of p16 in Line 130 cells throughout three days. A. The level of p16 at various days. p16 was probed with a mouse anti-p16 antibody (Santa Cruz). Actin was probed with a rabbit anti-actin antibody (Licor). IRDye 800CW goat anti-mouse antibody and IRDye 680LT goat anti-rabbit antibody (Licor) were used as secondary antibodies. B. Expression of p16 in relative to actin expression. Blue bars: negative control of siRNA, red bars: siRNA targeting T antigen).

5.14 Transcription of SIRT1 was down-regulated by silenced T antigen

The SIRT1 gene encodes the Sirtuin protein that belongs to the Silent information regulator (Sir2)-like family deacetylases. Sirtuin is an enzyme that catalyzes the removal of an acetyl group from lysine residues in histones and non-histone proteins, which is coupled to NAD^+ hydrolysis (139-141). Sirtuin does not act autonomously but as a component of large a multiprotein complex, such as Rb/E2F (142). These protein complexes mediate important transcription regulatory pathways and apoptosis (143). SirT1 inhibits p53 (144), implicating that SIRT1 is involved in regulating cell survival and stress response in mammalian organisms. The SIRT1 promoter is a target of E2F1, and increases expression of E2F1. E2F1 DNA binding and transcription activation are stimulated by acetylation (145-147). SIRT1 may regulate E2F1 by a combination of E2F1 deacetylation and promoter targeting. The tumor suppressor Rb inhibits E2F1 by binding to E2F1. In SV40 transfected cells, T antigen inactivates pRb and disrupts repressive Rb-E2F complexes, allowing transcription of E2F-dependent genes and progression into S-phase. We found that SIRT1 was up- regulated in SV40 transfected cell line. When T antigen was silenced in 130 cell lines, expression of SIRT1 mRNA was down regulated more than threefold; pRb was activated and bound to E2F1, leading to down regulation of SIRT1 (Figure 41. A). But the protein level of SIRT1 did not change (Figure 56). Therefore we continued to test SIRT1 protein level before any conclusion was reached. Reducing SIRT1 expression significantly increased cell death as a result of either apoptosis or senescence due to lack of acetylation of histone (146, 148).

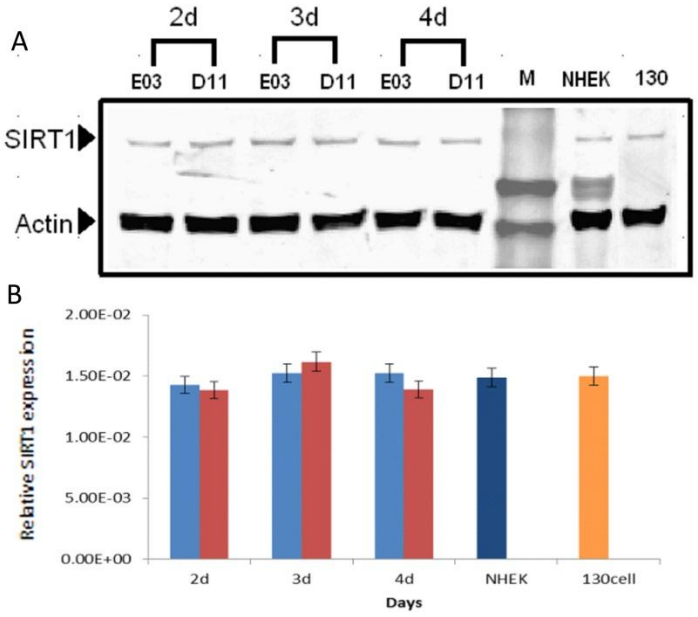

Figure 56. Protein expression of SIRT1 130 cells at various days after siRNA silencing. A. SIRT1 level at various days. SIRT1 was probed with a mouse anti-SIRT1 antibody (Santa Cruz), Actin was probed with a rabbit anti-actin antibody (Licor). IRDye 800CW goat anti-mouse antibody and IRDye 680LT goat anti-rabbit antibody (Licor) were used as secondary antibodies. B. The expression of SIRT1 in relative to expression of actin. Blue bars: negative control of siRNA, red bars: siRNA targeting T antigen.

5.15 Transcription of Fas is up-regulated by T antigen silencing.

Fas (member 6 of the tumor necrosis factor receptor superfamily) encodes the death receptor protein fas on the surface of the target cell. Fas ligand binds to fas receptor and recruits intracellular adaptor protein, which activates caspase-8 molecules and then activates downstream procaspases to induce apoptosis. Some stressed or damaged cells destroy themselves by producing the fas ligand and the fas protein (149-151).

Fas-dependent apoptosis is impaired by SV40 T-antigen in transgenic liver (152, 153) function for SV40 T-antigen which could contribute to viral pathogenesis by protecting infected cells against the host apoptotic defense mechanism (Figure 57).

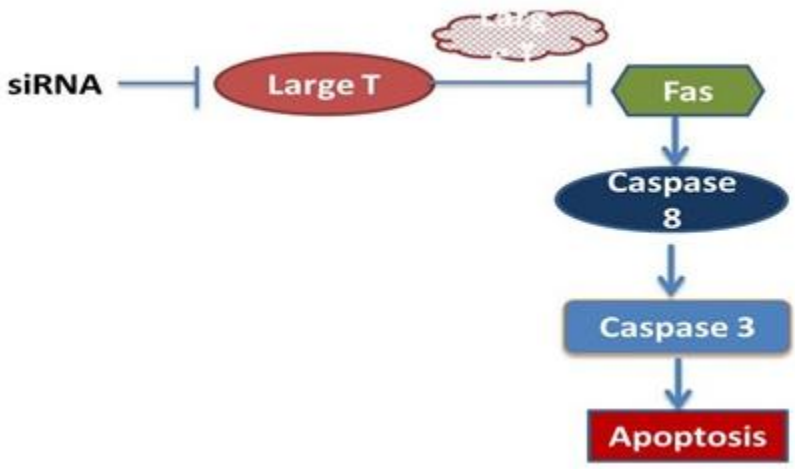

Figure 57. SV40 T antigen inhibits Fas- dependent apoptosis

We observed that *Fas* expression was up-regulated by knocking down the T antigen in 130 cells (Figure 41.B). This result was expected, because SV40 T antigen inhibits Fas-dependent apoptosis in SV40 transformed cells (154). But we did not detect significant changes in Fas protein level(Figure 58). We will try different primary Fas antibody in the future.

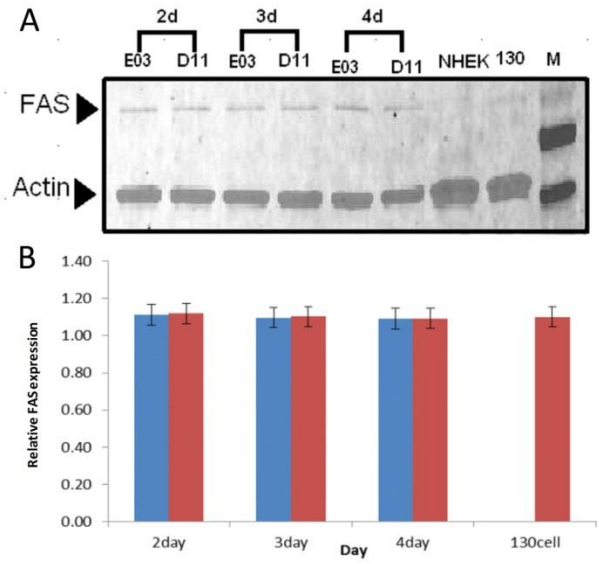

Figure 58. Protein expression of Fas 130 cells at various days after siRNA silencing. Protein expression of FAS in Line 130 cells at various days. A. FAS blot was probed with a rabbit anti-FAS antibody (Santa Cruz), Actin was probed with a mouse anti-actin antibody (Licor). IRDye 800CW goat anti-mouse antibody and IRDye 680LT goat anti-rabbit antibody (Licor) were used as second antibodies. B. Expression of FAS in relative to expression of actin. Blue bars: negative control of siRNA, red bars: siRNA targeting T antigen.

5.16 Transcription of TGF-β2 was down regulated by T antigen silencing

TGF-β2 (Transforming growth factor, beta 2) gene encodes a member of transforming growth factor-beta family of cytokines. TGF-β2 protein is a signal polypeptide. It acts as a hormone or a local mediator to regulate cellular processes, including cell division, proliferation, differentiation and extracellular matrix production. The regulation of TGF- β2 acts through enzyme-linked receptors, and single pass transmemberane protein TGF β2 receptors. TGF- β2 signals binds the TGF-beta type II receptor (TGF-betaRII) which transphosphorylates and activates the type I

receptor (TGF-betaRI). Activated TGF-beta RI recruits SMAD proteins and then phosphorylates a subset of SMAD proteins, such as Smad2 and Smad3 (155-157). These SMAD proteins then translocate to the nucleus where they form transcription complexes with DNA binding factors and co-activators/co-repressors. Whether TGF-β2 promotes or suppresses cellular proliferation depends on the cell type and context of stimulation. TGF β can act as a tumor suppressor or a tumor promoter in different cells. In non-transformed or carcinoma-associated epithelial cells, TGF-β2 is well known for its ability to inhibit cell proliferation and to promote an epithelial to mesenchymal transition (EMT) that has been associated with increased motility and invasiveness (158). Also TGF-β2 inhibits cyclin-dependent kinase (CDK) activity, which leads to accumulation of hypophosphorylated pRB and inhibits the cell cycle in the G1 phase (159). In our studies, mRNA level of TGF β2 was down regulated more than two-fold by SV40 T antigen silencing (Figure 41A). The protein level did not change (Figure 59). TGF β2 has been shown to be important in senescence induced by H_2O_2 (160). It may activate the cdc2 (p38) mitogen-activated protein kinase pathway (161). Further experiments will be carried out to determine the roll of TGF β2 in Line 130 cell cycle.

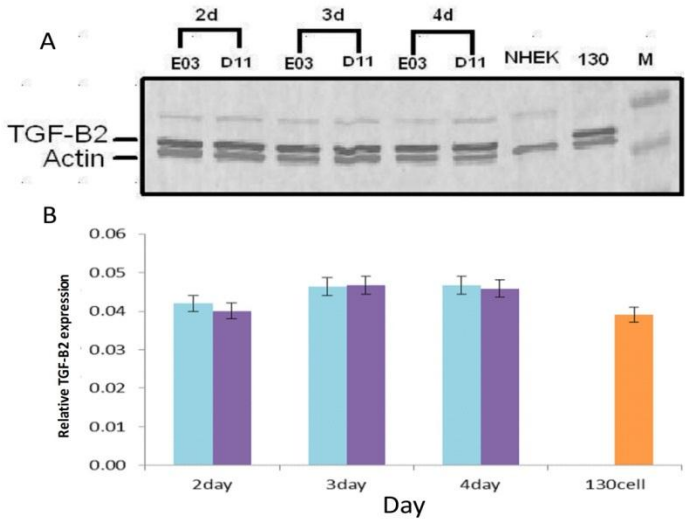

Figure 59. Protein expression of TGF-β2 at 130 cells at various days after siRNA silencing A. TGF-β2 level in western blots at various days after T antigen silencing. TGF-β2 was probed with a mouse anti-TGF-β2 antibody (Santa Cruz), Actin was probed with a rabbit anti-actin antibody (Licor). IRDye 800CW goat anti-mouse antibody and IRDye 680LT goat anti-rabbit antibody (Licor) were used as second antibodies. B. The expression of TGF-β2 in relative to expression of actin. Blue bars: negative control of siRNA, red bars: siRNA targeting T antigen.

5.17 Transcription of FRZB, WISP1, WNT2 and SOX17 were not affected by T antigen silencing

We designed primers for FRZB, WISP1, WNT2 and SOX17 to further investigate whether the expression of these genes is affected by T antigen knockdown. The FRZB gene encodes a frizzled-related protein-3, a seven-transmembrane receptor. The main function of frizzled-related protein-3 is to act as a modulator of Wnt signaling through direct interaction with Wnts (162). They have a role in regulating cell growth and differentiation in specific cell types. Wnt

signal pathway involves canonical and noncanonical signaling in proliferation. The WNT2 gene encodes WNT2 protein (Wingless-Type MMTV Integration Site2), a signal protein binding to Frizzled receptor, is crucially implicated in Wnt signaling pathway processes . WNT2 secretes a signal glycoprotein that binds to FRZB, a frizzled transmembrane receptor, and activates the Wnt pathway, which triggers a cascade signaling cascade resulting in transcript ion of cyclin D1 among others (163).

The *WISP1* gene encodes a Wnt-1 induced secreted protein 1, WISP1, which is a downstream regulator in the Wnt/Frizzled-signaling pathway and associated with cell survival. It induces p53- mediated apoptosis in response to DNA damage through activation of AKT kinase and up-regulates the anti-apoptotic Bcl-X(L) protein. In the absence of Wnt-signal (off state), β-catenin, an integral cell-cell adhension adaptor protein as well as transcriptional co-regulator, is targeted for degradation by the APC(adenomatous polyposis coli tumor suppressor)/Axin/GSK-3β9 glycogen synthase kinase-3β) –complex. β-catenin phosphorylated by GSK-3 β leads to its ubiquitination and proteasomal degradation (164-166).

In the presence of Wnt binding (on state), β-catenin phosphorylation and degradation are inhibited by moving GSK-3 β away from the degradation complex. As a result, unphosphorylated β-catenin accumulates in cytoplasm and nucleus. In the nucleus, the target genes for Wnt signaling are normally kept silent by an inhibitor complex LEF-1/TCF (lymphoid enhancer-binding factor 1 / T cell-specific transcription factor) bound to the corepressor protein Groucho. When β-catenin enters the nucleus, it binds to LEF-1/TCF and displaces Groucho protein, and induces transcription of the Wnt target genes (167, 168).

One of them is c-myc, which encodes an oncoprotein c-Myc. C-myc is a powerful stimulator of cell growth and proliferation. The resulting uncontrolled cell proliferation promotes the development of cancer. In our studies, transcriptions of *FRZB, WNT2* and *WISP1* as well as protein levels were up-regulated less than two-folds (Figure 41, 60 and 61). We did not focus on the Wnt signaling pathway study in this project (169-172).

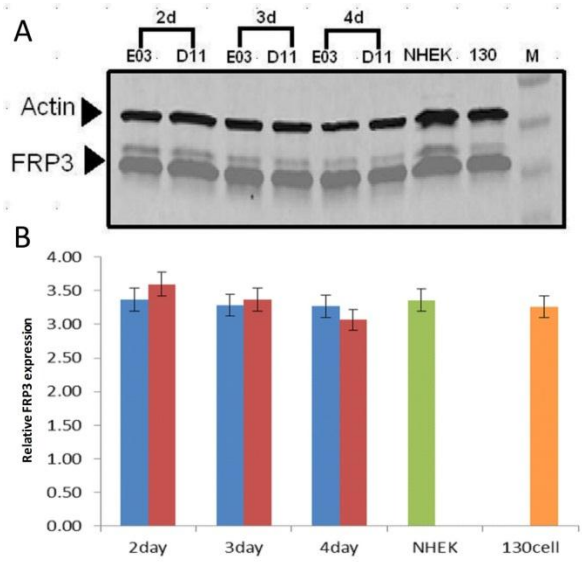

Figure. 60. Protein expression of FRP_3 at 130 cells at various days in after siRNA silencing A. FRP_3 level at various days. FRP_3 was probed with a rabbit anti-FRP_3 antibody (Santa Cruz), Actin was probed with a mouse anti-actin antibody (Licor). IRDye 800CW goat anti-mouse antibody and IRDye 680LT goat anti-rabbit antibody (Licor) were used as second antibodies. B. The expression of FRP_3 in relative to actin expression. Blue bars: negative control of siRNA, red bars: siRNA targeting T antigen.

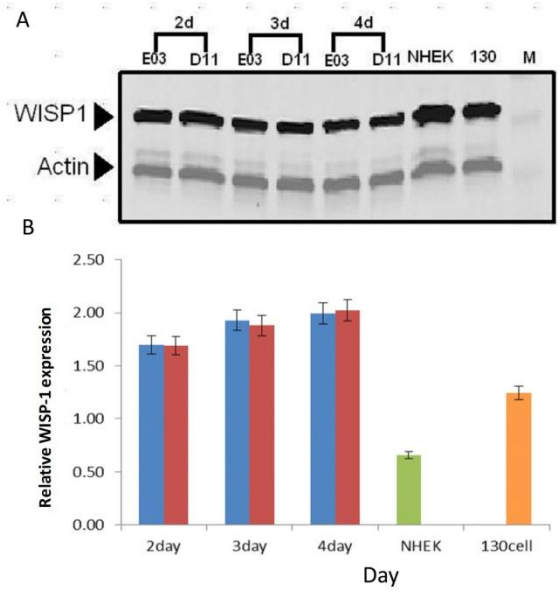

Figure. 61 Protein expression of WISP1 at 130 cells at various days in after siRNA silencing A. WISP1 level at various days after silencing of T antigen by siRNA. WISP1 was probed with a mouse anti-WISP1 antibody (Santa Cruz). Actin was probed with a rabbit anti-actin antibody (Licor). IRDye 800CW goat anti-mouse antibody and IRDye 680LT goat anti-rabbit antibody (Licor) were used as second antibodies. B. Expression of WISP1 in relative to actin expression. Blue bars: negative control of siRNA, red bars: siRNA targeting T antigen.

6. Establishing cell line with Stabilizing knockdown of L T-antigen

Synthetic Stealth siRNAs were used to knockdown T antigen in 130 cells. While siRNA transfection is an effective means for silencing of specifically targeted genes, silencing is limited by the fact that it is inherently transient. Long term continuous silencing of T antigen is not possible with siRNAs. Therefore, in order to make an effective silencing RNA for stable reduction of gene expression function, we employed a microRNA (miRNA) approach for a long term silencing of T antigen in 130 human keratinocyte line. The pcDNA6.2-GW/miR expression

vector (Invitrogen Inc.) was used to express engineered miRNA sequences from PolII promoters and facilitate the generation of an expression clone containing a double stranded oligo encoding a pre-miRNA sequence, which was designed by sequencing analysis. For this purpose we used BLOCK-iT™ RNAi Designer (Invitrogen) using SV40 776 strain (GenBank locus AF316139.1) T antigen as the reference genome to identify 3 viral target sequences:

1) beginning at SV40 nucleotide 4762: CACAAGTGGATCTTTCCTGTA

2) beginning at SV40 nucleotide 4924: TGCATCCCAGAAGCCTCCAAA

3) beginning at SV40 nucleotide 5028: CTTTATCAGGATGAAACTCCT

All 3 of the target sequences are located at an open reading frame (ORF). Three miRNA oligos were synthesized by Invitrogen. The constructs of miRNA are shown in Figure 62.

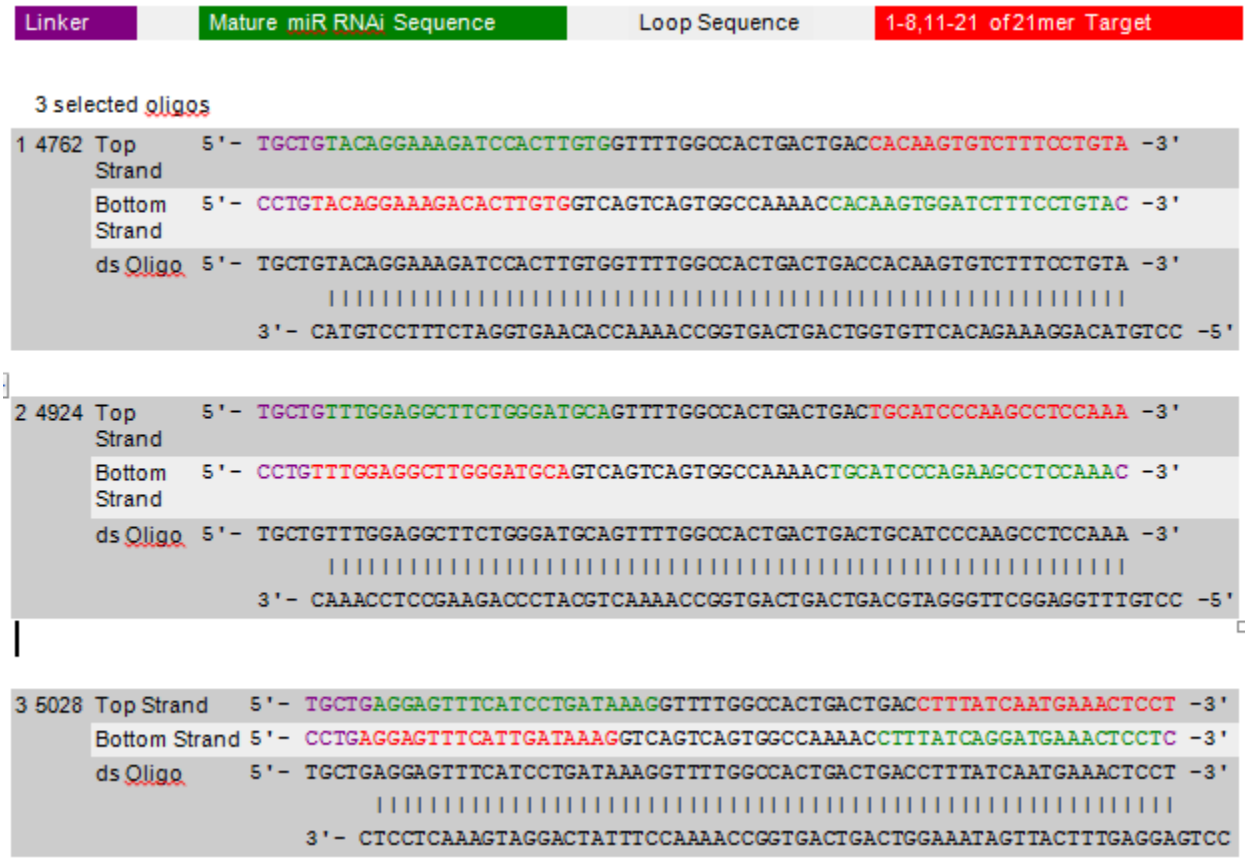

Figure 62. The three miRNAs cloned into the pcDNA6.2/miR expression vector

After cloning miRNAs into the pcDNA6.2-GW/miR expression vector, we analyzed the sequence of the recombinant plasmid DNA for each miRNA. The sequence of each miRNA was matched to the constructs of miRNA we designed. After transfection, recombinant plasmid DNA stably express the targeting miRNAs in mammalian cells, which are engineered to have 100% homology to target T antigen mRNA, subsequently, cleave the T antigen mRNA. In order to create a knock down T antigen cell line by 130 cells. Stable transfectants were selected with the antibiotic blasticidin over a period of 14 days. After that, a clonal cell subline was obtained by endpoint dilution (Figure. 63).

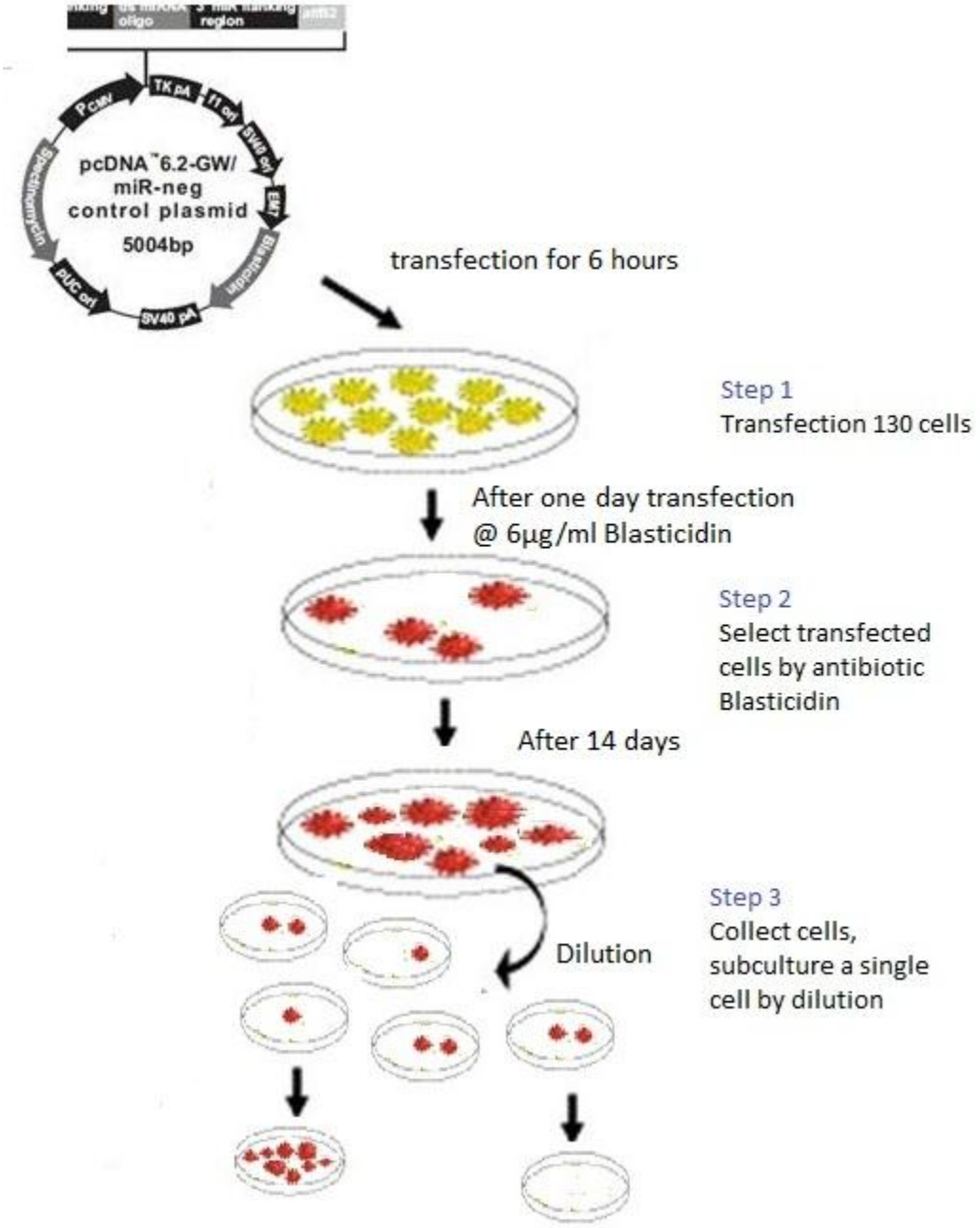

Figure 63. Diagram for the isolation of sublines stably maintaining the pcDNA6.2-GW/miR construct(s).

During the selection process in cell culture, most of cells died gradually. A few of the cells grew very slowly and took about three to four weeks to reach 70 to 80 % cell confluence in 6 well cell culture plates. To examine whether T antigen had been knocked down, the cells were harvested, T antigen mRNA level of cells was determined by qRT-PCR and T antigen protein level was evaluated by western blot (Figure 65.A and B). Our results indicated that T antigen showed little or no silencing by any of the 3 miRNAs.

In addition, there was no evidence of apoptosis as shown in the FACS results (Figure. 66).

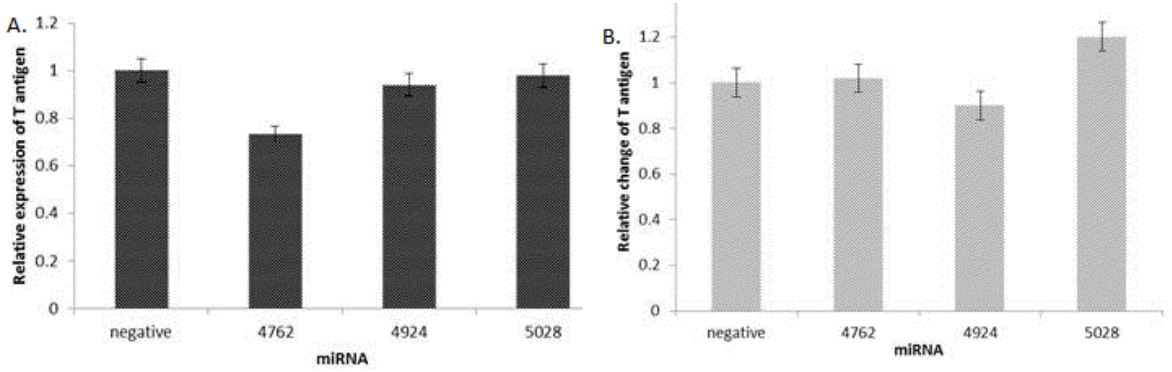

Figure 64. A) Expression of Large T-Antigen mRNA, B) Protein level of Large T-Antigen both graphs represent stable cell lines.

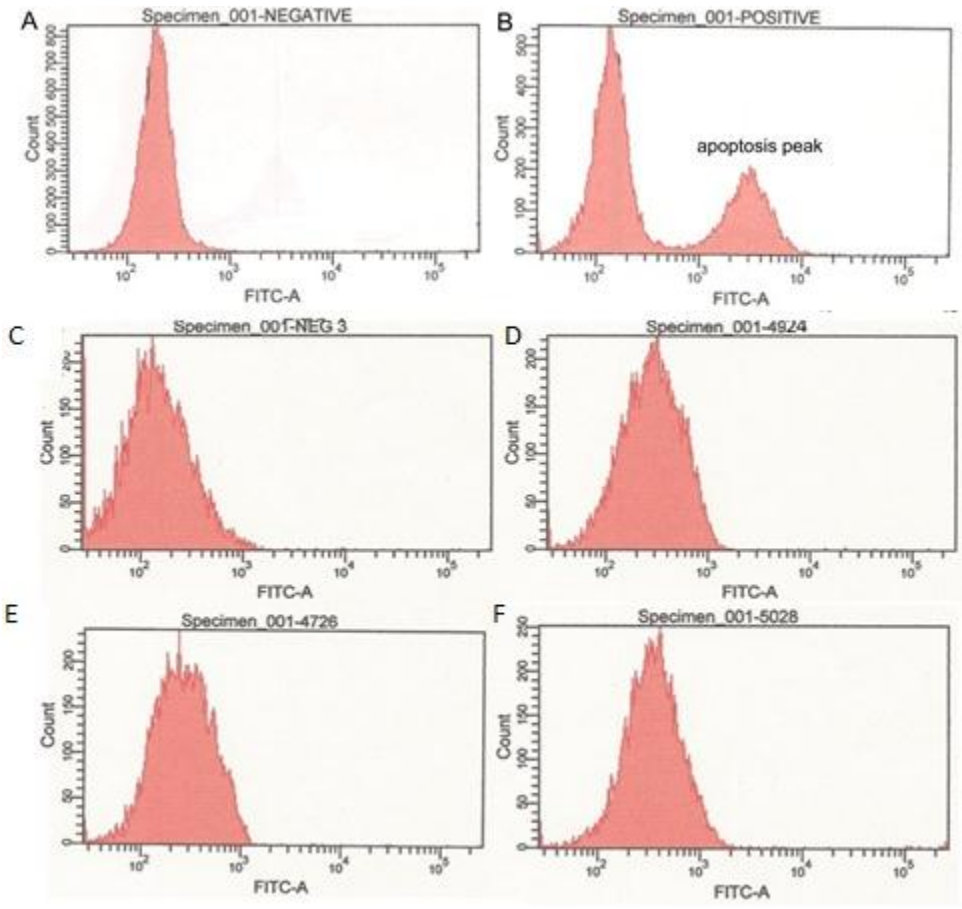

Figure 65. Apoptosis determination via FACS . A) An apoptosis negative control, B) An apoptosis positive control, C) miRNA negative control, D) miRNA 4924 E) miRNA 4762, F) miRNA 5028

In order to identify whether the cells in cell sublines still carried the miRNA sequences, we selected primers specific to pcDNA6.2 vector sequences and genomic DNA templates from the different sublines to carry out PCR. The PCR products were displayed on a 1% Agarose gel

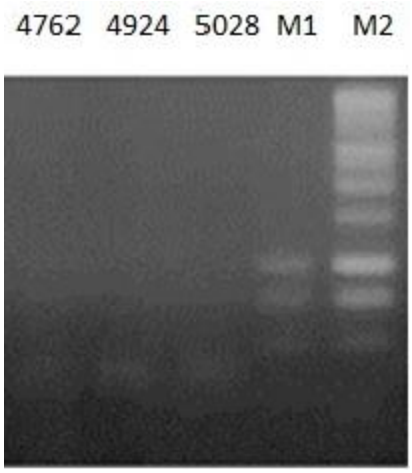

Figure 66. PCR products on 1% Agarose gel

4762(4924 and 5028) presents the template DNA from miRNA 4762 (4924 and 5028) transfection. M1 is PCR DNA ladder (Promega) M2 is 1Kb DNA ladder (Promega)

.

There was one band on each sample and the size(s) of the bands of each PCR product was of the exact size expected for the intact construct. Also, the purified PCR products were sequenced; the sequence of each of the PCR products confirmed that the PCR products matched the designed miRNA sequences. The results of the BLAST alignment are shown below (Figure.67). According to sequenced data, the recombinant plasmid DNAs, without any deletion or mutation, was transfected into the survival 130 cells. However, the T antigen did not knock down.

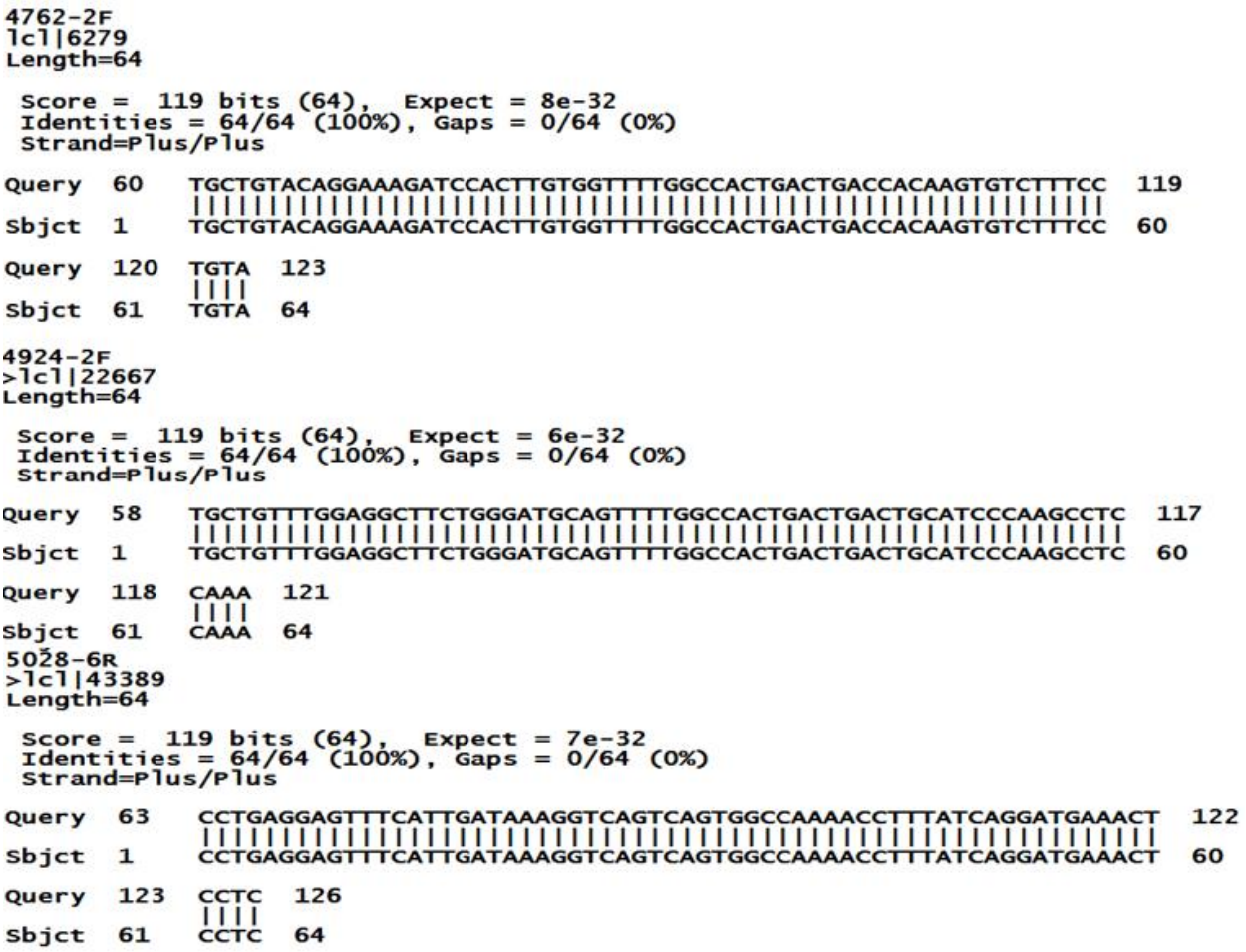

Figure 67. BLAST alignments of the sequences of the PCR products from stable sublines derived from pcDNA6.2/miR plasmid constructs for each of the miRNAs tested. The query sequence is recombinant plasmid DNA, the subject sequence is the designed miRNA.

In our previous studies, T antigen was integrated into human genomic DNA in 130 cells. It appears likely that T antigen may be essential for immortalization and so it is not possible to maintain cells in which viral early gene expression is knocked down over long periods of time. Thus, most of transfected cells in which T antigen was silenced probably died during the

selection process. A few of the cells that carried miRNA plasmid DNA survived, but T antigen did not knock down. It is difficult to explain the reason why T antigen was not silenced despite the presence of the intact constructs in the surviving cells. On the other hand, this experiment provided stronger evidence that T-antigen gene is essential for immortalized cell establishment. Previous reports on cells immortalized with SV40 virus have identified that the expression of a functional T antigen is required for maintenance of the immortalized phenotype (173, 174).

CONCLUSION

Transformation and immortalization of cultured human keratinocytes by Simian virus 40 was first reported by Steinberg and Defendi in 1979 (55). In this system the virus initiates a program of transformation in which the transformed phenotype evolves over a period of many serial passages following infection such that the properties associated with more highly transformed cells e.g anchorage independent growth or tumorigenic growth in a nude mouse host appear only many cell generations subsequent to infection. In contrast, replication of the viral DNA proceeds rapidly during the first few serial passages after infection but replicative capacity is gradually lost over time owing to the accumulation of defective viral DNA forms caused by intergenomic recombination. The loss of viral DNA from the cells occurs in parallel with the acquisition of the transformed phenotype suggesting that, over long term culture, the expression of transformed properties and immortalization may ultimately become independent from the initiating stimulus i.e. the SV40 early genes that encode the viral oncogenes. However, complete loss of the viral sequences has never been observed but rather, in cell lines studied, the viral sequences come to be retained in an integrated form in low copy number. Furthermore, sequence analyses of the integrated viral DNA have shown that the early gene region appears to be maintained integrated state arguing strongly that immortalization of the viral infected cells remains dependent on the

expression of the viral oncogenes. This study was initiated with the idea of using interfering RNA techniques to 1) test the dependence of immortalization on the continued expression of the viral early genes and, 2) to identify host genes involved in the expression of transformed properties whose expression is regulated by the SV40 T antigens.

We have studied a basic aspect of the SV40-transformed cell lines by carrying out experiments to test the essential nature of T antigen expression in the establishment of immortalization. Previous studies have sought to test whether immortalization remains dependent upon expression of T antigen using temperature-sensitive mutants of SV40 that expressed a thermolabile T antigen (175, 176). However, techniques that utilize temperature shift carry with them the inherent risk of introducing the pleiotropic effects of temperature on host metabolic pathways, thereby confounding interpretation of results. Here we have examined the dependence of immortalization on T antigen expression using RNA interference, a technique which specifically targets the function of one specific gene (T antigen) in order to demonstrate more clearly the relationship between T antigen expression and immortalization-related gene expression than was possible using temperature shift.

4.1 Integration of SV40 DNA in virus-immortalized human keratinocytes

Line 130 was chosen for these studies because previous analyses of the viral sequences in this line indicated that there was a single integrated copy of the viral early region thereby providing a unique target for the anticipated knockdown studies. Sequence analyses of the integrated virus in line 130 confirmed that this was in fact the case and also showed that the early region sequences were maintained in an intact form while, in contrast, the late region genes showed numerous alterations. These observations are consistent with the idea that the early genes continue to confer an essential vital function on the cells that harbor them. The fact that we were

unable to derive cell sublines carrying RNAi for long term T antigen knockdown also supports the idea that the T antigen continues to play an essential role in immortalization.

In two independently derived cell lines, viral integration was found to occur at a locus within chromosome 21 containing the human PKNOX1 gene. SV40 integration is not known to be mediated by a mechanism involving homologous recombination and no previous study of SV40 integration has ever demonstrated any degree of site specificity. It is not clear how SV40 virus DNA molecules insert into the human keratinocyte genome. According to our study, it seems to indicate the integration site of SV 40 DNA is not totally random. Previous reports suggest that viral DNA can integrate into the human genome by the viral-encoded integrases. The integration of SV40 DNA in mammalian cells may belong to this category, illegitimate mechanism. However, so far no SV40 viral –encoded integrases have been found. In our finding, there is TATA box at each junction, that TATA box binding protein (TBP) can bind to TATA box and melt the double strain DNA. By the way, D. W. Martin's research group found that human TATA-binding protein (TBP) can interact with T antigen by TBP co-immunoprecipitates with T antigen. The complex of TBP and T antigen can bind to the TATA box (177). Since SV40 T antigen possesses intrinsic DNA, RNA helicase and ATPase activity, we suggest T antigen unwinding double strain DNA which stimulates cleavage of the phosphodiester linkages in the covalent backbone of DNA. It may be part of mechanism. Recently, Kemian Gou's group found there were AT-rich domains on the 5' and 3' junction sequences that integrated fad2 gene into the X chromosome as well. It may also be that a form of recombination with low specificity may be involved in viral integration inasmuch as BLAST searches reveal that short segments of ~20-30 nucleotides are widely scattered throughout the human genome.

The commonality of integration in lines 22 and 130 is a potentially important finding since it suggests that SV40 integration itself might activate oncogenic processes in a manner similar to the "promoter insertion" model of oncogene activation that has been shown for retroviruses. Although we anticipated that the presence of the viral origin/promoter region might upregulate PKNOX1 expression, this turned out not to be the case. Nevertheless, it seems likely that gene activation related to integration of the virus in this region or near the integration site on chromosome 10 may turn out to play a role in the transformation process by SV40 in these cell lines.

4.2 Conversion of SV40-immortalized human keratinocytes to senescing cells by knock-down of T antigen

Normal human epithelial keratinocyte diploid cells (NHEK) become senescent after a definite number of divisions. 130 cells are immortalized cells established by SV40 virus transformation of NHEK cells. We sought to determine whether SV40 large T antigen is essential for this immortalization of 130 cells by introduction of an siRNA targeting T antigen into the cells. We found caspase 3/7 activity was increased on third day after siRNA transfection, but no apoptosis occurred. Whereas senescent cells were observed by β- galactasidase assay. Silencing of T antigen also was found to change the cell cycle progression. The relative number of cells in the S phase was decreased as compared to that in a negative control and about 50% of cells

accumulated at G_1 phase. The cell cycle transition at G1-S phase was blocked by silenced T antigen in 130 cell line.

4.3 Identification of senescence related Genes.

After silencing T antigen in the 130 cell line, we screened more than 250 genes to identify candidate genes correlated with loss of senescence that may be either directly or indirectly regulated by SV40 T antigen. When T antigen functions were reduced, both p53 and pRb tumor suppressors were activated by releasing the binding from T antigen. However, the mRNA level of p53 was decreased, whereas, expression of pRb did not change significantly. In our study, p16 was down regulated by activation of pRb transcription. Therefore, p16 does not play a role as a CDK inhibitor in this senescence pathway. Here we have focused on gene regulation downstream from p53 and pRb. We found transcription of BTG2, CDKN1A, GADD45A and MDM2 genes was significantly modulated after T antigen knockdown consistent with a model of transactivation by p53. This model is in agreement with models of gene transactivation involved in cell cycle arrest described in previous reports. In this connection we identified BTG2, a negative regulator of cell cycle progression as a possible novel mediator (Figure. 69).

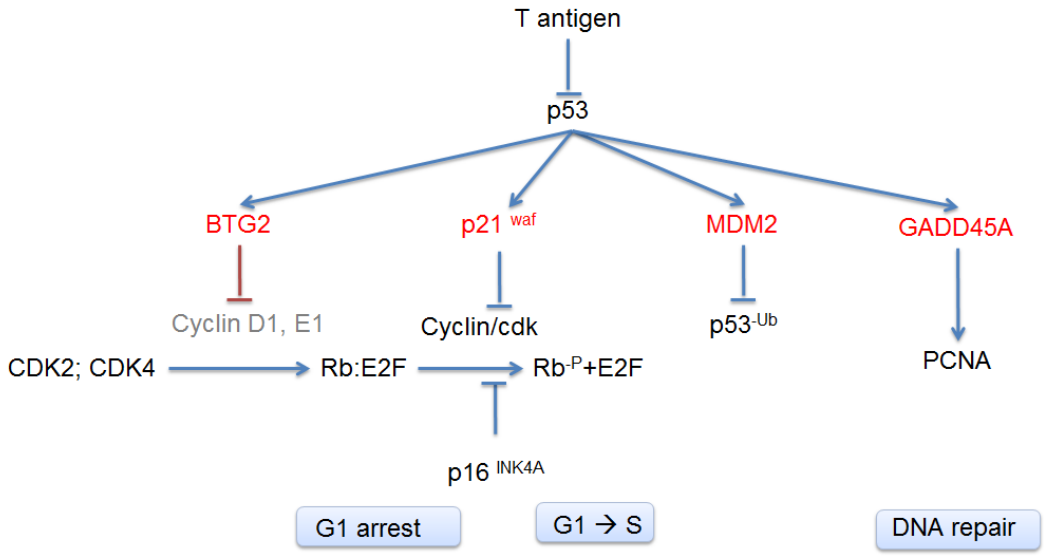

Figure 68. Diagram of genes of downstream of p53 affect the cell cycle.

BTG2, CDKN1A, GADD45A and MDM2 genes have anti-proliferation functions. Overexpression of these growth inhibitory genes cause the G1/S phase transition arrest or G2/M. Effects of CDKN1A, GADD45A and MDM2 on cell proliferation in SV40 T antigen model have been reported by Hsieh's research report. In our studies, we found that BTG2 , a novel anti-proliferation gene, was transactivated by p53 . BTG2 is also a negative transcriptional regulator of cyclin D1. Increased expression of BTG2 leads to the accumulation of hypophosphorlated form of pRb (67,68,114). As a result, the G1/S phase transition is blocked by a pRb dependent pathway. We suggest that in 130 cells in which T antigen has been knocked down, anti-proliferative pathways are dominated by p53 transactivation of downstream genes. Downstream functions of tumor suppressor Rb are inhibited by an increase in BTG2 expression. Therefore, BTG2 expression is as important as p21 for cell cycle arrest and cell senescence in 130 cells.

BIBLIOGRAPHY

1. Cullmann C*, et al.* (2009) Oncogenic human papillomaviruses block expression of the B-cell translocation gene-2 tumor suppressor gene. *International journal of cancer* 125(9):2014-2020.
2. Butel JS (2000) Simian virus 40, poliovirus vaccines, and human cancer: research progress versus media and public interests. *Bulletin of the World Health Organization* 78(2):195-198.
3. Eddy BE, Borman GS, Grubbs GE, & Young RD (1962) Identification of the oncogenic substance in rhesus monkey kidney cell culture as simian virus 40. *Virology* 17:65-75.
4. Gerber P (1963) Tumors induced in hamsters by simian virus 40: persistent subviral infection. *Science* 140(3569):889-890.
5. Blakeslee JR, von Muenchhausen W, & Cox HR (1973) Tumor rejection and immunotherapy studies with simian virus 40-induced tumors. *Journal of medicine* 4(4):233-247.
6. Manfredi JJ & Prives C (1994) The transforming activity of simian virus 40 large tumor antigen. *Biochimica et biophysica acta* 1198(1):65-83.
7. Chen W & Hahn WC (2003) SV40 early region oncoproteins and human cell transformation. *Histology and histopathology* 18(2):541-550.
8. Graessmann M & Graessmann A (1975) Regulation mechanism of simian virus 40 late gene expression in primary kidney cells and simian virus 40 transformed 3T3 cells. *Virology* 65(2):591-594.
9. Sweet BH & Hilleman MR (1960) The Vacuolating Virus, Sv40. *P Soc Exp Biol Med* 105(2):420-427.
10. Suda Y, Hirai S, Suzuki M, Ikawa Y, & Aizawa S (1988) Active ras and myc oncogenes can be compatible, but Sv40 large T antigen is specifically suppressed with normal differentiation of mouse embryonic stem cells. *Experimental cell research* 178(1):98-113.
11. Stetter G & Montenarh M (1989) Complex interaction of SV40 large T antigen with the control region on the SV40 DNA. *Oncogene* 4(11):1353-1357.
12. Marton A, Jean D, Delbecchi L, Simmons DT, & Bourgaux P (1993) Topoisomerase activity associated with SV40 large tumor antigen. *Nucleic acids research* 21(8):1689-1695.
13. Giacherio D & Hager LP (1980) A specific DNA unwinding activity associated with SV40 large T antigen. *The Journal of biological chemistry* 255(19):8963-8966.
14. Jones KA & Tjian R (1984) Essential contact residues within SV40 large T antigen binding sites I and II identified by alkylation-interference. *Cell* 36(1):155-162.
15. Tjian R (1981) Regulation of viral transcription and DNA replication by the SV40 large T antigen. *Current topics in microbiology and immunology* 93:5-24.
16. Stetter G, Braun MA, & Montenarh M (1991) A new DNA binding assay to study subclasses of SV40 large T antigen binding to individual binding sites on the SV40 DNA. *Oncogene* 6(3):389-396.
17. Dean FB*, et al.* (1987) Simian virus 40 (SV40) DNA replication: SV40 large T antigen unwinds DNA containing the SV40 origin of replication. *Proceedings of the National Academy of Sciences of the United States of America* 84(1):16-20.
18. Lobl TJ, Mitchell MA, & Maggiora LL (1990) SV40 large T-antigen nuclear signal analogues: successful nuclear targeting with bovine serum albumin but not low molecular weight fluorescent conjugates. *Biopolymers* 29(1):197-203.
19. Loeber G, Parsons R, & Tegtmeyer P (1989) A genetic analysis of the zinc finger of SV40 large T antigen. *Current topics in microbiology and immunology* 144:21-29.

20. Montenarh M, Vesco C, Kemmerling G, Muller D, & Henning R (1986) Regions of SV40 large T antigen necessary for oligomerization and complex formation with the cellular oncoprotein p53. *FEBS letters* 204(1):51-55.
21. Woods C, LeFeuvre C, Stewart N, & Bacchetti S (1994) Induction of genomic instability in SV40 transformed human cells: sufficiency of the N-terminal 147 amino acids of large T antigen and role of pRB and p53. *Oncogene* 9(10):2943-2950.
22. Simmons DT (2000) SV40 large T antigen functions in DNA replication and transformation. *Advances in virus research* 55:75-134.
23. Ali SH & DeCaprio JA (2001) Cellular transformation by SV40 large T antigen: interaction with host proteins. *Seminars in cancer biology* 11(1):15-23.
24. Lane DP*, et al.* (1985) Cellular targets for SV40 large T-antigen. *Proceedings of the Royal Society of London. Series B, Containing papers of a Biological character. Royal Society* 226(1242):25-42.
25. DeCaprio JA*, et al.* (1988) SV40 large tumor antigen forms a specific complex with the product of the retinoblastoma susceptibility gene. *Cell* 54(2):275-283.
26. Wang EH, Friedman PN, & Prives C (1989) The murine p53 protein blocks replication of SV40 DNA in vitro by inhibiting the initiation functions of SV40 large T antigen. *Cell* 57(3):379-392.
27. Deppert W, Steinmayer T, & Richter W (1989) Cooperation of SV40 large T antigen and the cellular protein p53 in maintenance of cell transformation. *Oncogene* 4(9):1103-1110.
28. Bargonetti J, Reynisdottir I, Friedman PN, & Prives C (1992) Site-specific binding of wild-type p53 to cellular DNA is inhibited by SV40 T antigen and mutant p53. *Genes & development* 6(10):1886-1898.
29. Reich NC & Levine AJ (1982) Specific interaction of the SV40 T antigen-cellular p53 protein complex with SV40 DNA. *Virology* 117(1):286-290.
30. Milner J & Gamble J (1985) The SV40 large T-p53 complex: evidence for the presence of two immunologically distinct forms of p53. *Virology* 147(1):206-209.
31. Bargonetti J, Friedman PN, Kern SE, Vogelstein B, & Prives C (1991) Wild-type but not mutant p53 immunopurified proteins bind to sequences adjacent to the SV40 origin of replication. *Cell* 65(6):1083-1091.
32. Ludlow JW*, et al.* (1989) SV40 large T antigen binds preferentially to an underphosphorylated member of the retinoblastoma susceptibility gene product family. *Cell* 56(1):57-65.
33. Kim HY, Ahn BY, & Cho Y (2001) Structural basis for the inactivation of retinoblastoma tumor suppressor by SV40 large T antigen. *The EMBO journal* 20(1-2):295-304.
34. Avantaggiati ML*, et al.* (1996) The SV40 large T antigen and adenovirus E1a oncoproteins interact with distinct isoforms of the transcriptional co-activator, p300. *The EMBO journal* 15(9):2236-2248.
35. Pipas JM (1998) Molecular chaperone function of the SV40 large T antigen. *Developments in biological standardization* 94:313-319.
36. Pallas DC*, et al.* (1990) Polyoma small and middle T antigens and SV40 small t antigen form stable complexes with protein phosphatase 2A. *Cell* 60(1):167-176.
37. Kamibayashi C*, et al.* (1994) Comparison of heterotrimeric protein phosphatase 2A containing different B subunits. *J Biol Chem* 269(31):20139-20148.
38. Yang SI*, et al.* (1991) Control of protein phosphatase 2A by simian virus 40 small-t antigen. *Molecular and cellular biology* 11(4):1988-1995.
39. Srinivasan A*, et al.* (1997) The amino-terminal transforming region of simian virus 40 large T and small t antigens functions as a J domain. *Molecular and cellular biology* 17(8):4761-4773.

40. Zhou J, Pham HT, Ruediger R, & Walter G (2003) Characterization of the Aalpha and Abeta subunit isoforms of protein phosphatase 2A: differences in expression, subunit interaction, and evolution. *Biochem J* 369(Pt 2):387-398.
41. Bikel I*, et al.* (1987) SV40 small t antigen enhances the transformation activity of limiting concentrations of SV40 large T antigen. *Cell* 48(2):321-330.
42. Boyapati A, Wilson M, Yu J, & Rundell K (2003) SV40 17KT antigen complements dnaj mutations in large T antigen to restore transformation of primary human fibroblasts. *Virology* 315(1):148-158.
43. Linskens MH, Harley CB, West MD, Campisi J, & Hayflick L (1995) Replicative senescence and cell death. *Science* 267(5194):17.
44. Larsson LG (2011) Oncogene- and tumor suppressor gene-mediated suppression of cellular senescence. *Seminars in cancer biology* 21(6):367-376.
45. Haferkamp S*, et al.* (2009) The relative contributions of the p53 and pRb pathways in oncogene-induced melanocyte senescence. *Aging (Albany NY)* 1(6):542-556.
46. Jarrard DF*, et al.* (1999) p16/pRb pathway alterations are required for bypassing senescence in human prostate epithelial cells. *Cancer research* 59(12):2957-2964.
47. Ruiz L*, et al.* (2008) Characterization of the p53 response to oncogene-induced senescence. *PloS one* 3(9):e3230.
48. Smeets SJ*, et al.* (2011) Immortalization of oral keratinocytes by functional inactivation of the p53 and pRb pathways. *International journal of cancer. Journal international du cancer* 128(7):1596-1605.
49. Di Micco R*, et al.* (2008) DNA damage response activation in mouse embryonic fibroblasts undergoing replicative senescence and following spontaneous immortalization. *Cell cycle* 7(22):3601-3606.
50. Smith JR & Pereira-Smith OM (1996) Replicative senescence: implications for in vivo aging and tumor suppression. *Science* 273(5271):63-67.
51. Berube NG, Smith JR, & Pereira-Smith OM (1998) The genetics of cellular senescence. *American journal of human genetics* 62(5):1015-1019.
52. Tominaga K, Olgun A, Smith JR, & Pereira-Smith OM (2002) Genetics of cellular senescence. *Mechanisms of ageing and development* 123(8):927-936.
53. Tominaga K, Tominaga E, Ausserlechner MJ, & Pereira-Smith OM (2010) The cell senescence inducing gene product MORF4 is regulated by degradation via the ubiquitin/proteasome pathway. *Experimental cell research* 316(1):92-102.
54. Eckhart W (1969) Cell transformation by polyoma virus and SV40. *Nature* 224(5224):1069-1071.
55. Steinberg ML & Defendi V (1979) Altered pattern of growth and differentiation in human keratinocytes infected by simian virus 40. *Proceedings of the National Academy of Sciences of the United States of America* 76(2):801-805.
56. Okada N*, et al.* (1989) Synthesis of epidermolysis bullosa acquisita antigen by simian virus 40-transformed human keratinocytes. *Archives of dermatological research* 281(1):1-4.
57. Okada N, Steinberg ML, & Defendi V (1984) Re-expression of differentiated properties in SV40-infected human epidermal keratinocytes induced by 5-azacytidine. *Experimental cell research* 153(1):198-207.
58. Montgomery MK, Xu S, & Fire A (1998) RNA as a target of double-stranded RNA-mediated genetic interference in Caenorhabditis elegans. *Proceedings of the National Academy of Sciences of the United States of America* 95(26):15502-15507.
59. Dudley NR & Goldstein B (2003) RNA interference: silencing in the cytoplasm and nucleus. *Current opinion in molecular therapeutics* 5(2):113-117.

60. Lin R & Avery L (1999) RNA interference. Policing rogue genes. *Nature* 402(6758):128-129.
61. Bernstein E, Caudy AA, Hammond SM, & Hannon GJ (2001) Role for a bidentate ribonuclease in the initiation step of RNA interference. *Nature* 409(6818):363-366.
62. Hannon GJ & Conklin DS (2004) RNA interference by short hairpin RNAs expressed in vertebrate cells. *Methods in molecular biology* 257:255-266.
63. Meister G & Tuschl T (2004) Mechanisms of gene silencing by double-stranded RNA. *Nature* 431(7006):343-349.
64. Duriez C, Moyret-Lalle C, Falette N, El-Ghissassi F, & Puisieux A (2004) BTG2, its family and its tutor. *Bulletin du cancer* 91(7-8):E242-253.
65. Duriez C*, et al.* (2002) The human BTG2/TIS21/PC3 gene: genomic structure, transcriptional regulation and evaluation as a candidate tumor suppressor gene. *Gene* 282(1-2):207-214.
66. Ryu MS*, et al.* (2004) TIS21/BTG2/PC3 is expressed through PKC-delta pathway and inhibits binding of cyclin B1-Cdc2 and its activity, independent of p53 expression. *Experimental cell research* 299(1):159-170.
67. Lim IK (2006) TIS21 (/BTG2/PC3) as a link between ageing and cancer: cell cycle regulator and endogenous cell death molecule. *Journal of cancer research and clinical oncology* 132(7):417-426.
68. Miyata S, Mori Y, & Tohyama M (2008) PRMT1 and Btg2 regulates neurite outgrowth of Neuro2a cells. *Neuroscience letters* 445(2):162-165.
69. Takahashi F*, et al.* (2011) Breast tumor progression induced by loss of BTG2 expression is inhibited by targeted therapy with the ErbB/HER inhibitor lapatinib. *Oncogene* 30(27):3084-3095.
70. Paruthiyil S*, et al.* (2011) Estrogen receptor beta causes a G2 cell cycle arrest by inhibiting CDK1 activity through the regulation of cyclin B1, GADD45A, and BTG2. *Breast cancer research and treatment* 129(3):777-784.
71. Karmakar S, Foster EA, & Smith CL (2009) Estradiol downregulation of the tumor suppressor gene BTG2 requires estrogen receptor-alpha and the REA corepressor. *International journal of cancer. Journal international du cancer* 124(8):1841-1851.
72. Jalava SE*, et al.* (2012) Androgen-regulated miR-32 targets BTG2 and is overexpressed in castration-resistant prostate cancer. *Oncogene*.
73. Hu XD*, et al.* (2011) BTG2 is an LXXLL-dependent co-repressor for androgen receptor transcriptional activity. *Biochemical and biophysical research communications* 404(4):903-909.
74. Wada K, Hamaguchi Y, Furukawa K, & Taniguchi A (2009) DNA damage sensible engineered promoter for cellular biosensing of cytotoxicity. *Biotechnology and bioengineering* 102(5):1460-1465.
75. Cortes U*, et al.* (2000) BTG gene expression in the p53-dependent and -independent cellular response to DNA damage. *Molecular carcinogenesis* 27(2):57-64.
76. Guardavaccaro D*, et al.* (2000) Arrest of G(1)-S progression by the p53-inducible gene PC3 is Rb dependent and relies on the inhibition of cyclin D1 transcription. *Molecular and cellular biology* 20(5):1797-1815.
77. Tirone F (2001) The gene PC3(TIS21/BTG2), prototype member of the PC3/BTG/TOB family: regulator in control of cell growth, differentiation, and DNA repair? *Journal of cellular physiology* 187(2):155-165.
78. Liu M*, et al.* (2009) Regulation of the cell cycle gene, BTG2, by miR-21 in human laryngeal carcinoma. *Cell research* 19(7):828-837.
79. Cho BO*, et al.* (2008) Up-regulation of the BTG2 gene in TPA- or RA-treated HL-60 cell lines. *Oncology reports* 19(3):633-637.

80. Hong JW, Ryu MS, & Lim IK (2005) Phosphorylation of serine 147 of tis21/BTG2/pc3 by p-Erk1/2 induces Pin-1 binding in cytoplasm and cell death. *The Journal of biological chemistry* 280(22):21256-21263.
81. Mauxion F, Faux C, & Seraphin B (2008) The BTG2 protein is a general activator of mRNA deadenylation. *The EMBO journal* 27(7):1039-1048.
82. Yang X*, et al.* (2008) Crystal structures of human BTG2 and mouse TIS21 involved in suppression of CAF1 deadenylase activity. *Nucleic acids research* 36(21):6872-6881.
83. Steinberg ML & Defendi V (1983) Transformation and immortalization of human keratinocytes by SV40. *The Journal of investigative dermatology* 81(1 Suppl):131s-136s.
84. Chen G, Baez JM, & Steinberg ML (1996) Integration of the SV40 promoter/enhancer sequences in an anchorage-independent clonal subline of SV40-infected human keratinocytes. *Gene* 183(1-2):41-45.
85. Steinberg ML, Rossman TG, Morris A, & Chen GT (1989) Specific high frequency rearrangements induced by MNNG in SV40-infected human keratinocytes. *Carcinogenesis* 10(10):1801-1807.
86. Steinberg ML (1996) Culture of Immortalized Cells. pp 95-120.
87. Wang S, He J, Cui Z, & Li S (2007) Self-formed adaptor PCR: a simple and efficient method for chromosome walking. *Applied and environmental microbiology* 73(15):5048-5051.
88. Li X & Darzynkiewicz Z (1995) Labelling DNA strand breaks with BrdUTP. Detection of apoptosis and cell proliferation. *Cell proliferation* 28(11):571-579.
89. Dimri GP*, et al.* (1995) A biomarker that identifies senescent human cells in culture and in aging skin in vivo. *Proceedings of the National Academy of Sciences of the United States of America* 92(20):9363-9367.
90. Defendi V, Naimski P, & Steinberg ML (1982) Human cells transformed by SV40 revisited: the epithelial cells. *Journal of cellular physiology. Supplement* 2:131-140.
91. Sanchez-Font MF, Bosch-Comas A, Gonzalez-Duarte R, & Marfany G (2003) Overexpression of FABP7 in Down syndrome fetal brains is associated with PKNOX1 gene-dosage imbalance. *Nucleic acids research* 31(11):2769-2777.
92. Elbashir SM*, et al.* (2001) Duplexes of 21-nucleotide RNAs mediate RNA interference in cultured mammalian cells. *Nature* 411(6836):494-498.
93. Kothakota S*, et al.* (1997) Caspase-3-generated fragment of gelsolin: effector of morphological change in apoptosis. *Science* 278(5336):294-298.
94. Aggarwal S & Gupta S (1999) Increased activity of caspase 3 and caspase 8 in anti-Fas-induced apoptosis in lymphocytes from ageing humans. *Clinical and experimental immunology* 117(2):285-290.
95. Canbakan B, Senturk H, Canbakan M, Toptas T, & Tuncer M (2011) Reliability of caspase activity as a biomarker of hepatic apoptosis in nonalcoholic fatty liver disease. *Biomarkers in medicine* 5(6):813-815.
96. Galluzzi L, Kepp O, & Kroemer G (2012) Caspase-3 and prostaglandins signal for tumor regrowth in cancer therapy. *Oncogene* 31(23):2805-2808.
97. Florentin A & Arama E (2012) Caspase levels and execution efficiencies determine the apoptotic potential of the cell. *The Journal of cell biology* 196(4):513-527.
98. Walsh JG*, et al.* (2008) Executioner caspase-3 and caspase-7 are functionally distinct proteases. *Proceedings of the National Academy of Sciences of the United States of America* 105(35):12815-12819.
99. Larsson O*, et al.* (2004) Kinetics of senescence-associated changes of gene expression in an epithelial, temperature-sensitive SV40 large T antigen model. *Cancer research* 64(2):482-489.

100. Shay JW, Pereira-Smith OM, & Wright WE (1991) A role for both RB and p53 in the regulation of human cellular senescence. *Experimental cell research* 196(1):33-39.
101. Fujii M*, et al.* (1999) The introduction of dominant-negative p53 mutants suppresses temperature shift-induced senescence in immortal human fibroblasts expressing a thermolabile SV40 large T antigen. *Journal of biochemistry* 125(3):531-536.
102. Lin WJ, Chang YF, Wang WL, & Huang CY (2001) Mitogen-stimulated TIS21 protein interacts with a protein-kinase-Calpha-binding protein rPICK1. *The Biochemical journal* 354(Pt 3):635-643.
103. Struckmann K*, et al.* (2004) Impaired expression of the cell cycle regulator BTG2 is common in clear cell renal cell carcinoma. *Cancer research* 64(5):1632-1638.
104. Lehman TA*, et al.* (1993) p53 mutations in human immortalized epithelial cell lines. *Carcinogenesis* 14(5):833-839.
105. Ying H & Xiao ZX (2006) Targeting retinoblastoma protein for degradation by proteasomes. *Cell cycle* 5(5):506-508.
106. Sdek P*, et al.* (2005) MDM2 promotes proteasome-dependent ubiquitin-independent degradation of retinoblastoma protein. *Molecular cell* 20(5):699-708.
107. Brown DR, Deb S, Munoz RM, Subler MA, & Deb SP (1993) The tumor suppressor p53 and the oncoprotein simian virus 40 T antigen bind to overlapping domains on the MDM2 protein. *Molecular and cellular biology* 13(11):6849-6857.
108. Henning W*, et al.* (1997) MDM2 is a target of simian virus 40 in cellular transformation and during lytic infection. *Journal of virology* 71(10):7609-7618.
109. Sengupta PS*, et al.* (2000) p53 and related proteins in epithelial ovarian cancer. *European journal of cancer* 36(18):2317-2328.
110. He G*, et al.* (2005) Induction of p21 by p53 following DNA damage inhibits both Cdk4 and Cdk2 activities. *Oncogene* 24(18):2929-2943.
111. Ueda Y*, et al.* (2001) Immunohistochemical study of p53, p21 and PCNA in pterygium. *Acta histochemica* 103(2):159-165.
112. Jin S*, et al.* (2000) BRCA1 activation of the GADD45 promoter. *Oncogene* 19(35):4050-4057.
113. Harkin DP*, et al.* (1999) Induction of GADD45 and JNK/SAPK-dependent apoptosis following inducible expression of BRCA1. *Cell* 97(5):575-586.
114. Maekawa T*, et al.* (2008) ATF-2 controls transcription of Maspin and GADD45 alpha genes independently from p53 to suppress mammary tumors. *Oncogene* 27(8):1045-1054.
115. Chen IT, Smith ML, O'Connor PM, & Fornace AJ, Jr. (1995) Direct interaction of Gadd45 with PCNA and evidence for competitive interaction of Gadd45 and p21Waf1/Cip1 with PCNA. *Oncogene* 11(10):1931-1937.
116. Smith ML*, et al.* (1994) Interaction of the p53-regulated protein Gadd45 with proliferating cell nuclear antigen. *Science* 266(5189):1376-1380.
117. Shu J, Hitomi M, & Stacey D (1996) Activation of JNK/SAPK pathway is not directly inhibitory for cell cycle progression in NIH3T3 cells. *Oncogene* 13(11):2421-2430.
118. Gao M, Guo N, Huang C, & Song L (2009) Diverse roles of GADD45alpha in stress signaling. *Current protein & peptide science* 10(4):388-394.
119. Zhan Q (2005) Gadd45a, a p53- and BRCA1-regulated stress protein, in cellular response to DNA damage. *Mutation research* 569(1-2):133-143.
120. Yoshida T*, et al.* (2005) Quercetin induces gadd45 expression through a p53-independent pathway. *Oncology reports* 14(5):1299-1303.
121. Milde-Langosch K, Bamberger AM, Methner C, Rieck G, & Loning T (2000) Expression of cell cycle-regulatory proteins rb, p16/MTS1, p27/KIP1, p21/WAF1, cyclin D1 and cyclin E in breast

cancer: correlations with expression of activating protein-1 family members. *International journal of cancer. Journal international du cancer* 87(4):468-472.

122. Baba Y*, et al.* (2000) Nasal natural killer/T cell lymphoma: case report with molecular biologic examination on Epstein-Barr virus and cell cycle regulatory p16, cyclin D1, Rb, and p53 genes. *The Journal of otolaryngology* 29(2):121-125.
123. Zhang K & Kumar R (1994) Interferon-alpha inhibits cyclin E- and cyclin D1-dependent CDK-2 kinase activity associated with RB protein and E2F in Daudi cells. *Biochemical and biophysical research communications* 200(1):522-528.
124. Boiko AD*, et al.* (2006) A systematic search for downstream mediators of tumor suppressor function of p53 reveals a major role of BTG2 in suppression of Ras-induced transformation. *Genes & development* 20(2):236-252.
125. Goss VL*, et al.* (2003) SAPK/JNK regulates cdc2/cyclin B kinase through phosphorylation and inhibition of cdc25c. *Cellular signalling* 15(7):709-718.
126. Qian YW, Erikson E, Taieb FE, & Maller JL (2001) The polo-like kinase Plx1 is required for activation of the phosphatase Cdc25C and cyclin B-Cdc2 in Xenopus oocytes. *Molecular biology of the cell* 12(6):1791-1799.
127. Roshak AK*, et al.* (2000) The human polo-like kinase, PLK, regulates cdc2/cyclin B through phosphorylation and activation of the cdc25C phosphatase. *Cellular signalling* 12(6):405-411.
128. Ohkubo Y, Kishimoto T, Nakata T, Yasuda H, & Endo T (1994) SV40 large T antigen reinduces the cell cycle in terminally differentiated myotubes through inducing Cdk2, Cdc2, and their partner cyclins. *Experimental cell research* 214(1):270-278.
129. Yuan L, Yu WM, & Qu CK (2003) DNA damage-induced G2/M checkpoint in SV40 large T antigen-immortalized embryonic fibroblast cells requires SHP-2 tyrosine phosphatase. *The Journal of biological chemistry* 278(44):42812-42820.
130. Chang TH, Ray FA, Thompson DA, & Schlegel R (1997) Disregulation of mitotic checkpoints and regulatory proteins following acute expression of SV40 large T antigen in diploid human cells. *Oncogene* 14(20):2383-2393.
131. Prevot D*, et al.* (2000) The leukemia-associated protein Btg1 and the p53-regulated protein Btg2 interact with the homeoprotein Hoxb9 and enhance its transcriptional activation. *The Journal of biological chemistry* 275(1):147-153.
132. Gayther SA*, et al.* (2007) Tagging single nucleotide polymorphisms in cell cycle control genes and susceptibility to invasive epithelial ovarian cancer. *Cancer research* 67(7):3027-3035.
133. Aprelikova O, Xiong Y, & Liu ET (1995) Both p16 and p21 families of cyclin-dependent kinase (CDK) inhibitors block the phosphorylation of cyclin-dependent kinases by the CDK-activating kinase. *The Journal of biological chemistry* 270(31):18195-18197.
134. Davies BR*, et al.* (2003) Immortalisation of human ovarian surface epithelium with telomerase and temperature-sensitive SV40 large T antigen. *Experimental cell research* 288(2):390-402.
135. Huschtscha LI, Neumann AA, Noble JR, & Reddel RR (2001) Effects of simian virus 40 T-antigens on normal human mammary epithelial cells reveal evidence for spontaneous alterations in addition to loss of p16(INK4a) expression. *Experimental cell research* 265(1):125-134.
136. Modi S*, et al.* (2000) Protein expression of the RB-related gene family and SV40 large T antigen in mesothelioma and lung cancer. *Oncogene* 19(40):4632-4639.
137. Wang A & Jiang H (2010) Rumen fluid inhibits proliferation and stimulates expression of cyclin-dependent kinase inhibitors 1A and 2A in bovine rumen epithelial cells. *Journal of animal science* 88(10):3226-3232.
138. Ip C, Dong Y, Thompson HJ, Bauman DE, & Ip MM (2001) Control of rat mammary epithelium proliferation by conjugated linoleic acid. *Nutrition and cancer* 39(2):233-238.

139. Du J, Jiang H, & Lin H (2009) Investigating the ADP-ribosyltransferase activity of sirtuins with NAD analogues and 32P-NAD. *Biochemistry* 48(13):2878-2890.
140. Aksoy P*, et al.* (2006) Regulation of SIRT 1 mediated NAD dependent deacetylation: a novel role for the multifunctional enzyme CD38. *Biochemical and biophysical research communications* 349(1):353-359.
141. Sauve AA*, et al.* (2001) Chemistry of gene silencing: the mechanism of NAD+-dependent deacetylation reactions. *Biochemistry* 40(51):15456-15463.
142. Pickard A, Wong PP, & McCance DJ (2010) Acetylation of Rb by PCAF is required for nuclear localization and keratinocyte differentiation. *Journal of cell science* 123(Pt 21):3718-3726.
143. Vinall RL, Ripoll AZ, Wang S, Pan CX, & deVere White RW (2012) MiR-34a chemosensitizes bladder cancer cells to cisplatin treatment regardless of p53-Rb pathway status. *International journal of cancer. Journal international du cancer* 130(11):2526-2538.
144. Zhang Q*, et al.* (2012) A small molecule Inauhzin inhibits SIRT1 activity and suppresses tumour growth through activation of p53. *EMBO molecular medicine* 4(4):298-312.
145. Guarani V*, et al.* (2011) Acetylation-dependent regulation of endothelial Notch signalling by the SIRT1 deacetylase. *Nature* 473(7346):234-238.
146. Peck B*, et al.* (2010) SIRT inhibitors induce cell death and p53 acetylation through targeting both SIRT1 and SIRT2. *Molecular cancer therapeutics* 9(4):844-855.
147. Solomon JM*, et al.* (2006) Inhibition of SIRT1 catalytic activity increases p53 acetylation but does not alter cell survival following DNA damage. *Molecular and cellular biology* 26(1):28-38.
148. Seo JS*, et al.* (2012) SIRT1, a histone deacetylase, regulates prion protein-induced neuronal cell death. *Neurobiology of aging* 33(6):1110-1120.
149. Ferreira KS*, et al.* (2012) Caspase-3 feeds back on caspase-8, Bid and XIAP in type I Fas signaling in primary mouse hepatocytes. *Apoptosis : an international journal on programmed cell death* 17(5):503-515.
150. Mendilcioglu I*, et al.* (2011) Apoptosis and expression of Bcl-2, Bax, p53, caspase-3, and Fas, Fas ligand in placentas complicated by preeclampsia. *Clinical and experimental obstetrics & gynecology* 38(1):38-42.
151. Zuo XL*, et al.* (2008) [Relation of apoptosis of K562 cells induced by naringenin in vitro to enzyme activity changes of caspase-3 and caspase-8 and expression of FAS/FASL proteins]. *Zhongguo shi yan xue ye xue za zhi / Zhongguo bing li sheng li xue hui = Journal of experimental hematology / Chinese Association of Pathophysiology* 16(2):286-289.
152. Rouquet N*, et al.* (1996) Protection of hepatocytes from Fas-mediated apoptosis by a non-transforming SV40 T-antigen mutant. *Cell death and differentiation* 3(1):91-96.
153. Rouquet N*, et al.* (1995) Fas-dependent apoptosis is impaired by SV40 T-antigen in transgenic liver. *Oncogene* 11(6):1061-1067.
154. Gonin S*, et al.* (1999) p53/T-antigen complex disruption in T-antigen transformed NIH3T3 fibroblasts exposed to oxidative stress: correlation with the appearance of a Fas/APO-1/CD95 dependent, caspase independent, necrotic pathway. *Oncogene* 18(56):8011-8023.
155. Sethi A, Jain A, Zode GS, Wordinger RJ, & Clark AF (2011) Role of TGFbeta/Smad signaling in gremlin induction of human trabecular meshwork extracellular matrix proteins. *Investigative ophthalmology & visual science* 52(8):5251-5259.
156. Tiwari R, Bargmann W, & Bose HR, Jr. (2011) Activation of the TGF-beta/Smad signaling pathway in oncogenic transformation by v-Rel. *Virology* 413(1):60-71.
157. Li J, Tang X, & Chen X (2011) Comparative effects of TGF-beta2/Smad2 and TGF-beta2/Smad3 signaling pathways on proliferation, migration, and extracellular matrix production in a human lens cell line. *Experimental eye research* 92(3):173-179.

158. Lu T*, et al.* (2012) Targeting Androgen Receptor to Suppress Macrophage-induced EMT and Benign Prostatic Hyperplasia (BPH) Development. *Molecular endocrinology*.
159. Campisi G*, et al.* (2007) Human papillomavirus: its identity and controversial role in oral oncogenesis, premalignant and malignant lesions (review). *International journal of oncology* 30(4):813-823.
160. Yu AL*, et al.* (2009) Subtoxic oxidative stress induces senescence in retinal pigment epithelial cells via TGF-beta release. *Investigative ophthalmology & visual science* 50(2):926-935.
161. Li H & Wicks WD (2001) Retinoblastoma protein interacts with ATF2 and JNK/p38 in stimulating the transforming growth factor-beta2 promoter. *Archives of biochemistry and biophysics* 394(1):1-12.
162. Witte F, Dokas J, Neuendorf F, Mundlos S, & Stricker S (2009) Comprehensive expression analysis of all Wnt genes and their major secreted antagonists during mouse limb development and cartilage differentiation. *Gene expression patterns : GEP* 9(4):215-223.
163. Elston MS*, et al.* (2008) Wnt pathway inhibitors are strongly down-regulated in pituitary tumors. *Endocrinology* 149(3):1235-1242.
164. Wang S, Chong ZZ, Shang YC, & Maiese K (2012) Wnt1 inducible signaling pathway protein 1 (WISP1) blocks neurodegeneration through phosphoinositide 3 kinase/Akt1 and apoptotic mitochondrial signaling involving Bad, Bax, Bim, and Bcl-xL. *Current neurovascular research* 9(1):20-31.
165. Venkatesan B*, et al.* (2010) WNT1-inducible signaling pathway protein-1 activates diverse cell survival pathways and blocks doxorubicin-induced cardiomyocyte death. *Cellular signalling* 22(5):809-820.
166. Su F, Overholtzer M, Besser D, & Levine AJ (2002) WISP-1 attenuates p53-mediated apoptosis in response to DNA damage through activation of the Akt kinase. *Genes & development* 16(1):46-57.
167. Dorfman DM, Greisman HA, & Shahsafaei A (2003) Loss of expression of the WNT/beta-catenin-signaling pathway transcription factors lymphoid enhancer factor-1 (LEF-1) and T cell factor-1 (TCF-1) in a subset of peripheral T cell lymphomas. *The American journal of pathology* 162(5):1539-1544.
168. Wu L & Strasser A (2001) "Decisions, decisions.": beta-catenin-mediated activation of TCF-1 and Lef-1 influences the fate of developing T cells. *Nature immunology* 2(9):823-824.
169. Muncan V*, et al.* (2006) Rapid loss of intestinal crypts upon conditional deletion of the Wnt/Tcf-4 target gene c-Myc. *Molecular and cellular biology* 26(22):8418-8426.
170. Calvisi DF*, et al.* (2005) Activation of the canonical Wnt/beta-catenin pathway confers growth advantages in c-Myc/E2F1 transgenic mouse model of liver cancer. *Journal of hepatology* 42(6):842-849.
171. Fahnert B*, et al.* (2004) Murine Wnt-1 with an internal c-myc tag recombinantly produced in Escherichia coli can induce intracellular signaling of the canonical Wnt pathway in eukaryotic cells. *The Journal of biological chemistry* 279(46):47520-47527.
172. You Z*, et al.* (2002) Wnt signaling promotes oncogenic transformation by inhibiting c-Myc-induced apoptosis. *The Journal of cell biology* 157(3):429-440.
173. Stins MF, Prasadarao NV, Zhou J, Arditi M, & Kim KS (1997) Bovine brain microvascular endothelial cells transfected with SV40-large T antigen: development of an immortalized cell line to study pathophysiology of CNS disease. *In vitro cellular & developmental biology. Animal* 33(4):243-247.

174. La Rosa FG*, et al.* (1997) Inhibition of proliferation and expression of T-antigen in SV40 large T-antigen gene-induced immortalized cells following transplantations. *Cancer letters* 113(1-2):55-60.
175. May T, Wirth D, Hauser H, & Mueller PP (2005) Transcriptionally regulated immortalization overcomes side effects of temperature-sensitive SV40 large T antigen. *Biochemical and biophysical research communications* 327(3):734-741.
176. Takazawa Y*, et al.* (1999) Articular cartilage cells immortalized by a temperature sensitive mutant of SV40 large T antigen survive and form cartilage tissue in articular cartilage environment. *Journal of cellular biochemistry* 75(2):338-345.
177. Martin DW*, et al.* (1993) p53 and SV40 T antigen bind to the same region overlapping the conserved domain of the TATA-binding protein. *Biochemical and biophysical research communications* 195(1):428-434.